UNITED STATES DEPARTMENT OF THE INTERIOR

GEOLOGICAL SURVEY

Geology of Precambrian Rocks and Isotope Geochemistry of Shear Zones in the Big Narrows Area, northern Front Range, Colorado

By

Jeffrey T. Abbott

Open-file report

1970

70-1

This report is preliminary and has not been edited or reviewed for conformity with U.S. Geological Survey standards and nomenclature.

Geology of Precambrian Rocks and Isotope Geochemistry of Shear Zones in the Big Narrows Area, northern Front Range, Colorado

By Jeffrey T. Abbott

U.S. Geological Survey, Denver, Colo.

ABSTRACT

Rocks within the Big Narrows and Poudre Park quadrangles located in the northern Front Range of Colorado are Precambrian metasedimentary and metaigneous schists and gneisses and plutonic igneous rocks. These are locally mantled by extensive late Tertiary and Quaternary fluvial gravels. The southern boundary of the Log Cabin batholith lies within the area studied.

A detailed chronology of polyphase deformation, metamorphism and plutonism has been established. Early isoclinal folding (F_1) was followed by a major period of plastic deformation (F_2), sillimanite-microcline grade regional metamorphism, migmatization and synkinematic Boulder Creek granodiorite plutonism (1.7 b.y.). Macroscopic doubly plunging antiformal and synformal structures were developed. P-T conditions at the peak of metamorphism were probably about 670°C and 4.5 Kb. Water pressures may locally have differed from load pressures.

The 1.4 b.y. Silver Plume granite plutonism was post kinematic and on the basis of petrographic and field criteria can be divided into three facies. Emplacement was by forcible injection and assimilation. Microscopic and mesoscopic folds which postdate the formation of the characteristic mineral phases during the 1.7 b.y. metamorphism are correlated with the emplacement of the Silver Plume Log Cabin batholith. Extensive retrograde metamorphism

was associated with this event.

A major period of mylonitization postdates Silver Plume plutonism and produced large E-W and NE trending shear zones. A detailed study of the Rb/Sr isotope geochemistry of the layered mylonites demonstrated that the mylonitization and associated recrystallization homogenized the Rb^{87}/Sr^{86} ratios. Whole-rock dating techniques applied to the layered mylonites indicate a probable age of 1.2 b.y. Petrographic studies suggest that the mylonitization-recrystallization process produced hornfels facies assemblages in the adjacent metasediments.

Minor Laramide faulting, mineralization and igneous activity occurred within this area. A sinuous band of gravel deposits trending into the Livermore embayment and lying well above the present drainage is believed to represent a late Tertiary course of the Cache La Poudre river.

TABLE OF CONTENTS

PAGE

PAGE

PAGE

PAGE

INTRODUCTION

This study was undertaken to investigate the structural geology and petrology of an area in the northern Front Range adjacent to the southern boundary of the Log Cabin batholith.

The area mapped includes the northwestern third of the Poudre Park quadrangle and the eastern three quarters of the adjacent Big Narrows quadrangle in the northern Front Range, Larimer County, Colorado (fig. 1).

It was hoped that a detailed analysis of this area would clarify the relationship of deformation, metamorphism and plutonism in an area of high metamorphic grade and pervasive migmatization. The study has demonstrated that the chronology of events in the area studied is subtly different from that established by earlier workers to the south suggesting that there may be a significant areal variation in the timing of these events.

During the course of the field work large Precambrian shear zones were recognized and a detailed whole rock Rb-Sr study was undertaken to establish both their age and the effect of cataclasis on Rb-Sr systems. Many of these large shear zones have well-developed layered blastomylonites suggesting that processes of metamorphic differentiation may have been important. The recognition of possible metamorphic aureoles related to these zones reinforced these ideas and the Rb-Sr study demonstrates their validity.

A trend-surface analysis of modal variation within a granitic gneiss unit was carried out to test the usefulness of that technique in determining the petrogenesis of such units in the northern Front Range. The random nature of the results has some potentially

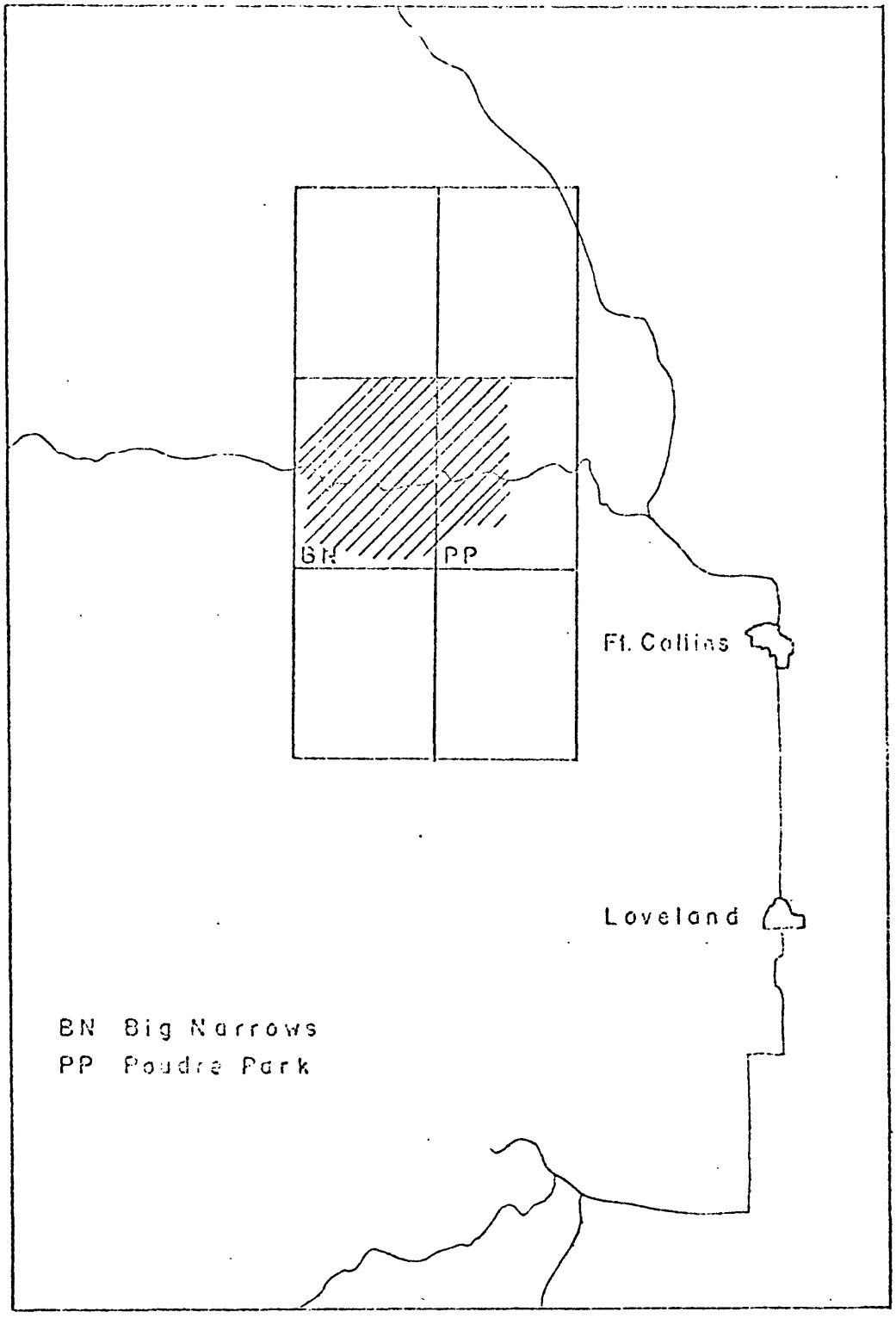

Figure 1: Location of area mapped

interesting applications in the discussion on the origin of these units.

All field work was carried out during the summers of 1967 through 1969. Mapping was done at a scale of 1:24,000 or 1:15,840 on topographic base maps produced by the U.S. Geological Survey. Field data was compiled at a scale of 1:24,000. Aerial photos proved of little value because of heavily timbered slopes or lack of contrast in geologic units.

The only previous geologic work in the Big Narrows-Poudre Park area is the reconnaissance study of Lovering and Goddard (1950). Detailed mapping to the east and the south has been carried out by students at the University of Colorado under the direction of Professor W. A. Braddock and much data is available in unpublished Ph.D. dissertations.

ACKNOWLEDGEMENTS

Primary support for the work reported in this study came from the U.S. Geological Survey. The author has been a member of the Northeast Front Range Project directed by Professor William A. Braddock who also served as chief thesis advisor. His guidance and constructive criticism are deeply appreciated. His commitment to his research and his students is equally great--a noteworthy achievement in these times.

All of the Rb-Sr isotope geochemistry was done at the Denver laboratories of the U.S. Geological Survey by permission of Thomas W. Stern. The work was carried out under the guidance of Robert E. Zartman to whom the author is very grateful.

Drs. James L. Munoz, Edwin E. Larson and William C. Bradley have all contributed valuable criticism and advice during the preparation of this report.

Field assistance was ably provided by Tim Grove during the 1969 field season.

The Department of Geological Sciences and the W. O. Thompson fund have supplied financial assistance. The Graduate School of the University of Colorado provided a NASA traineeship to the author during the academic year 1969-1970. This aid was of singular importance in allowing the author time for the laboratory studies carried out as part of this research.

DESCRIPTION OF ROCK UNITS

Introduction

This section includes a brief field description and a detailed petrographic description of all of the bedrock units shown on the geologic map (plate 1). The major discussion of petrogenesis of the rocks follows in separate sections, but petrologic interpretations are included in the following section where appropriate.

All plagioclase composition determinations were made optically using the PM section method (Van der Plas, 1966). Low temperature structural states were assumed. The structure and the composition of the potassium feldspar phase were determined using the X-ray techniques of Wright (1968) and Orville (1967).

All modal analyses were counted on standard 20 by 40 mm thin sections stained for potassium feldspar. With a few exceptions 1000 points uniformly distributed over each slide were counted.

Metamorphic rocks

Quartzofeldspathic mica schist (qms)

This unit is characterized by the abundance of quartz and feldspar, and by the presence of a strong foliation due to the preferred orientation of micas and the development of a mineralogical banding (fig. 2). The rock has an average grain size of about 0.5 mm. Much of the unit weathers to a tannish brown or gray color; the more massive biotite gneiss layers weather to dark gray or blue gray. Locally the unit is quite migmatitic.

The dominant mineral phases are quartz, plagioclase, microcline and biotite. Subordinate amounts of sillimanite, andalusite,

Figure 2: Typical exposure of quartzofeldspathic mica schist showing strong foliation, S_1.

muscovite and garnet are present. Important accessory phases include zircon, apatite, magnetite, ilmenite and sphene. Chlorite is occasionally present as a retrograde alteration product of biotite or garnet. Representative modal analyses are presented in table 1.

The quartz-feldspar fabric is granoblastic and generally equigranular. The average grain size of the quartz (0.1 - 0.4 mm) is perhaps somewhat less than that of the feldspars (0.2 - 0.5 mm). Plagioclase shows slight to moderate sericitic alteration and is commonly poorly twinned; no zoning was recognized. The potassium feldspar phase is perthitic (string perthitite) and shows microcline grid twinning. X-ray analysis of the potassium feldspar indicates that it is triclinic; however no detailed analysis of the structural state was attempted. In the sillimanite-bearing layers the quartz commonly contains numerous fine needles of sillimanite. No rutile was identified.

The biotite is pleochroic in tans, browns, reddish browns and greenish browns. No systematic variation in color with geographic location or structural setting was recognized. The mica fabric varies from lepidoblastic to random. The accessory mineral phases are usually associated with the biotite-rich layers.

Muscovite is present in three forms: small plates with a preferred orientation similar to that of biotite (fig. 3), large plates with a random orientation that commonly enclose fibrolitic sillimanite (fig. 4), and fine to medium grained shimmer aggregates in thin parallel seams (fig. 5). The latter two types are generally recognizable in hand specimen.

Sillimanite is occasionally present as fibrolite. These fine

TABLE 1. Modal analyses of quartzofeldspathic mica schist

Sample	12-4-10	4-4-1C	4-4-48	12-5-22	12-4-2	12-4-169
Quartz	44.7	27.7	60.5	37.3	40.0	39.2
Plagioclase	24.2	30.2	13.4	10.1	33.9	16.4
Microcline	5.5	0.1	6.6	21.7	4.0	-
Biotite	17.5	41.7	10.2	20.6	20.9	30.5
Muscovite	6.3	Tr.	0.8	10.1	1.0	12.8
Chlorite	-	-	-	-	-	-
Epidote	-	-	-	-	-	-
Amphibole	-	-	-	-	-	-
Opaque	1.2	-	Tr.	0.2	0.1	0.3
Apatite	0.5	0.2	-	Tr.	0.1	-
Zircon	0.1	0.1	-	-	-	-
Sphene	-	-	-	-	-	-
Garnet	-	-	Tr.	-	-	-
Sillimanite	-	-	8.5	Tr.	-	0.8
% An in plagioclase	17	26	12	35	15	-

Figure 3: Photomicrograph of quartzofeldspathic mica schist showing lepidoblastic biotite (B) and muscovite (M) in a granoblastic quartz and feldspar aggregate. The micas show a strong preferred orientation parallel with S_1. Sample 4-4-22. Crossed nicols. 60X.

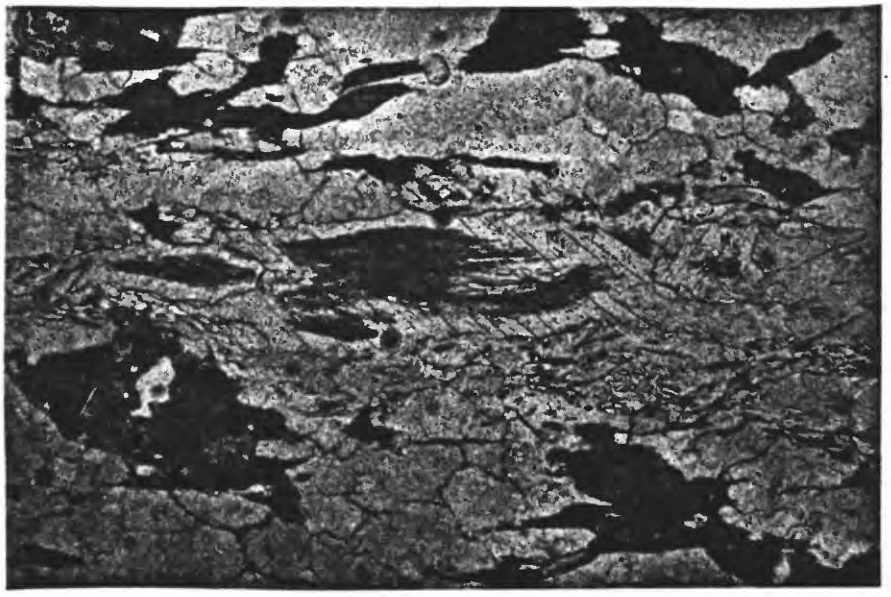

Figure 4: Photomicrograph of porphyroblastic muscovite (M_1 on plate 6) enclosing fibrolitic sillimanite. Sample 4-2-27. Uncrossed nicols. 50X.

Figure 5: Photomicrograph of fine to medium grained shimmer aggregates of muscovite (M_2 on plate 6). Some minor development of late lepidoblastic muscovite (M_3 on plate 6) is present on the righthand edge of the photomicrograph. Sample 4-4-99. Uncrossed polars. 60X.

grained aggregates of thin sillimanite crystals show a moderate preferred orientation. Only in exceptional cases was sillimanite recognizable on the megascopic scale. In a few samples coarse sillimanite rods were present possibly indicating second generation sillimanite. Similar textures have also been found to the east (Connor, 1962).

Andalusite is present in only a few samples. It is not recognizable in hand specimen and is present as small, anhedral corroded grains.

Almandine garnet is present occasionally as highly corroded porphyroblasts with associated secondary biotite, chlorite, feldspar and quartz.

Locally the more massive biotite gneiss units contain distinctive augen consisting of subhedral to euhedral crystals of magnetite with associated tabular crystals of ilmenite surrounded by an elliptical envelope of quartz, feldspar, sphene and minor mica (fig. 6).

Detailed studies of the opaques within these augen were limited to a few selected specimens. Observations on these indicate that the oxidation of magnetite to hematite was extensive.

Knotted mica schist (mks)

Much of the rocks of the southeastern corner of the map have distinctive flat, elliptical aggregates of quartz, feldspar and fibrolitic sillimanite set in a biotite schist matrix. These aggregates stand out on weathered surfaces as lighter colored knots and because of their distinctive appearance permit the mapping of

Figure 6: Quartzofeldspathic mica schist showing magnetite-bearing augen.

these biotite schists as a separate unit.

These rocks weather to a tan, brown or dark brown color. Average grain size is similar to that of the migmatitic biotite schists. Units gradational into both quartzofeldspathic mica schist and migmatitic biotite schist are present. At the northern limits of the unit the degree of migmatization is high. The knots vary in length from a few mm to 5 cm. Sillimanite is quite apparent in the larger knots; some knots are now largely secondary muscovite.

Quartz, plagioclase, biotite and sillimanite are the dominant mineral phases. Subordinate microcline, garnet, and muscovite are present. Accessory phases include apatite, zircon, sphene, magnetite, and hematite.

Quartz, the feldspars and the micas are similar to those in the migmatitic biotite schists and the quartzofeldspathic mica schists. The plagioclase composition ranges from An_{18} to An_{27}. Potassium feldspar is slightly perthitic and shows microcline grid twinning. The feldspar content varies considerably. Representative modal analysis are presented in table 2.

The knots are primarily aggregates of fibrolitic sillimanite set in a quartz matrix. Locally minor plagioclase is present in the quartz matrix. In the larger knots the quartz-feldspar matrix is present as a distinct border around the fibrolite. Secondary muscovite is very common and in many samples the fibrolite mats are set in large plates of muscovite. The origin of these ellipsoidal mineral aggregates is an enigma. Perhaps they represent the high-grade equivalent of earlier andalusite or staurolite

TABLE 2. Modal analyses of knotted mica schist

Sample	4-4-10	4-4-16A	4-4-137	4-4-139A	4-4-142
Quartz	45.0	36.6	63.2	23.3	54.8
Plagioclase	11.8	0.8	4.8	3.2	16.2
Microcline	4.8	-	8.4	0.6	3.6
Biotite	21.6	26.6	10.4	39.7	11.6
Muscovite	4.0	33.2	1.2	9.1	2.0
Chlorite	2.6	-	-	-	-
Epidote	-	-	-	-	-
Amphibole	-	-	-	-	-
Opaque	T	0.8	0.4	4.5	4.6
Apatite	T	T	-	T	T
Zircon	T	T	T	0.1	T
Sphene	-	-	-	-	-
Allanite	-	-	-	-	-
Sillimanite	10.2	2.0	11.6	19.5	7.2
% An in plagioclase	24		25		27

porphyroblasts or they may represent the product of metamorphic segregation processes. In two samples small subhedral grains of andalusite (?) associated with these knots were recognized. In other areas to the east and south other researchers have found porphyroblasts of cordierite, andalusite, staurolite and sillimanite in units similar to this one (Nutalaya, 1966). Muscovite textures are similar to those in the migmatitic biotite schists and the quartzofeldspathic mica schists.

Migmatitic biotite schist (mbs)

A number of exposures of a buff, tan to brown weathering, highly migmatitic, biotite schist are present in the central and western portions of the mapped area. It is characteristically highly variable in mineral composition with alternating biotite-rich seams and quartzofeldspathic layers (fig. 7). Abundant fibrolitic sillimanite is clearly visible in hand specimen. The rock has an average grain size of 1 mm and is, therefore, noticeably coarser grained than the quartzofeldspathic mica schists. The unit is distinguished from the migmatitic members of the quartzofeldspathic mica schist on the basis of coarser grain size, abundant sillimanite (or andalusite) and biotite, weathered color and characteristic response to deformation. Units gradational with quartzofeldspathic mica schist and knotted mica schist are present.

The dominant mineral phases are quartz, plagioclase, microcline and sillimanite. Subordinate amounts of andalusite, cordierite and muscovite are locally present. Accessory phases include apatite, zircon and the opaques. Chlorite and sercite are

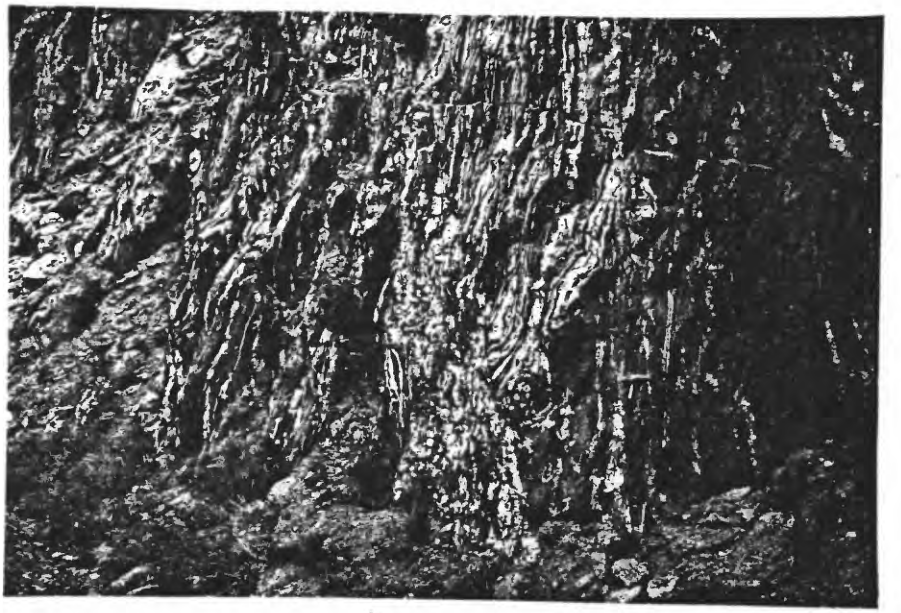

Figure 7: Exposure of migmatitic biotite schist.

secondary alteration products. Modal analyses are presented in table 3.

The quartz-feldspar fabric is similar to that in the quartzofeldspathic mica schists. Feldspar-quartz proportions are quite variable. Only rarely does plagioclase show twinning and except where it is extensively sericitized it is difficult to distinguish it from cordierite. Microcline is slightly perthitic and has the typical microcline grid twinning.

Sillimanite occurs as fibrolitic mats either intergrown with biotite and muscovite or enclosed within anhedral mosaic quartz. Andalusite is present locally as anhedral to subhedral, highly poikiolitic porphyroblasts up to 2 cm in size. Inclusions include quartz, feldspar, biotite, opaques and sillimanite. The quartz, feldspar and biotite inclusions seem to have no preferred orientation whereas the opaques occur as long, well defined trains of small subhedral to euhedral crystals. The lenticular shape of the andalusite porphyroblasts suggests that they may have replaced lenticular fibrolite aggregates.

Cordierite occurs in the andalusite-rich migmatitic biotite schist units as irregular, anhedral porphyroblasts, commonly quite poikiolitic. The hexagonal basal twinning of cordierite was never observed. Pinnitic alteration is rare.

Biotite in migmatitic biotite schists differs from that in the quartzofeldspathic mica schists in being coarser grained, and often possessing a more demonstrable association with sillimanite. Biotite inclusions in andalusite are finer grained than the surrounding biotite.

TABLE 3. Modal analyses of migmatitic biotite schist

Sample	12-6-37	12-4-2	12-4-28B	12-4-49	12-4-78
Quartz	40.3	40.0	44.8	39.5	34.6
Plagioclase	20.0	33.9	21.6	5.7	9.8
Microcline	-	4.0	-	0.1	2.6
Biotite	17.9	20.9	22.6	31.2	33.0
Muscovite	20.5	1.0	1.0	5.0	12.4
Chlorite	-	-	-	-	0.8
Epidote	-	-	-	-	-
Amphibole	-	-	-	-	-
Opaque	0.7	0.1	T	0.2	T
Apatite	-	0.1	0.6	T	T
Zircon	T	-	T	T	T
Sphene	-	-	-	-	-
Allanite	-	-	-	-	-
Sillimanite	0.6	-	9.4	18.6	6.8
% An in plagioclase		15	20		

Muscovite is present either as large plates intergrown with biotite or as fine-to medium-grained, shimmer aggregates. These aggregates seem certainly to be the result of retrograde alteration of fibrolitic sillimanite. Figure 4 illustrates a rare example of a muscovite aggregate with a core of sillimanite.

Clinozoisite-biotite schist (cbs)

Exposures of this unit occur over a sizeable area in the southwest portion of the Big Narrows quadrangle. It is a fine-grained, well-foliated schist which weathers to a dark, greenish-gray color. Interlayered with this unit are thin lenses of calc-silicate gneiss, biotite schist, pegmatite and aplite. The color, fine grain size and interlayered calc-silicate lenses give the unit a distinctive appearance.

In thin section the rock has a granoblastic to lepidoblastic texture. Important mineral phases include quartz, oligoclase, microcline, biotite and clinozoisite-epidote. Accessory phases include muscovite, sphene, apatite and very minor opaques. Oligoclase is more abundant than microcline. Microcline is only slightly perthitic. Biotite is abundant and occurs as small equant plates crudely to strongly aligned. Muscovite is rare and it is unclear whether it is primary or secondary.

Clinozoisite-epidote was present in all samples. The content was quite variable ranging from trace quantities to as much as five percent. It occurs as subhedral to euhedral grains, some slightly zoned. It is non-pleochroic to very weakly pleochroic. In some samples it appears to be associated with sphene, in others it is scattered throughout the sample.

Amphibolite (am)

Throughout the mapped area are bodies of amphibolite ranging in size from very thin layers extending great distances parallel to the strike of the conformable metasediments to very thick units which appear to pinch out abruptly into the metasediments or pinch out on the noses of large F_2 fold structures.

The thin amphibolite layers are clearly conformable with the adjacent metasediments on both the local and regional scales. A foliation defined by a crude mineralogical banding is usually present in the larger, more massive amphibolite bodies. Lineations defined by the parallel orientation of amphibole crystals are exceedingly rare, possibly due to the high metamorphic grade. No crosscutting relationships between the larger amphibolite bodies and the enclosing metasediments were every observed.

The amphibolites are gray to black in color and have a medium grained, equigranular granoblastic texture. Representative modal analyses are presented in table 4.

Important mineral phases include hornblende, plagioclase, biotite and quartz. Accessory phases include microcline, actinolite, diopside, garnet, opaques, apatite, sphene, pyrite and clinozoisite-epidote. Secondary phases include muscovite, sericite, chlorite, clay, and calcite.

Hornblende occurs as subhedral, equant grains pleochroic in tans, browns, greens and blue-greens.

Plagioclase is present as anhedral interstitial grains, polysynthetically twinned and usually strongly altered to secondary sericite and clay. The composition of the plagioclase ranges from

TABLE 4. Modal analyses of amphibolite

Sample	4-4-189A	12-4-145A	12-5-132B	4-4-38
Quartz	8.2	T	2.7	14.0
Plagioclase	21.0	34.3	32.4	35.2
Microcline	-	-	-	-
Biotite	0.4	-	-	7.8
Muscovite	0.6	-	-	-
Chlorite	T	-	-	-
Epidote	-	T	6.8	-
Amphibole	67.4	64.8	55.4	42.2
Opaque	2.4	0.2	-	0.8
Apatite	-	0.1	0.1	T
Zircon	-	-	-	-
Sphene	-	0.1	2.0	-
Diopside	-	-	0.6	-
Ortho-Amphibole Anthophyllite ?	-	0.4	-	0
% An in plagioclase		38		55

An_{25} to An_{77} but the majority of samples have compositions in the range An_{45} to An_{60}. A few samples appear to have two distinct populations of plagioclase, one with a composition in the oligoclase range and one with a composition in the labradorite range. Too few samples were available to check the extent of the anomalous plagioclase compositions or their possible association with a particular type of amphibolite body.

Quartz occurs as anhedral interstial grains in amounts varying from trace contents to over 14 percent. Undulatory extinction is common.

Microcline occurs as small anhedral interstial grains in a few samples.

Diopside, actinolite and garnet are restricted to only a few samples. Diopside occurs as irregular anhedral grains with a very weak pale-green pleochroism and is restricted to discrete layers within the samples. Actinolite occurs as bladed aggregates in thin lenses within a normal hornblende-plagioclase amphibolite. It is strongly pleochroic in pale green and green. Garnet occurs in only one sample.

Clinozoisite-epidote is more common than the preceeding three phases and also occurs in thin well defined bands within the amphibolite. It has an equant subhedral form and is only weakly pleochroic in pale greens.

Apatite occurs scattered throughout as tiny subhedral to euhedral grains. Sphene is rare. The opaques consist of subhedral grains of magnetite slightly oxidized to hematite.

Secondary alteration of the feldspars and chloritization of the biotite is common. Fresh plagioclase is very rare. In a few samples the alteration is restricted to discrete zones at a high angle to the foliation (fig. 8). Some veins of secondary "muscovite" and calcite are present in a few samples.

Calc-silicate gneiss (cgn)

Interlayered with the metasediments are thin layers of strongly banded gneiss rich in calcium-bearing silicate minerals, many too thin to show on the geologic map at the scale of 1:24,000. These units are generally associated with the thin amphibolite layers although they are not restricted to such associations. They are always conformable with adjacent metasediments and the contacts appear quite gradational.

A large unit crops out in the south-central part of the Big Narrows quadrangle. It has a thickness of four hundred meters, extends over a distance of two kilometers and grades into migmatitic biotite schists. Numerous thin conformable lenses of biotite schist and microcline gneiss are present within the layer. Mineralogical banding is well developed, some of the individual layers are quite rich in calcite. This unit and the smaller layers have been mapped as calc-silicate gneisses.

The calc-silicate gneisses are fine to medium grained, strongly foliated and weather to a white, green, gray or buff color. Locally an extreme color banding is present where monomineralic layers of amphibole, clinopyroxene, garnet or calcite are present.

Figure 8: Amphibolite showing alteration bands at a high angle to S_1. Sample 12-5-107. 8X.

The mineralogy of these units is quite variable. The important mineral phases (not necessarily all present in each unit) include quartz, plagioclase, microcline, biotite, diopside, hornblende, clinozoisite, epidote, actinolite, tremolite and garnet. Accessory phases or phases with only very limited occurrences include augite, cummingtonite, scapolite, idocrase, forsterite, hypersthene, spene, zircon and opaques. Secondary phases (some of the previously mentioned phases are also late in the paragenetic history of this unit) include chlorite, muscovite and sericite.

In thin section these rocks have a granoblastic to decussate texture and are locally strongly banded with individual bands 2 mm to 2 cm in width. Many of the units, in particular those near the Skin Gulch Shear zone, show evidence of cataclasis and recrystallization. These are both megascopically and microscopically flaser gneisses with clinozoisite and amphibole restricted to thin anastomosing seams. Quartz textures range from equant mosaic fabrics with undulatory extinction to strongly deformed fabrics with elongated grains, sutured contacts and finally to completely recrystallized polygonal fabrics showing no residual strain. Plagioclase is quite common but is almost always strongly altered to sericite and clay. The composition of the plagioclase lies in the andesine-labradorite range. Microcline distribution is extremely irregular varying from zero to 40 percent of the rock.

Amphiboles identified include hornblende, actinolite, tremolite and cummingtonite (?). Hornblende occurs as equant strongly pleochroic grains, actinolite as prismatic or acicular grains with a mottled pale green pleochroism and tremolite as prismatic

grains with no pleochroism. Cummingtonite occurs as non pleochroic prismatic grains associated with quartz and plagioclase.

Pyroxene phases include diopside, augite and hypersthene. All occur as equant, subhedral grains. Diopside is nonpleochroic and in many cases is strongly corroded showing a probable reaction relationahip with tremolite-actinolite. Augite occurs as highly corroded anhedral grains surrounded by epidote and minor actinolite. Exsolution lamellae are developed parallel to (100). Some grains show extensive alteration to secondary iron oxides. Diopside is the most common pyroxene phase. Diopside and augite were not observed in the same sample. Both occur with hornblende. Hypersthene is restricted to one occurrence where it is associated with forsterite, tremolite and spinel (?). It has a very weak pink pleochroism and occurs as equant subhedral grains in a matrix of tremolite. The associated spinel occurs as very small deep olive green subhedral grains.

Scapolite, idocrase and forsterite were each identified only once in separate samples. Scapolite occurs as a single large subhedral grain in a plagioclase diopside-actinolite-clinozoisite-calcite assemblage. Idocrase occurs as very large subhedral to euhedral grains in a tactite. It was not observed in thin section. Forsterite occurs as anhedral corroded and altered grains with tremolite, hypersthene and spinel. Calcite is an abundant constituent of the large calc-silicate gneiss unit in the Big Narrows quadrangle and occurs in a granoblastic aggregate with quartz and diopside. Elsewhere it occurs as a late alteration product as irregular patches and veins in tremolite.

Clinozoisite-epidote aggregates are quite common and make up over 50 percent of some samples. Much of the clinozoisite shown anomalous blue extinction colors and is present as anhedral to subhedral masses. The epidote is coarse grained, pleochroic in yellow and yellow-green and occurs as granular masses that are possibly the product of recrystallization contemporaneous with the mylonitization. Some of the clinozoisite may also be late, replacing earlier amphibole.

Secondary alteration products include chlorite derived from biotite, sericite developed in plagioclase, muscovite present as fine grained aggregates in the flaser gneisses and calcite and epidote in veins cutting across the metamorphic foliation.

Accessory phases include magnetite, apatite, zircon, sphene and spinel. Locally sphene is abundant enough to qualify as a major rock component. It is usually slightly corroded.

Microcline-quartz-plagioclase-biotite gneiss (mbgn)

Two large bodies of microcline-quartz-plagioclase-biotite gneiss are present in the Big Narrows quadrangle, one south and one north of the river. The former is very well exposed over an area of some $10km^2$ and was utilized in a detailed study of modal variation (appendix 2).

The rocks in both bodies are fine to medium grained, generally equigranular, and poorly to well-foliated with the foliation defined by discontinuous seams of biotite and/or quartzofeldspathic-rich seams. Occasionally augen of feldspar and quartz are present and these are subparallel to the rare mineral streaking linear. In one

sample large subhedral quartz grains were present with a form suggestive of relict bipyramidal quartz phenocrysts (fig. 9). The unit weathers to a tan, reddish-tan or gray color. Interlayered lenses up to twenty meters in thickness of quartzofeldspathic mica schist, amphibolite and migmatitic biotite schist are present although uncommon. The foliation within this unit is parallel with the foliation in the enclosing metasediments. Crosscutting contacts were not observed.

In thin section the rock has an equigranular to inequigranular granoblastic texture with a crude mineralogic banding only rarely developed. The augen are primarily microcline with minor quartz, plagioclase and biotite. The feldspar is somewhat coarser grained within these lenses. Modal data on over ninety samples is summarized in table 5 and in figure 10. Four chemical analyses are reported in table 12. The calculated CIPW norms for these samples are shown on figure 11. Although their modal composition is quite variable these rocks are modally and chemically equivalent to quartz monzonite. Results from a trend-surface analysis of modal variation of quartz, microcline, plagioclase and biotite indicate that the variation is essentially random (appendix 2).

In thin section cataclastic textures are exceedingly common--virtually all samples show some evidence of postcrystallization strain. In some samples the anastomosing, subparallel seams of milled quartz, feldspar and mica constitute the only recognizable foliation.

Major mineral phases include quartz, potassium feldspar, plagioclase and biotite. Accessory and secondary phases include

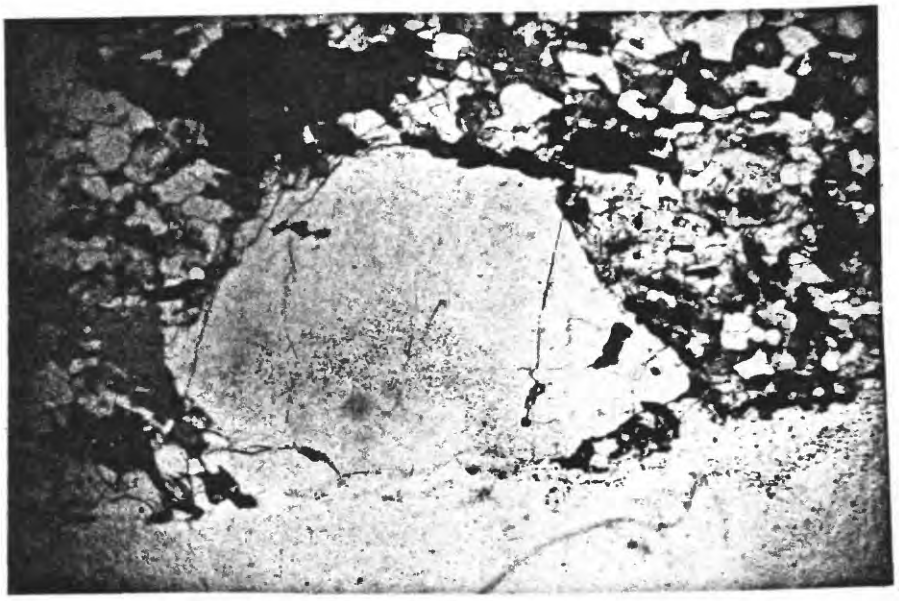

Figure 9: Photomicrograph of relict (?) bipyramidal quartz grain in microcline-quartz-plagioclase-biotite gneiss. Sample 12-1-32. 18X.

Table 5: Summary of modes of microcline-quartz-plagioclase-biotite gneiss

Mean and range of 92 modal analyses		
	Mean	Range
Quartz	37.3	27.1 - 51.8
Plagioclase	33.4	17.2 - 62.6
Microcline	21.8	0.0 - 43.3
Biotite	5.7	0.3 - 16.4
Muscovite	1.1	0.0 - 7.9
Opaques	0.4	0.0 - 2.1

Accessory phases present include epidote, chlorite, apatite, zircon, sphene and allanite.

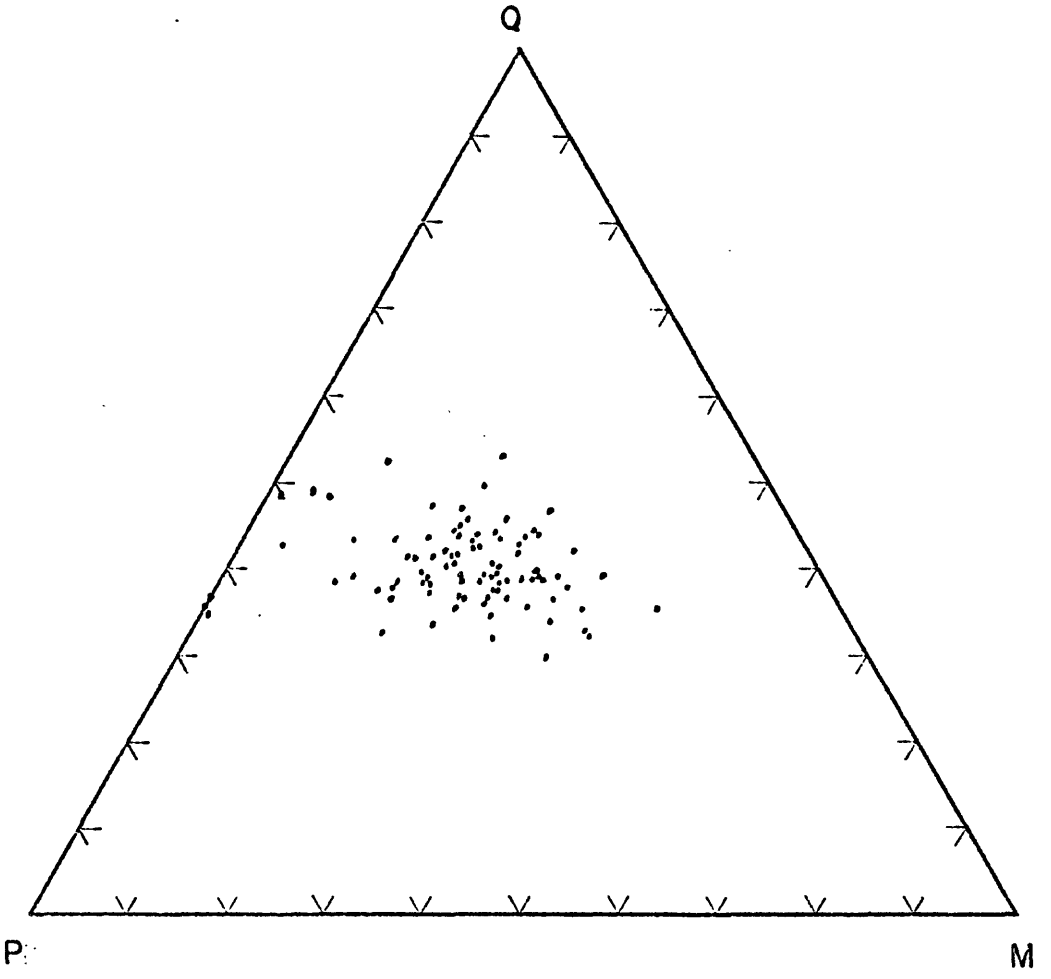

Figure 10: Ternary plot of modal analyses of microcline-quartz-plagioclase-biotite gneiss.

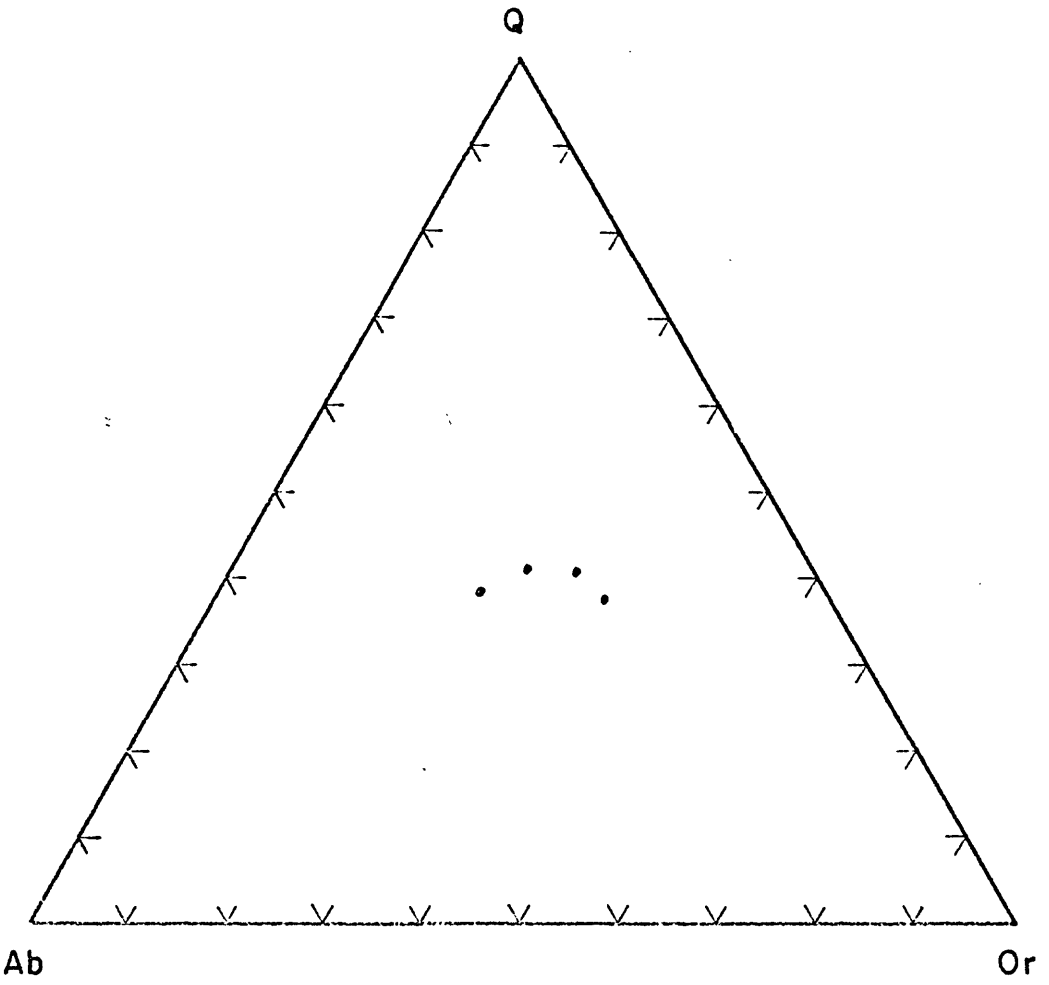

Figure 11: Ternary plot of CIPW norms of four samples of microcline-quartz-plagioclase-biotite gneiss.

muscovite, opaques, zircon, apatite, calcite, sphene, epidote and allanite (?).

Potassium feldspar occurs as anhedral grains ranging in size from 0.1 mm to 3 mm, and commonly has abundant quartz and minor plagioclase inclusions. Virtually all of the potassium feldspar is perthitic having both vein and patch perthite. It commonly shows undulatory extinction. Both the perthitic character and the extensive strain contribute to poor powder X-ray diffraction traces. The available X-ray data and the twinning both suggest a microcline structure.

Plagioclase occurs as anhedral grains generally less than 1 mm in size, polysynthetically twinned and weakly to strongly altered to secondary sericite and clay. Undulatory extinction and bent twin lamellae occur rarely. The plagioclase ranges in composition from An_{13} to An_{30} and averages approximately An_{23}. It is very rarely antiperthitic and quartz inclusions are common. Myrmekitic textures are quite uncommon but where developed they appear to be restricted to plagioclase adjacent to microcline.

Quartz occurs as anhedral interstitial grains showing undulatory extinction, sutured contacts and locally development of recrystallized (?) mosaic textures. Biotite generally occurs as small ragged plates often with only a crude parallel preferred orientation. It is pleochroic in browns and greenish-brown and commonly associated with muscovite, apatite and zircon. In most samples the biotite is partially altered to aggregates of clay and iron oxides. Muscovite occurs as fine grained aggregates associated with biotite and quartz in thin discontinuous seams

probably developed during secondary recrystallization associated with the cataclasis. It also occurs as larger ragged plates up to one mm in size. It is unclear whether these are also late secondary products or represent primary metamorphic phases.

Epidote-clinozoisite is a common minor accessory phase. It is weakly to nonpleochroic and occurs as anhedral grains commonly associated with the late biotite and muscovite. It is presumed to be the product of the alteration of plagioclase. Calcite and sericite are additional secondary phases--the latter present in virtually all plagioclase grains.

Apatite and zircon occur as subhedral to euhedral grains 0.1 to 0.3 mm in size and usually associated with biotite-muscovite aggregates. Sphene is quite rare. It is associated with the opaque phases.

The opaque phases include magnetite, hematite and ilmenite. There appear to be two types of occurrences: large subhedral grains (1-2 mm in size) and tiny irregular grains associated with the biotite-muscovite aggregates. The large grains are principally magnetite with minor subhedral blades of ilmenite. In some samples much of the magnetite has been oxidized to hematite and in a few samples pseudobrookite has been tentatively identified associated with ilmenite and hematite after magnetite. The large grains usually have a border of muscovite and rarely small grains of sphene. The tiny opaque grains associated with the micas are all now aggregates of hematite (?) and hydrous iron oxides (?). These may be related to the breakdown of biotite and the widespread oxidation possibly associated with the cataclastic phenomena.

Precambrian igneous rocks

Boulder Creek Granodiorite (bcg)

In the Front Range the term Boulder Creek Granodiorite has been used for a diverse group of granitic rocks ranging in composition from quartz diorite to quartz monzonite. Previous work on granitic rocks of this group has been extensive. Work in the central Front Range includes that of Lovering and Goddard, 1950; Moench, 1964; Sheridan and others, 1967 and Wells, 1967. Work in the northern Front Range includes that of Connor, 1962; Nutalaya, 1966, and Bucknam, 1969.

Throughout the south-central portion of the mapped area are bodies of Boulder Creek Granodiorite with modal and normative compositions which range from quartz diorite to granodiorite. These bodies range in size from small plugs to plutons a few kilometers across and commonly are phacoliths emplaced in the hinge regions of macroscopic fold structures (F_2 folds of this report; "older deformation" of Moench, 1964). Contacts with the enclosing metasediments are generally concordant but locally are discordant particularly along the boundaries of some of the larger plutons. They are commonly gradational in the Big Narrows-Poudre Park area where the wall rocks are migmatitic biotite schists and it is difficult to distinguish between the two rock types.

The foliation is due to a combination of the preferred orientation of biotite and feldspar and the development of a crude mineralogical layering defined by biotite-rich seams. The foliation is consistently parallel with the regional foliation of the adjacent metasediments. Numerous pegmatitic and aplitic veins are associated

with some of the larger plutons (Wells, 1967) but they are uncommon in the phacolithic bodies in the Big Narrows-Poudre Park area. Some large conformable pegmatites have been correlated with the emplacement of the Boulder Creek Granodiorite. Mafic inclusions are common and are parallel with the foliation. The rock is medium grained and weathers to a dark gray color. In the larger exposures the unit tends to weather spheroidally into large subrounded boulders.

In thin section the rock has a hypidiomorphic, equigranular to seriate porphyritic texture locally modified by cataclastic processes which have produced a mortar texture with a matrix of finer grained quartz, feldspar and mica. Representative modal analyses are presented in table 6 and plotted in figure 12.

Plagioclase is polysynthetically twinned, commonly shows slight sericitic alteration and occurs in subhedral to euhedral crystals 1-10 mm in size.

Potassium feldspar is present as anhedral crystals showing good microcline grid twinning. It is generally finer grained than the plagioclase and with quartz and biotite constitutes the matrix of the rock. The composition and structural state of the microcline was not determined. It is slightly perthitic.

Quartz has an average grain size of 0.5 to 1 mm and shows weak to strong undulatory extinction. Locally quartz grain boundaries are strongly sutured indicating extensive postcrystallization strain.

Biotite occurs as fresh plates, 0.5 - 2 mm in size and pleochroic in tans, greenish browns and browns. Only rarely is any preferred orientation evident in thin section.

Muscovite occurs as ragged plates to euhedral tabular crystals.

TABLE 6. Modal analyses of Boulder Creek Granodiorite

Sample	4-6-81A	4-6-81B	13-1-1A	12-5-96	12-3-8	12-3-13
Quartz	28.9	32.1	30.3	30.0	34.0	32.2
Plagioclase	48.0	46.7	41.4	39.4	40.6	35.6
Microcline	-	Tr.	10.6	0.9	7.7	6.6
Biotite	20.1	18.6	15.1	27.0	14.1	19.4
Muscovite	2.3	2.1	1.2	1.5	1.4	1.2
Chlorite	0.1	Tr.	Tr.	-	-	-
Epidote	-	-	0.3	-	-	0.6
Amphibole	-	-	-	-	-	-
Opaque	0.4	0.2	0.2	0.2	1.5	2.4
Apatite	0.1	0.3	0.5	0.6	0.5	1.8
Zircon	0.1	Tr.	Tr.	0.4	Tr.	0.2
Sphene	-	-	Tr.	Tr.	-	-
Allanite	-	Tr.	0.4	-	-	-
% An in plagioclase	30	-	30	32	24	28

TABLE 6. (continued)

Sample	12-3-222	4-4-50	4-4-56	4-4-66	4-4-69B	4-4-73B	4-4-78	4-4-118	4-4-122
Quartz	32.8	32.1	30.3	30.1	30.1	28.5	43.1	37.6	34.5
Plagioclase	47.3	42.7	43.2	47.7	46.2	39.9	33.9	36.5	45.0
Microcline	1.1	0.2	9.1	-	1.0	10.9	1.7	-	-
Biotite	15.5	20.6	15.5	9.5	19.6	18.2	19.9	21.3	15.4
Muscovite	1.7	3.5	1.1	11.2	1.1	0.9	0.4	3.3	4.5
Chlorite	-	-	-	0.7	-	-	-	-	-
Epidote	-	-	0.1	-	-	0.1	-	0.2	-
Amphibole	-	-	-	-	-	-	-	-	-
Opaque	1.5	0.7	0.4	0.7	1.1	0.6	0.6	0.8	0.1
Apatite	0.1	0.2	0.3	0.1	0.8	0.6	0.1	0.3	0.5
Zircon	Tr.	Tr.	Tr.	Tr.	0.1	0.3	0.4	Tr.	Tr.
Sphene	-	-	-	-	-	-	-	-	-
Allanite	-	-	-	-	-	-	-	-	-
% An in plagioclase	25	28	-	22	23	-	24	28	28

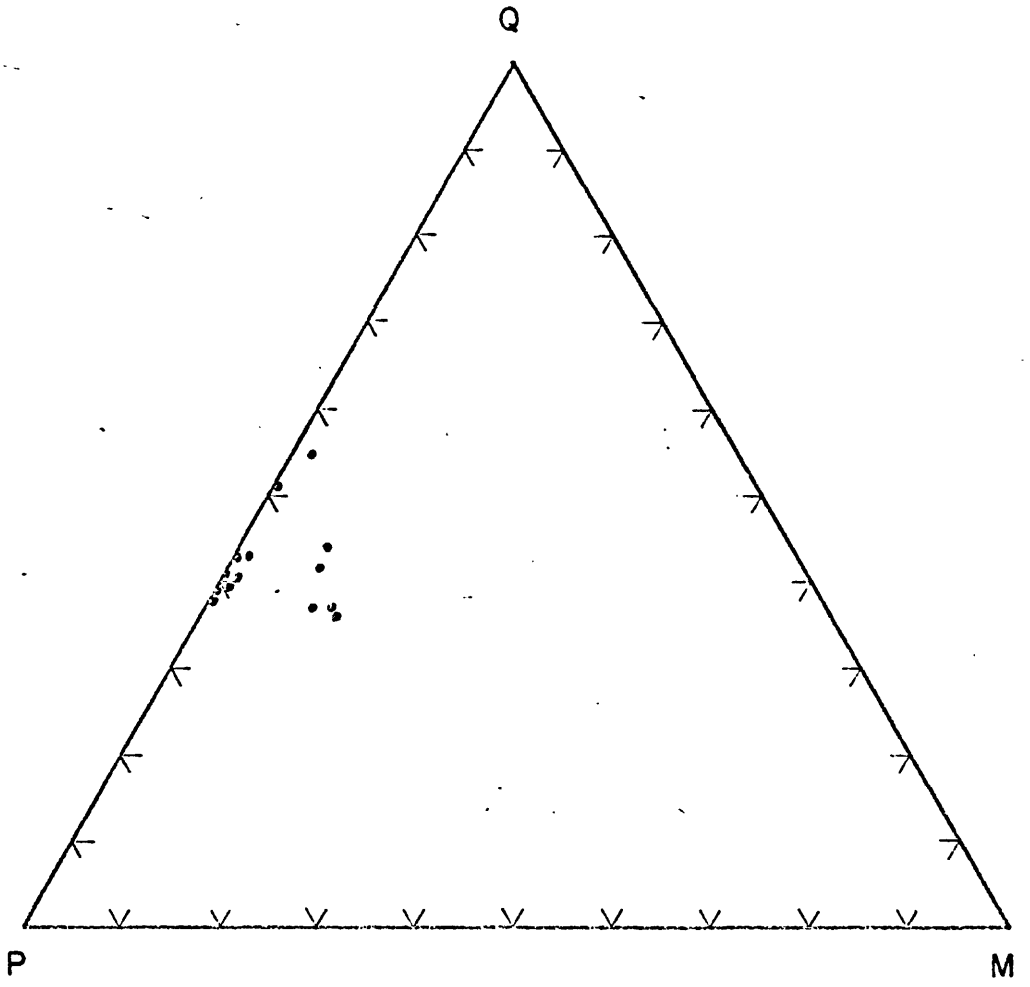

Figure 12: Ternary plot of modal analyses of Boulder Creek Granodiorite

from less than 0.1 mm to 2 mm in size. Some of it is clearly secondary, developing along preferred crystallographic planes in plagioclase; some of it may be primary. Muscovite-biotite aggregates are consistantly rich in opaques.

Chlorite occurs as an alteration product of biotite.

Sherman Granite (shg)

The Sherman Granite was first named by Darton and others (1910). Other more recent studies include Eggler (1967, 1968). It is distinguished from Silver Plume Granite primarily on the basis of its coarse grain size, presence of hornblende, absence of primary muscovite, and rarity of associated pegmatites (Eggler, 1967, p. 19).

In the northwestern corner of the Poudre Park quadrangle the southern portion of a pluton of Sherman Granite is exposed. The main body of the pluton lies to the north in the Livermore Mountain quadrangle. This pluton is probably a satellitic pluton related to the larger batholith of Sherman Granite which is present to the northeast.

Specimens of this unit are very similar in appearance to specimens of the porphyritic quartz monzonite facies of the Silver Plume and correlation of this unit with the Sherman granite rather than the Silver Plume granite is problematical.

The rock is a coarse-grained gray-to buff-colored quartz monzonite with prominent tabular potassium feldspar grains. Flow layering is uncommon. Petrographically it is similar to the porphyritic quartz monzonite. Hornblende, considered typical of much of the Sherman Granite (Eggler, 1967), occurs in only a few

samples (W. A. Braddock, personal communication, 1970).

A ring dike complex on the southwestern margin of the Sherman batholith has been studied in detail by Eggler (1967, 1968). The igneous rocks are corundum normative subsolvus granitic rocks and, although the history of individual facies of Sherman within the ring dike complex is quite complicated, the magma was formed by partial melting in the lower crust (Eggler, 1967).

Hornblende-microcline granite (hmg)

Three small bodies of coarse grained, equigranular, mafic granitic rock occur in the northeastern corner of the Big Narrows quadrangle where they are enclosed in alaskite and pegmatite. No clear cut structural relationships between this rock type and the host rock are evident. These small elliptical bodies are oriented parallel with the foliation in the nearby metasedimentary xenoliths in a large irregular body of alaskite and pegmatite. No evidence was observed which would permit an accurate estimate of even a relative age for this unit.

In thin section the granite has a hypidiomorphic-equigranular to seriate porphyritic texture. Essential mineral phases include quartz, microcline, plagioclase, hornblende and biotite. Accessory phases include epidote, apatite, sphene and opaques.

The potassium feldspar phase shows excellent development of both albite-pericline and carlsbad twinning. It is presumed to be microcline. The microcline grains are subhedral to euhedral, slightly perthitic and average about one cm in length. Plagioclase is polysynthetically twinned, has a composition in the oligoclase

range and is weakly to moderately altered to secondary sericite and clay. Microcline contains minor plagioclase inclusions some of which appear to have more albitic borders. Locally the plagioclase occurs as anhedral to subhedral grains somewhat smaller than microcline. Quartz occurs as interstitial anhedral grains showing little evidence of cataclastic strain.

Hornblende is abundant and occurs as coarse interlocking anhedral grains. It is pleochroic in tans, greens and blue greens and strongly poikiolitic with inclusions of sphene, apatite and quartz. Biotite is considerably less abundant than hornblende and is pleochroic in tans and greenish browns. It also contains quartz and sphene inclusions.

Sphene is abundant occuring as both tiny subhedral grains in hornblende and biotite and larger anhedral grains generally at grain boundaries. Sphene does not occur as inclusions in the feldspars. Apatite is present as large subhedral crystals 0.1 - 0.4 mm across. Magnetite is anhedral to euhedral. Epidote is rare. It is strongly pleochroic in yellow and yellow-green.

Overall mineral proportions are microcline > hornblende > plagioclase > quartz > biotite. No modal analyses were made.

Andesite dikes (and)

A swarm of north-northwest trending andesite dikes are present in the south-central part of the mapped area. Few are present north of the Poudre River fault. The dikes are from less than a meter to a few meters thick. They weather to a dull gray-black color, sometimes in negative relief, and are quite apparent on air photos.

They are fine-to medium-grained and the plagioclase phenocrysts commonly weather out in relief. Crosscutting relationships indicate that the andesites postdate both Boulder Creek Granodiorite and Sherman Granite plutonism and predate Silver Plume plutonism.

In thin section they are porphyritic hypidiomorphic to automorphic-granular in texture. The groundmass has an intergranular texture. The major mineral constituents are plagioclase, biotite and hornblende. Plagioclase crystals are euhedral, strongly zoned and clouded, and have an average composition of andesine. The degree of sericitization varies considerably from slide to slide.

Hornblende occurs as ragged subhedral grains associated with biotite and opaques in the groundmass. In a few specimens it is present as phenocrysts up to 3 mm in size with abundant quartz inclusions and is strongly chloritized. Occasionally aggregates of hornblende, biotite, sphene and magnetite are present suggesting that these represent alteration products of an earlier mafic phase such as a pyroxene. Hepp (1966) has discussed these textures in greater detail. Biotite is present as ragged plates in the groundmass and as coarser crystals in the hornblende-biotite-magnetite-sphene aggregates. Biotite and hornblende are locally altered to chlorite.

Accessory phases include quartz, microcline, apatite, sphene and magnetite. Quartz occurs as anhedral interstitial grains as does microcline. Apatite is present both as tiny euhedral rods and needles and much larger, 1 mm tabular subhedral crystals. Sphene and magnetite are usually closely associated as anhedral corroded grains. Sphene rims magnetite in many specimens and suggests that

it may be produced by the breakdown of a Ti-rich magnetite.

In the west-central portion of the Big Narrows quadrangle a group of flat lying quartz andesite dikes crop out in a migmatitic biotite schist terrain. These are thin tabular bodies dipping gently to the north and occur as a number of subparallel sheets. Their structural setting is quite different from that of the north-northwest trending dike swarm.

In thin section these flat dikes have a porphyritic xenomorphic-granular texture very different from the other andesites. The plagioclase phenocrysts are up to 3 mm in size and are subhedral to euhedral and are neither zoned nor clouded. The biotite-plagioclase-quartz fabric of the groundmass is almost granoblastic. The biotite plates show a subparallel alignment. Hornblende is not present in some specimens; microcline is absent from all specimens except those showing extensive cataclastic deformation. Quartz is considerably more abundant than in the andesites of the dike swarm; thus, these are termed quartz andesites.

The petrographic features suggest that the quartz andesites are completely recrystallized. Their style of emplacement is different from the andesites of the dike swarm and their composition is different. It is apparent then that there may be two generations of andesites. Both types are found as inclusions in Silver Plume Granite.

Alaskite (als)

In the northern part of the area there are a number of large irregular bodies of medium to coarse grained, very leucocratic

granitic rock. The modal mineralogy is quite variable ranging from granite to quartz monzonite. The name alaskite has been adopted because of the very low color index and the mineralogy. It weathers to a cream, buff or tan color, and is only rarely slightly foliated. Locally portions of the alaskite bodies are pegmatitic or aplitic in texture.

Much of the unit is spatially associated with bodies of microcline gneiss; however, relationships are somewhat ambiguous. In the Livermore Mountain quadrangle field relationships indicate that the quartz monzonite facies of the Silver Plume crosscuts this unit (W.A. Braddock, 1970, personal communication).

In thin section the alaskite has a xenomorphic to hypidiomorphic equigranular to seriate porphyritic texture. Important mineral phases include quartz, microcline, plagioclase and muscovite. Subordinate and accessory phases include biotite, garnet, apatite, sillimanite and opaques. Secondary alteration products include sericite and iron oxides. Modal analyses are given in table 7.

Quartz occurs as interstitial anhedral grains showing undulatory extinction and locally evidence of more extensive strain. Microcline is anhedral to subhedral, slightly perthitic, has well developed albite-pericline twinning and locally contains abundant round quartz blebs. Plagioclase is subhedral to euhedral, complexely twinned, slightly altered to sericite and has a composition in the albite-oligoclase range. Muscovite is abundant, commonly representing 10 percent or more of the rock and occurs as equant plates, locally rather wormy at the edges. Biotite is absent or present only in trace quantities usually strongly altered to iron oxides, clays and

TABLE 7. Modal analyses of alaskite

Sample	4-2-43	4-2-48	4-2-84C	4-2-102	4-2-114
Quartz	32.8	34.0	34.6	36.2	25.4
Plagioclase	30.6	25.6	26.0	35.0	11.2
Microcline	29.0	25.6	29.2	13.2	62.6
Biotite	5.2	3.0	-	-	T
Muscovite	2.2	11.6	9.0	14.6	0.6
Chlorite	-	-	-	-	-
Epidote	-	-	-	-	-
Amphibole	-	-	-	-	-
Opaque	0.2	T	T	0.4	0.2
Apatite	-	-	-	-	-
Zircon	-	-	-	-	-
Sphene	-	-	-	-	-
Garnet	-	-	1.2	0.2	-
Sillimanite ?	T	T	-	-	-
% An in plagioclase	17	16	6	7	8

chlorite (?). Garnet occurs only in a few samples as subhedral grains 0.5 - 1 mm in size. Magnetite is very rare; hematite associated with the muscovite is common but present only in trace quantities.

Silver Plume Granite

The name Silver Plume Granite was first applied to granitic rocks in the Georgetown quadrangle by Ball in Spurr and Garrey (1908). The rock of the type locality is equigranular to porphyritic and has a hypidiomorphic-granular texture in thin section. This name is now applied to granitic rocks of Precambrian age emplaced as small batholiths, plutons and stocks throughout the Front Range. They are characterized by prominent lathlike feldspar crystals which have a subparallel alignment (Lovering and Goddard, 1950, p. 28).

Much work has been carried out on the various bodies of Silver Plume Granite beginning with Ball and including Fuller (1924) and Lovering and Goddard (1950). More recent studies include those of Bucknam (1969), Braddock (1969), Moench and others (1962), Nutalaya (1966), Connor (1962), Sheridan and others (1967) and Wells (1967). The widespread occurence of granitic rocks of similar composition, age and plutonic setting throughout the Front Range justifies the use of the term Silver Plume Granite.

Three types of granitic intrusives have been mapped within the Big Narrows-Poudre Park area which on the basis of megascopic and microscopic criteria can be related to the Silver Plume group of granitic rocks in the Front Range. The three units are:

porphyritic quartz monzonite, quartz monzonite and mafic quartz monzonite. These three rock units are probably distinct facies of the Silver Plume Granite.

The northern third of the Big Narrows quadrangle is almost entirely granitic rock and represents the southern boundary of the Log Cabin batholith; a small composite batholith believed to be composed entirely of Silver Plume Granite but as yet only mapped on a reconnaissance basis (Lovering and Goddard, 1950).

In the field these units were distinguished entirely on the basis of grain size (the porphyritic quartz monzonite facies is coarse grained), color (the mafic quartz monzonite is distinctively darker) and the presence of subhedral to euhedral, lath-shaped feldspar crystals (well developed in the porphyritic quartz monzonite and mafic quartz monzonite facies). Crosscutting relationships which would permit assigning relative ages were either not observed or were ambiguous. The mafic quartz monzonite facies was never observed in contact with the other facies. The quartz monzonite and porphyritic quartz monzonite facies are mutually crosscutting. Unlike the other facies the porphyritic quartz monzonite commonly develops a moderately good tor topography with subrounded boulders bounded by a nearly orthogonal joint set. No attemps was made to map these joints.

Contacts with the wall rocks are locally sharp and discordant particularly along the contacts of the satellitic dikes and sills (fig. 13). Excellent exposures of dike and sill injection are present in the Hallet's Peak area adjacent to the Long's Peak-St. Vrain batholith (Boos and Boos, 1934; Ludington, personal

Figure 13: Contact between intrusive mafic quartz monzonite and microcline-quartz-plagioclase-biotite gneiss.

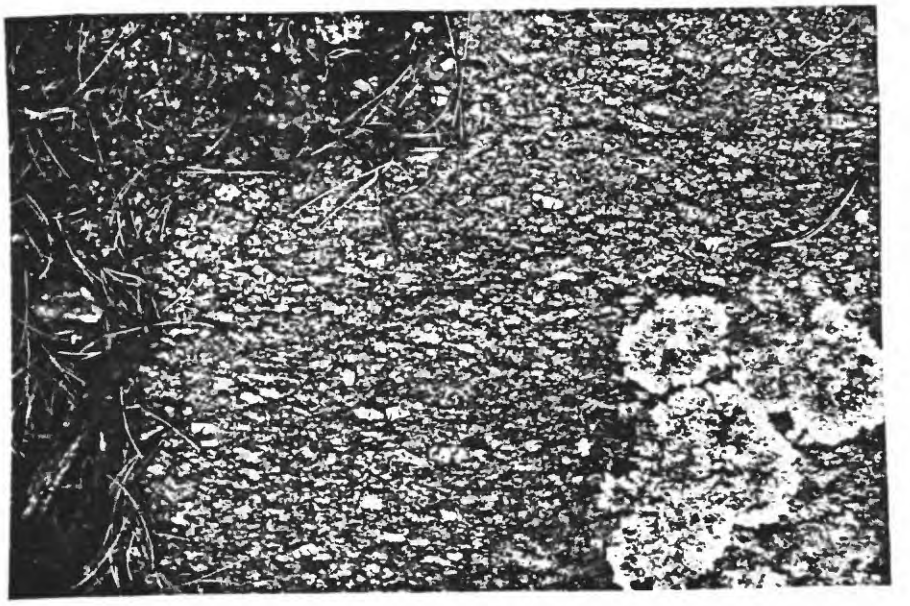

Figure 14: Flow foliation in porphyritic quartz monzonite.

communication). Contacts of the larger bodies of granitic rock in the Log Cabin batholith with their wall rocks are sometimes gradational. In the coarser-grained facies the feldspar crystals are aligned along what is interpreted as a flow foliation (fig. 14) although due to lack of exposures flow layering paralleling the walls of the intrusive was never observed. Associated pegmatites and aplites are common in the area adjacent to the southern boundary of the Log Cabin batholith.

Chill zones are absent and there is no evidence of contact metamorphism. In general few xenoliths are present. All of those observed within the coarse-grained porphyritic quartz monzonite were quartzofeldspathic mica schist. However, in every example the granitic phase immediately adjacent to the metasediments was a fine grained phase with only rare large phenocrysts. Excellent examples of magmatic injection are present within these xenoliths (fig. 15).

Porphyritic quartz monzonite (sppm): A large portion of the northwest corner of the mapped area consists of a coarse-grained buff-to gray-weathering granitic rock. In thin section the rock is a hypidiomorphic granular, porphyritic to seriate porphyritic quartz monzonite. Representative modal analyses are presented in table 8 and plotted in figure 16. Two chemical analyses are listed in table 12.

Potassium feldspar occurs as subhedral to euhedral phenocrysts up to 3 cm in length. The potassium feldspar phase has a maximum-microcline structural state. Compositions were determined on homogenized samples and average Or_{83}. The microcline is subhedral

Figure 15: Interior of large quartzofeldspathic mica schist xenolith in Silver Plume Granite showing extensive injection of magma parallel with the foliation within the xenolith.

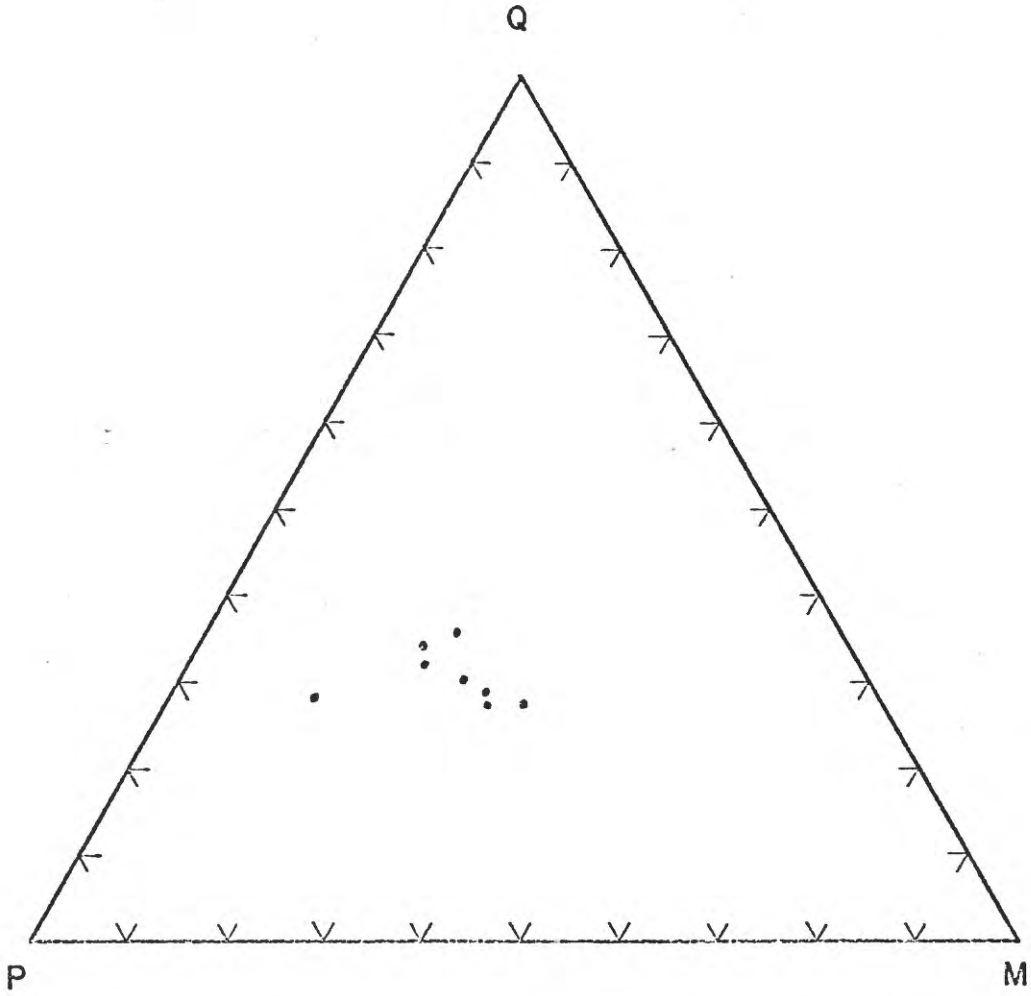

Figure 16: Ternary plot of modal analyses of porphyritic quartz monzonite.

TABLE 8. Modal analyses of porphyritic quartz monzonite

Sample	12-2-11	12-2-25A	12-2-9	12-1-20	12-1-21	12-1-22A	12-1-75	12-2-35B
Quartz	25.9	23.8	24.5	31.2	33.7	27.5	30.0	26.2
Plagioclase	35.3	48.6	35.6	38.0	36.7	36.3	41.3	33.6
Microcline	28.7	12.5	29.4	20.7	23.8	26.0	22.4	34.1
Biotite	6.7	12.2	8.4	7.1	3.9	7.2	3.8	4.5
Muscovite	0.3	0.5	0.8	1.4	0.6	1.0	0.7	0.4
Chlorite	-	-	-	-	0.2	T	-	0.1
Epidote	-	0.2	-	0.1	0.2	0.3	0.4	0.1
Amphibole	-	-	-	-	-	-	-	-
Opaque	1.1	1.3	1.2	0.9	0.6	1.2	1.0	0.7
Apatite	0.8	0.6	T	0.5	0.1	0.5	0.2	T
Zircon	0.5	0.1	T	T	0.2	T	T	T
Sphene	0.9	-	-	T	-	T	T	0.1
Allanite	-	0.2	0.1	0.1	T	T	0.2	0.2
Rutile ?			T			T		
% An in plagioclase	20	23	19	21	21	23		

to euhedral and slightly perthitic with both string and patch perthite. It is poikiolitic containing quartz blebs, euhedral plagioclase crystals and irregular biotite plates.

Plagioclase is present as subhedral to euhedral crystals that usually contain quartz and biotite inclusions, and patches of antiperthitic microcline. Myrmekitic intergrowth of quartz and plagioclase are occasionally found adjacent to microcline. Minor late sericitic alteration is widespread.

Accessory minerals are unusually abundant and permit easy petrographic distinction of this rock type from other types of Silver Plume granite.

Secondary alteration products include muscovite, chlorite, hematite and epidote. Some of the muscovite is primary but volumetrically it is very minor. Chlorite is an alteration product of biotite and hematite and magnetite.

Locally this unit shows pervasive effects of post-crystallization strain including undulatory extinction in the feldspars and quartz, sutured quartz contacts, polygonized quartz and bent and fractured feldspars.

Mafic quartz monzonite (spmm): This unit is present as a small stock and numerous related satellitic pods, dikes and irregular intrusive bodies a few meters to a few hundred meters in dimensions in the central portion of the mapped area. It has clearly crosscutting contacts with the surrounding metasediments and microcline-quartz-plagioclase-biotite gneiss. The rock weathers to a dark gray with a distinctively dark matrix. It is medium grained and strongly

porphyritic.

In thin section the texture is hypidiomorphic seriate porphyritic. Virtually all samples show evidence of cataclastic deformation. Representative modal analyses are given in table 9 and plotted in figure 17. One chemical analysis is listed in table 12.

Anhedral to subhedral potassium feldspar is moderately perthitic, shows well developed microcline grid twinning and has a maximum microcline structure.

Plagioclase crystals are subhedral to euhedral, are polysynthetically twinned and unzoned. Sericitic alteration is common.

Quartz forms anhedral fine-grained aggregates in the matrix. Biotite forms fine-grained aggregates and is unusually rich in very small inclusions of zircon (?) with pronounced pleochroic halos. Secondary muscovite is intergrown with biotite and chlorite is present as an alteration product of biotite. Some larger, possibly primary, muscovite plates are present. Sillimanite occurs as very small needles scattered throughout the quartz matrix. Epidote is associated with biotite and muscovite in fine-grained seams which cut through the rock and which have been formed by cataclastic processes.

Quartz monzonite (spqm): Throughout the central portion of the mapped area are small (100 meters) to large (>1 km) bodies of fine to medium grained slightly porphyritic quartz monzonite with the characteristic tabular feldspar crystals of the Silver Plume granite. The unit clearly crosscuts the metasedimentary wall rocks

TABLE 9. Modal analyses of mafic quartz monzonite

Sample	12-3-146	12-3-185	12-3-207	12-3-89	12-3-69	12-3-79A	12-3-81	12-3-84	12-3-86A
Quartz	33.3	34.4	35.5	31.5	27.0	28.3	28.8	29.4	36.3
Plagioclase	22.3	31.8	22.2	23.7	31.4	21.3	21.9	23.4	20.9
Microcline	31.9	22.6	28.5	35.4	30.2	42.9	39.7	34.2	34.0
Biotite	9.0	8.6	10.8	6.8	8.9	3.4	4.8	7.5	6.3
Muscovite	3.5	2.4	6.5	2.5	2.5	4.1	4.3	4.9	2.5
Chlorite	-	-	-	-	-	-	-	-	Tr.
Epidote	-	-	-	-	-	-	-	-	-
Amphibole	-	-	-	-	-	-	-	-	-
Opaque	-	0.1	0.6	Tr.	Tr.	Tr.	0.5	0.6	-
Apatite	Tr.	-	0.3	0.1	Tr.	-	Tr.	-	-
Zircon	Tr.	0.1	-	Tr.	Tr.	Tr.	Tr.	Tr.	Tr.
Sphene	-	-	-	-	-	-	-	-	-
Allanite	-	-	-	-	-	-	-	-	-
Sillimanite	Tr.	Tr.	-	Tr.	-	-	-	-	Tr.
% An in plagioclase	20	16	17	16	-	18	-	13	25

TABLE 9. (continued)

Sample	12-3-86B	12-3-95A	12-3-95B	12-3-99A	12-3-211A	12-3-174	12-3-176	12-3-184C	12-3-199
Quartz	40.5	31.8	34.2	39.6	29.6	32.7	33.5	33.0	27.5
Plagioclase	20.9	22.9	20.4	28.0	30.2	27.0	27.6	25.4	25.6
Microcline	27.6	35.5	35.4	25.6	37.9	30.7	30.0	33.1	36.1
Biotite	6.8	7.5	7.2	5.3	7.7	7.7	7.1	4.3	7.8
Muscovite	4.3	2.2	2.6	1.5	3.6	1.9	1.7	3.8	2.6
Chlorite	-	-	Tr.	-	-	-	-	-	-
Epidote	-	-	0.1	Tr.	0.3	-	0.1	0.2	0.1
Amphibole		-	-	-	-	-	-	-	-
Opaque	-	Tr.	Tr.	Tr.	0.7	-	Tr.	0.1	0.3
Apatite	-	0.1	0.1	Tr.	Tr.	-	-	Tr.	-
Zircon	-	Tr.	Tr.	Tr.	Tr.	-	Tr.	0.1	Tr.
Sphene	-	-	-	-	-	-	-	-	-
Allanite	-	-	-	-	-	-	-	-	-
Sillimanite	Tr.	-	-	Tr.	Tr.	Tr.	Tr.	Tr.	Tr.
% An in plagioclase	-	23	23	-	-	17	17	13	12

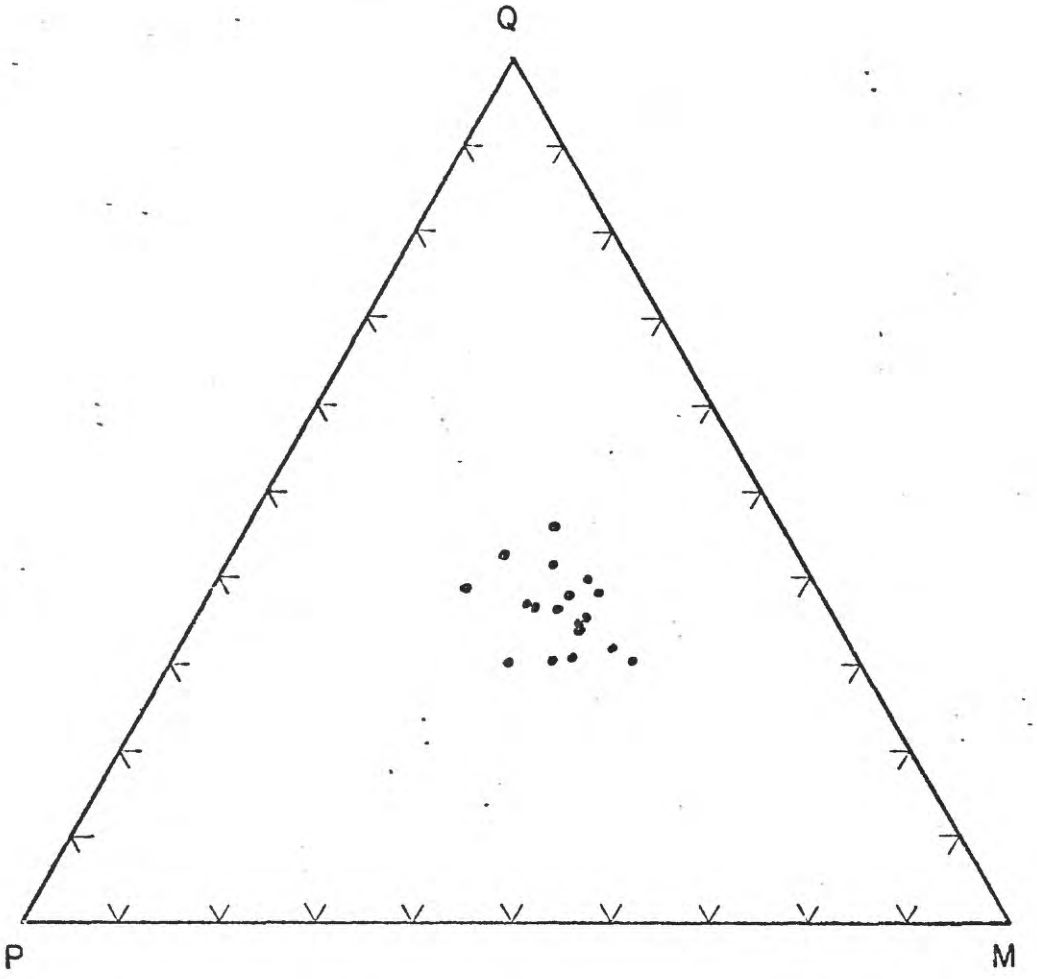

Figure 17: Ternary plot of modal analyses of mafic quartz monzonite

on both the outcrop and the regional scale. It weathers to a gray, tan or buff color and locally develops a tor topography. Representative modal analyses are listed in table 10 and plotted in figure 18. Six chemical analyses are listed in table 12.

The potassium feldspar phase is generally subhedral to euhedral and non-perthitic to slightly perthitic. Inclusions of quartz, plagioclase and biotite are common. It has a maximum-microcline structure and albite-pericline twinning is common. Plagioclase is subhedral to euhedral, unzoned, and contains inclusions of quartz and biotite. The feldspars as a group have fewer inclusions in this rock type than in the porphyritic quartz monzonite. Sericitic alteration of plagioclase is very common.

Quartz is present as anhedral grains showing undulatory extinction and locally sutured contacts. It commonly contains scattered very fine sillimanite needles.

By comparison with the porphyritic quartz monzonite this unit is poor in accessory phases. Allanite is rare. Sphene was not recognized. Trace quantities of sillimanite are nearly ubiquitous. Sillimanite was not observed in the porphyritic quartz monzonite.

Muscovite is present in all samples and varies in habit from very fine-grained "sericitic" aggregates to large plates 1-3 mm in size. Some of it is clearly secondary as it is present as tabular crystals parallel to crystallographic planes in the plagioclase. Chlorite as an alteration product of biotite and epidote is particularly prevalent in those specimens showing evidence of cataclastic deformation. Virtually all samples show evidence of some post-crystallization strain.

TABLE 10. Modal analyses of quartz monzonite

Sample	12-4-127	12-3-55	12-3-171	12-3-205A	12-3-212A
Quartz	33.5	33.1	35.0	28.9	31.9
Plagioclase	21.3	30.2	20.9	25.1	29.5
Microcline	34.8	26.3	34.5	36.4	29.4
Biotite	5.7	7.6	7.6	4.8	6.3
Muscovite	3.8	2.8	1.9	4.2	2.7
Chlorite	-	-	-	-	-
Epidote	0.7	-	-	-	0.1
Amphibole	-	-	-	-	-
Opaques	Tr.	Tr.	0.1	0.1	0.1
Apatite	-	-	-	0.5	Tr.
Zircon	Tr.	Tr.	-	Tr.	Tr.
Sphene	-	-	-	-	-
Allanite	Tr.	-	-	-	-
Sillimanite	Tr.	-	Tr.	Tr.	Tr.
% An in plagioclase	-	-	20	7	17

TABLE 10. (continued)

Sample	12-1-8	12-2-8	12-2-15C	12-2-25C	12-4-65	12-4-85	12-4-98	12-4-110	12-4-113
Quartz	36.0	32.2	30.5	31.7	32.3	32.3	32.6	27.5	28.3
Plagioclase	20.7	28.4	26.0	22.8	29.1	25.4	14.8	27.4	27.1
Microcline	35.2	35.2	35.1	37.0	23.2	32.3	40.4	38.0	35.5
Biotite	4.9	3.5	4.8	7.1	9.1	3.8	5.4	4.6	6.9
Muscovite	3.2	0.6	2.0	0.9	6.3	6.2	6.3	2.4	1.0
Chlorite	-	-	Tr.	-	-	-	-	-	-
Epidote	-	Tr.	0.6	-	-	-	-	-	0.4
Amphibole	-	-	-	-	-	-	-	-	-
Opaque	-	0.1	1.0	0.4	Tr.	-	-	0.1	0.6
Apatite	-	Tr.	Tr.	0.1	Tr.	0.1	0.4	-	0.2
Sphene	-	-	-	-	-	-	-	-	-
Allanite	-	-	Tr.	-	-	-	-	-	-
Sillimanite	Tr.	-	-	Tr.	Tr.	Tr.	Tr.	Tr.	-
% An in plagioclase	-	20	22	27	26	-	-	17	-

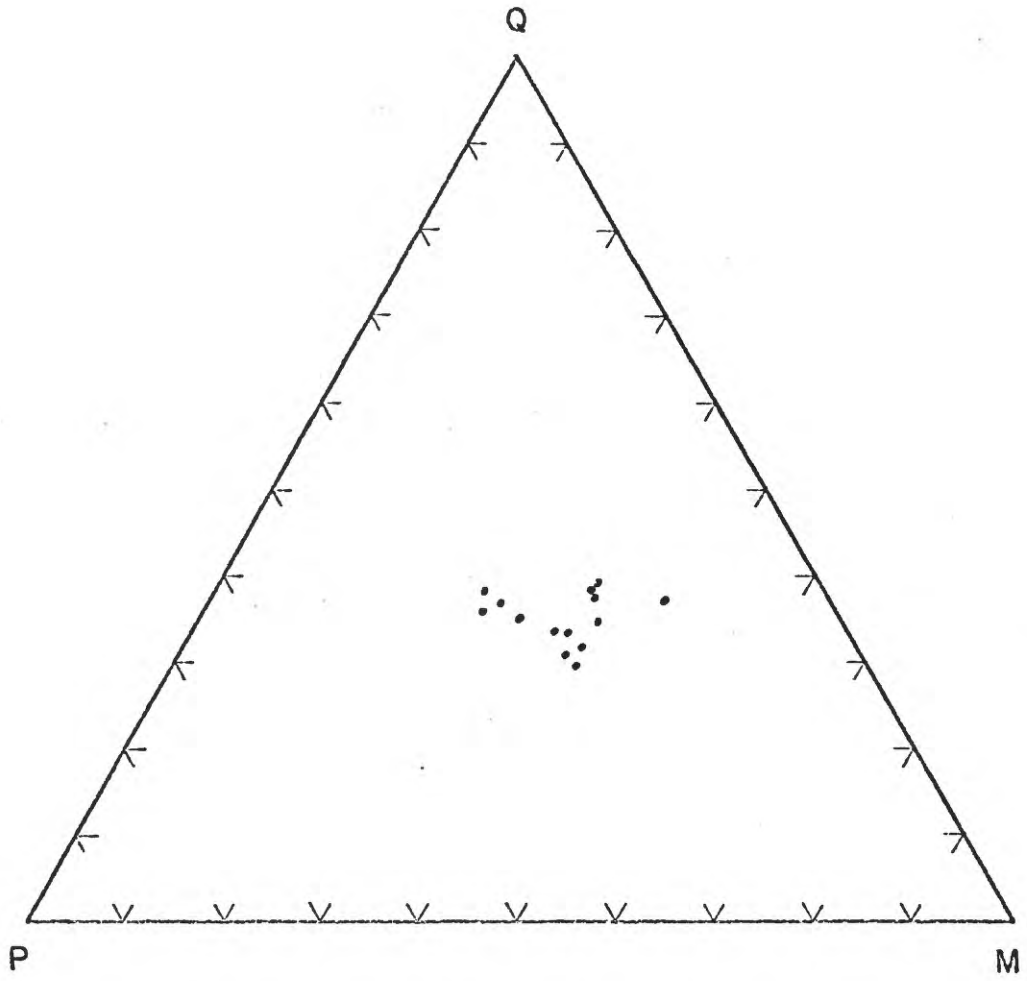

Figure 18: Ternary plot of modal analyses of quartz monzonite.

Biotite-muscovite granite (bmg)

A number of bodies of granitic rock characterized by the presence of two micas, albitic plagioclase, xenomorphic granular textures and abundant associated aplites and pegmatites are present in the northern Front Range. Although modal and normative plagioclase contents are high the plagioclase is albitic and the term biotite-muscovite granite is used. Previous work on these rocks includes that of Bucknam (1969) and Nutalaya (1966).

A small stock of reddish-tan weathering, medium-grained quartz monzonite is present just west of the Little Narrows near the center of the mapped area. The southern edge of the stock is cut by the Poudre River fault and much of the southern portion of the stock shows a shear foliation due to cataclastic deformation and recrystallization. The reddish color of the weathered rock distinguishes it from the other granitic rocks in the surrounding area. It clearly crosscuts the metamorphic wall rocks. The stock has no primary internal structure either near the stock contacts or in the center of the body. Xenoliths are rare to absent throughout the stock. Pegmatites and aplites are present in the adjacent rocks and the aplites in particular may be related to this unit. No clear cut field relationships between the Silver Plume group of intrusives and this stock were observed either in the Big Narrows quadrangle or to the south (Nutalaya, 1966).

In thin section the rock is xenomorphic to hypidiomorphic-equigranular; a fabric distinctly different from that of the various facies of the Silver Plume. Representative modal analyses are given in table 11 and plotted in figure 19; a chemical analysis is listed in table 12.

TABLE 11. Modal analyses of biotite muscovite granite

Sample	12-3-26A	12-3-34	12-3-44B	12-3-50	12-3-51	12-3-59A	12-3-59B	12-3-169A	12-3-169B
Quartz	33.4	38.4	32.7	35.0	33.7	31.0	34.0	33.1	30.8
Plagioclase	25.8	21.9	29.0	30.1	31.6	24.2	29.7	27.8	29.3
Microcline	25.2	26.8	32.8	19.7	27.0	37.6	24.3	32.2	27.5
Biotite	3.1	1.6	0.2	Tr.	0.9	1.1	7.7	2.4	2.9
Muscovite	12.5	11.3	3.5	15.2	6.0	5.4	3.9	3.5	8.6
Chlorite	-	-	-	-	-	-	Tr.	-	-
Epidote	-	-	-	-	-	-	-	-	-
Amphibole	-	-	-	-	-	-	-	-	-
Opaque	-	-	1.0	Tr.	0.8	0.7	Tr.	0.5	0.5
Apatite	-	-	-	Tr.	-	-	-	-	-
Zircon	-	-	0.1	Tr.	Tr.	-	-	-	Tr.
Sphene	-	-	-	-	-	-	-	-	-
Allanite	-	-	-	-	-	-	-	-	-
Flourite	-	-	0.7	-	-	-	-	0.5	0.4
% An in plagioclase	10	-	11	10	5	7	-	-	8

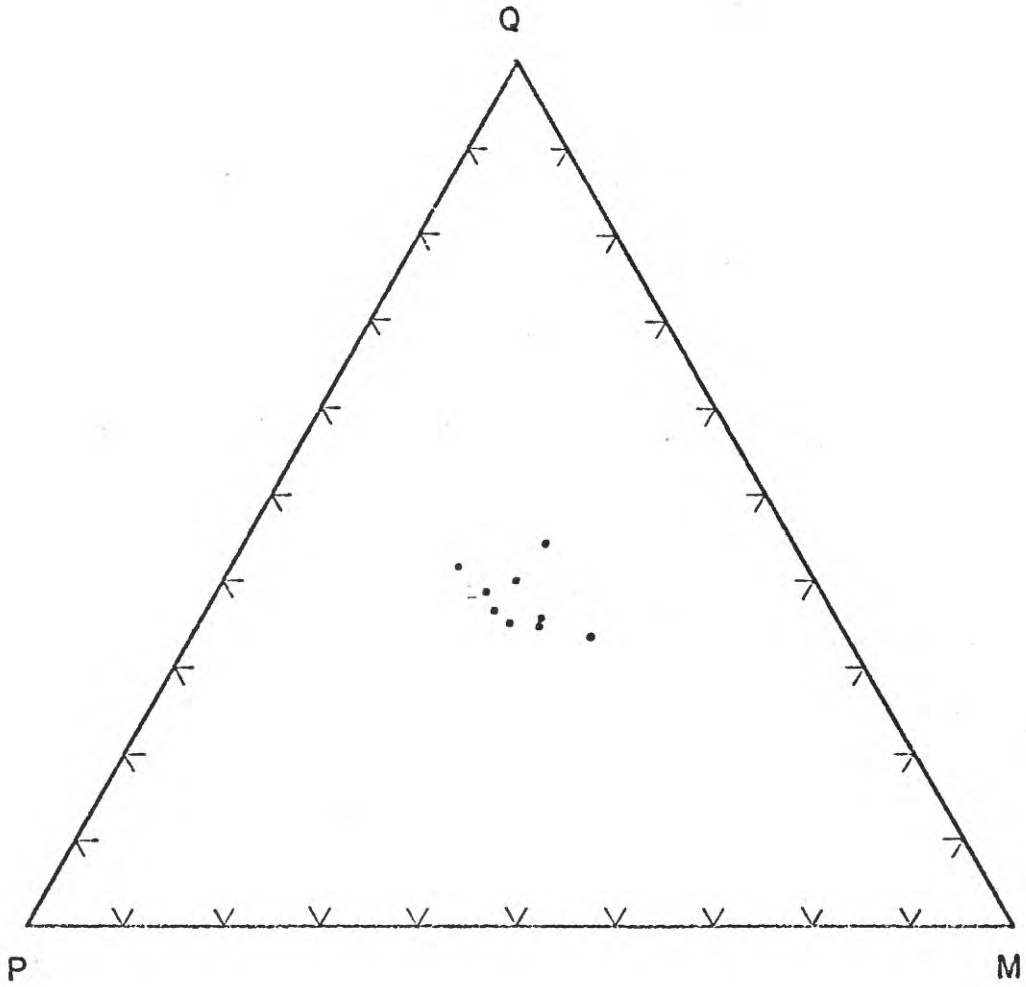

Figure 19: Ternary plot of modal analyses of biotite-muscovite granite.

Potassium feldspar occurs as anhedral grains with albite-pericline grid twinning. Although no specific structural state determinations were made it is presumed to be microcline. It is moderately perthitic and contains some quartz inclusions as anhedral rounded blebs. Plagioclase is anhedral to subhedral, polysynthetically twinned and has a mean anorthite content of An_9. The composition of the plagioclase is distinctly more albitic than that of any of the other granitic rocks in the region and compares well with the composition of the biotite-muscovite granites of the Glen Haven quadrangle to the south (Bucknam, 1969). Quartz occurs as anhedral grains showing undulatory extinction and locally sutured contacts.

Biotite content averages about 2 percent, considerably less than the other granitic rocks in the area. Considerable quantities of iron oxide are present along cleavage planes. Muscovite occurs as anhedral to subhedral plates up to 3 mm across. It is considerably more abundant than in any other granitic rock type, averaging 8 percent.

Fluorite occurs as anhedral grains, and was only recognized in this rock type. Opaque dust present in the feldspar grains is responsible for the reddish weathering color of the rock.

Aplite and pegmatite (ap,p)

Bodies of pegmatite and aplite are common throughout the area and range in size from unmappable up to plugs as much as two kilometers across. The bodies may be either conformable or notably

discordant to the structure of the enclosing rocks. The smaller conformable lenses are difficult to distinguish from the metasome in the more extensively migmatized biotite schists. Some of the conformable pegmatites are present as phacolithic bodies in the hinge regions of F_2 folds. The large irregular plugs are definitely discordant, and flat discordant sheets of pegmatite are common in the eastern part of the area.

It is clear that there are at least two ages of pegmatites, inasmuch as some of them are cut by andesite dikes while others either cut andesite dikes or cut rocks which are younger than andesites. It is probable that all older pegmatites are conformable while younger ones may be conformable or more commonly discordant. The older pegmatites and aplites are probably related to the Boulder Creek Granodiorite and/or regional migmatization while the younger are probably related to the Silver Plume Granite or the biotite-muscovite granite.

All of the units weather to a buff, cream, pink or tan color. Grain size is quite variable in most units ranging from very coarse to fine.

The aplite bodies are distinguished from the pegmatites on the basis of a more uniform equigranular, fine-to medium-grained texture and the presence of garnet; but there is complete gradation from aplite to pegmatite.

In thin section the aplites have xenomorphic-equigranular textures. Microcline appears to be as abundant or more abundant than plagioclase; it is strongly perthitic. The plagioclase is

polysynthetically twinned and slightly altered to sericite and clay. Quartz shows minor undulatory extinction. Where plagioclase is in contact with microcline, thin albitic (?) rims are present. Biotite is absent or present in minor quantities and altered to iron oxides and muscovite (?). Muscovite, which is abundant, occurs as large ragged plates and smaller equant plates. Garnet, as subhedral rounded grains, is a common accessory phase.

Adamellite porphyry dikes (adp)

A small number of adamellite porphyry dikes are present in the central and northeastern portions of the map area. They are exposed only for short distances and do not exceed a meter in width. The dikes weather to a reddish brown or gray-black color and possess a marked foliation parallel with the dike walls. The dikes were emplaced both parallel with and at an angle to the regional foliation. The feldspar phenocrysts are present as buff to reddish-colored augen.

Dikes of this type are more common to the east and Connor (1962), who termed them adamellite dikes, presents a detailed analysis of their modal and chemical composition. The term adamellite porphyry is used here to emphasize their texture and their distinction from the other quartz monzonite intrusive plutonic rocks.

In thin section these rocks possess a distinctive xenomorphic-granular groundmass with an average grain size of 0.1 - 0.2 mm. Biotite present in the groundmass has a strong preferred orientation. The "phenocrysts" of quartz, microcline and plagioclase

are subhedral to euhedral. In many cases the "phenocryst" grain boundaries appear to be interlocking with the quartz-feldspar fabric of the groundmass, suggesting recrystallization. Thin seams of fine-grained biotite and muscovite occur in the samples parallel to the prominent megascopic foliation. A weak undulatory extinction is characteristic of the quartz and feldspars in these samples. Many of these dikes have undergone cataclastic deformation and recrystallization.

Tertiary igneous rocks

Rhyolite porphyry (Trp)

A small plug of rhyolite porphyry is present near the western edge of the Big Narrows quadrangle. The plug is emplaced in quartz monzonite of the Log Cabin batholith near the southern edge of the batholith. It is apparently the easternmost of a series of small hypabyssal porphyritic intrusives of probable Tertiary age which are centered in the Manhattan district some ten miles to the west.

The unit weathers to a pale tan-white to violet-white color. On a fresh exposure it has a distinctly violet-white color. The groundmass is aphanitic and the average grain size of the phenocrysts is 0.4 cm.

In thin section it is porphyritic with phenocrysts of plagioclase, sanidine, quartz, altered amphibole, biotite and opaques (see figure 20). The groundmass is aphanitic, microfelsitic to glassy, with a suggestion of a flow banding. Most of the mineral phases are present both as angular fragments and as anhedral to euhedral grains. Quartz occurs only as anhedral to subhedral

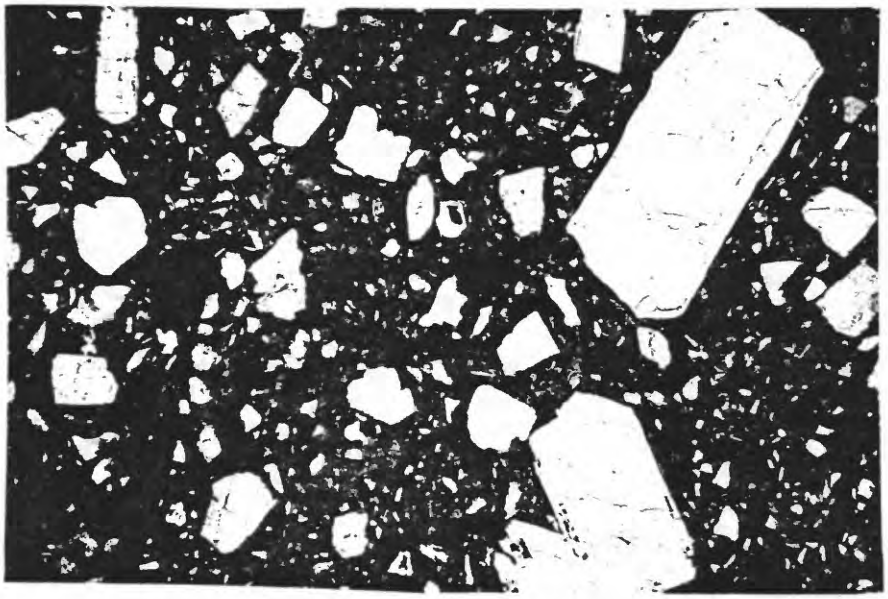

Figure 20: Photomicrograph of rhyolite porphyry showing an aphanitic, microfelsitic to glassy groundmass. Sample 12-4-74. 10X.

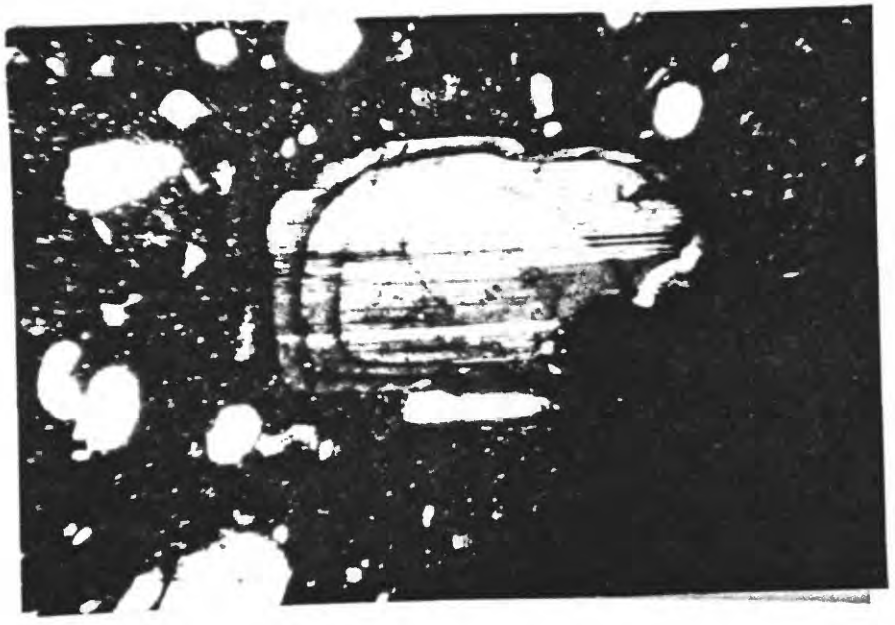

Figure 21: Photomicrograph of plagioclase in rhyolite porphyry showing rounded internal zone boundaries. Sample 12-4-74. 60X.

embayed crystals. One large phenocryst has numerous irregular patches of optically continuous plagioclase.

Plagioclase occurs as subhedral to euhedral crystals and as broken grain fragments. Grain morphology, zoning and twinnning suggests at least two distinct populations of plagioclase. A small proportion of the crystals are nearly euhedral and show rounded internal zone boundaries not parallel with the present crystal boundaries (fig. 21). Some larger grains show internal zone boundaries which closely parallel present crystal boundaries. It is not clear whether these constitute a second distinct group or whether they simply represent a gradational variant of the first group. A third group of grains are both complexely zoned and twinned.

Textures of the first group suggest an early history of crystallization and resorbtion followed by renewed crystallization. The apparent mechanical (?) rounding and fracturing of these grains and their presence in a glassy, dense matrix suggests a rapid, forceful, perhaps explosive, emplacement. The heterogeneity of the plagioclase phenocrysts suggests mixing of different rhyolite (?) magmas prior to or during emplacement.

Quartz latite porphyry dike (Tlp)

A narrow dike of quartz latite porphyry crops out near the western edge of the Big Narrows quadrangle. It has an aphanitic groundmass with phenocrysts averaging about 0.5 cm in size. It weathers to a dull gray color.

In thin section it has a microfelsitic groundmass; phenocrysts include quartz, plagioclase and amphibole. The plagioclase is commonly strongly zoned and complexly twinned. Composition of the core of the slightly zoned larger crystals showing albite and carlsbad twinning is about An_{14}. The quartz phenocrysts are strongly embayed bipyramidal quartz crystals (fig. 22). Euhedral partially altered phenocrysts of hornblende are abundant.

Accessory phases include sphene, allanite (?), and opaques in the groundmass. No potassium feldspar phenocrysts are present, however, staining suggests that potassium feldspar is present in the groundmass.

Aphanitic felsite dike (Tap)

One dike of very fine-grained pale violet-gray weathering igneous rock occurs in the west-central area. It is less than half a meter in width and exposed over a total length of about two kilometers.

In thin section the groundmass is very fine grained but appears to be rich in material with a high birefringence, possibly micas, and potassium feldspar (?) as the groundmass takes a strong yellow stain. The rare phenocrysts are subhedral to euhedral plagioclase crystals less than 0.5 mm in size.

Additional hypabyssal Tertiary (?) intrusives are known to exist to the west in the Manhattan district (Lovering and Goddard, 1950). A more detailed study of these rocks and their possible relationship with the known Tertiary volcanics in the

Figure 22: Photomicrograph of quartz latite porphyry showing corroded quartz (Q), euhedral plagioclase (P) and altered hornblende (H). Sample 12-4-92. 10X.

Cameron Pass area to the west is desirable.

Mixed rock units (iu, mu, imu)

In a few areas near the edges of the Log Cabin batholith the rocks become a heterogeneous mixture of metasediments and granitic rocks. Subdivision of these rocks into discrete units proved impractical and they have been mapped as one of three catagories of mixed rock: granitic rocks undivided (primarily Silver Plume quartz monzonite, aplites, alaskite and pegmatites), metasediments undivided (primarily quartzofeldspathic mica schist, migmatitic biotite schist and amphibolite) and igneous and metamorphic rocks undivided (including all of the above rock types).

STRUCTURAL GEOLOGY

Introduction

Previous work on the structural geology of the northern Front Range has been extensive and includes that of Braddock (1970), Bucknam (1969), Connor (1962), Gawarecki (1963), Nutalaya (1966), Swann (1962) and Wohlford (1965). Their efforts resulted in a detailed structural chronology for the area south and east of the Big Narrows area.

To the south, in the Drake and Masonville quadrangles, Gawarecki (1963) recognized abundant examples of primary sedimentary structures in the metamorphic rocks. Superimposed on this relict bedding (So) is a second S surface, a schistosity (S_1) defined by the parallelism of lepidoblastic micas (Nutalaya, 1966). In some outcrops bedding and schistosity are parallel, while in others they are at small angles to each other. A large syncline was recognized on the basis of the repetition of lithologic units and reversal of graded beds; the schistosity may be axial planar to the structure (Nutalaya, 1966, p. 30). The folding that produced this syncline is the earliest recognized deformation in the northeast Front Range.

A second and third period of deformation produced superposed folds with axial plane crenulation cleavages trending NE and NW: these are S_2 and S_3 respectively. The high-grade regional metamosphism followed the third period of deformation and has been dated as about 1.7 b.y. (Peterman and others, 1968).

Within the Big Narrows-Poudre Park area the major structural

features are macroscopic and mesoscopic folds whose axial planes are subvertical and whose axial plane traces are from ENE to E to ESE. The high grade regional metamorphism dated at about 1.7 b.y. is apparently syntectonic as are conformable, phacolithic bodies of Boulder Creek Granodiorite, also dated at about 1.7 b.y. (Peterman and others, 1968).

Problems exist in correlating this structural-metamorphic-plutonic event with the three stages of deformation recognized in the south. These folds might be correlated with F_1 in the south because of a similarity in axial plane orientation. However, this must be rejected because: (a) hinges of F_1 folds in the south are characterized by an axial plane schistosity while in the north the schistosity wraps around the hinges of the folds. (b) In the south F_1 is separated by several structural episodes from the 1.7 metamorphism whereas in the north the folding and the 1.7 metamorphism appear to be synchronous.

Alternatively the folds in the north might be correlated with F_2 in the south because of similar axial plane orientation and to a limited extent a similarity in style--ie. a crude axial plane crenulation cleavage. The axial plane orientation of the F_2 folds changes progressively north towards the Big Narrows-Poudre Park area, becoming more closely parallel with the regional foliation in that area. In addition the axial plane crenulation cleavage becomes less well developed to the north particularly within the migmatitic rocks.

A difficulty with this correlation is the apparent difference in the timing of metamorphism and deformation in the north and in

the south. In the south the F_2 deformation occurred earlier than the 1.7 b.y. metamorphism. Perhaps this difficulty can be rationalized in the following manner. Both of these areas may have undergone deformation at essentially the same time while the time of the peak intensity of metamorphism was earlier in the north than in the south. Therefore the major folds in the Big Narrows-Poudre Park area are correlated with F_2 in the south.

Only very minor evidence for F_1 structures exists in the north, particularly small isoclinal folds, but it is a distinct possibility that the major F_2 structures owe some of their complexity to superposition on older but unrecognized F_1 folds.

No folds were recognized with a consistent attitude parallel with the third period crenulation cleavage of the area to the south. A subsequent period of deformation (F_4) is, however, recognized in the Big Narrows-Poudre Park area.

Mapping was begun in the Big Narrows-Poudre Park area with this chronology in mind. Subsequent work indicated that the timing and style of deformation in the north differs from that in the south. The F_2 deformation in the Big Narrows-Poudre Park area is synchronous in age with the high-grade regional metamorphism and is not characterized by a consistent axial plane crenulation cleavage. No folds were recognized with a consistent attitude parallel with the third period crenulation cleavage of the area to the south. A subsequent period of deformation (F_4) is, however, recognized in the Big Narrows-Poudre Park area.

S-surfaces

The oldest recognizable S surface in the map area is a prominent metamorphic foliation defined by both mineralogical banding and by parallelism of micas. No primary structures were observed although graded bedding has been identified in the Buckhorn Mountain quadrangle to the south of the Poudre Park quadrangle (W.A. Braddock, personal communication, 1968).

As one progresses to the north from the Drake-Masonville area the rocks are of continually higher metamorphic grade and the recrystallization and increase in grain size obscure the relationship of bedding and schistosity previously recognized by other workers. Within the Poudre Park-Big Narrows area it is assumed that the present regional metamorphic foliation is at least subparallel to the earlier schistosity (S_1) preserved in the low-grade terrain to the south. In places the prominent lithologic layering is almost certainly parallel to original bedding. The regional foliation is referred to as S_1.

True crenulation (slip) cleavages were not recognized in the Big Narrows-Poudre Park area. However, locally, F_2 fold structures have small crinkle folds developed in the hinge regions whose axial planes are subparallel to the axial planes of the larger structures. These probably represent the incipient development of a true slip cleavage. This axial plane orientation is referred to as S_2.

No consistent axial-plane orientation comparable to S_3 of the region to the south was recognized although, locally, folds with such an orientation are present.

In the west-central part of the map area there are mesoscopic

crinkle folds that formed after regional metamorphism and in which sillimanite and biotite are deformed. The axial planes of these folds are defined as S_4. S_2 and S_4 are often subparallel and it is then difficult to distinguish between them. S_4 was only mapped where the associated crinkle folds clearly deform biotite and sillimanite. S_4 is best developed in an exposure of migmatitic biotite schist immediately adjacent to the southern edge of the Log Cabin batholith.

Cataclastic deformation of rocks within this area is widespread and a number of shear zones are present which contain large thicknesses of flaser gneiss, blastomylonite and ultramylonite. The cataclastic foliation in these rocks is termed S_5. In many cases S_5 and S_1 are parallel to sub-parallel. However, the processes which produced them are quite different.

Lineations

Four types of lineations were recognized in these rocks: fold axes, mineral streaking unrelated to cataclastic deformation, mineral streaking related to cataclastic deformation, and slickensides. The vast majority of all lineations measured were fold axes of mesoscopic folds probably related to the second period of folding, F_2, and are therefore labeled L_2 lineations. No fold axes of F_1 folds could be accurately measured. Where possible fold axes of large macroscopic F_2 structures were calculated using π diagrams (see plate 5) and are shown on plates one and three.

All mineral streaking lineations definitely unrelated to cataclastic processes are referred to as L_U lineations since it is

usually impossible to determine their specific origin. They may be relicts from the F_1 period of folding, or they may have originated during the synmetamorphic F_2 folding. In only a few instances were early (?) mineral streaking lineations clearly refolded about the hinge of an F_2 fold.

Lineations related to the cataclastic processes in the shear zones are termed L_s lineations. True slickensides distinct from L_s were observed; however, they were uncommon. Since the distribution of cataclastic textures is so widespread in this area, L_s lineations were observed well outside the large delineated shear zones. In some instances they are difficult to distinguish from L_U lineations. Locally small intrafolial folds are present within the blastomylonites with axes subparallel with L_s. These are shown separately on the map.

The paucity of lineations is remarkable. Immediately to the south multiple S surfaces and related lineations are abundant (L. LaFountain, personal communication, 1970). There appears to be a correlation between metamorphic grade and the presence of slip cleavages and lineations; this may be due to the more highly migmatitic character and increased grain size of the high-grade rocks.

Folds

F_1 structures

Small isoclinal folds of distinctive style occur locally and may be the only direct evidence to indicate an older fold period. These are small, isoclinal intrafolial folds in which the amplitude is much greater than the wavelength. They would be described as

"close" to "tight" folds in the descriptive terminology of Fleuty (1964). Examples of this type of fold are illustrated in figures 23 and 24. Their axial planes are parallel to the regional metamorphic foliation, S_1. The style of these folds is distinctively different than that of all F_2 and F_4 folds. Contrast, for example, the folds illustrated in figure 24 with those in figure 25. In all examples observed the folds were rootless, showing only one hinge with the limbs disappearing into the regional foliation. The foliation, S_1, is observed to cross the hinge of the fold in figure 24 deomonstrating that these must have formed prior, or during, the regional metamorphism (with which the F_2 deformation is correlated). For these reasons these folds are classed as F_1.

The axes of these folds appear to be steep, subparallel to the dip of S_1. It was not possible to accurately measure the attitude of these axes. Lineations related to these folds were rarely recognized. No unequivocal example of the refolding of an F_1 axial plane by an F_2 fold was found.

F_2 structures

The second period of folding probably produced the large macroscopic structures which establish the present map pattern of the major lithologic units. Folds of this period range in size from structures with amplitudes and wavelengths of a meter to structures with closures kilometers across. The variation in the style of these folds is exemplified by the variation in the style of closure in the hinge regions. This ranges from quite sharp,

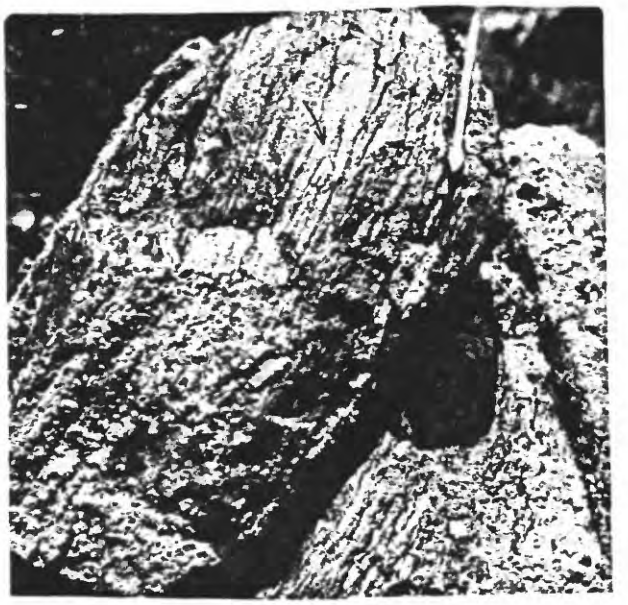

Figure 23: Isoclinal F_1 fold in quartzofeldspathic mica schist. Fold hinge indicated by arrow.

Figure 24: Isoclinal F_1 fold in migmatitic biotite schist. Fold hinge indicated by arrow. Note that biotite within hinge is parallel to S_1 and axial planar.

typical of chevron folds, to very broad and open, typical of concentric folds. The attitude of the limbs of the larger folds indicates that they are isoclinal structures. Examples of mesoscopic F_2 structures are illustrated in figures 25 and 26.

Locally the mesoscopic folds are exceedingly disharmonic with pronounced thickening in the crestal regions and thinning on the limbs. This is particularly evident in the folds developed in the migmatitic biotite schists. Those in the more massive biotite gneisses are less disharmonic. This correlation of style of deformation with rock lithology indicates that the latter has had an important role in the development of the different folds of this period in this area.

The distribution of the mesoscopic F_2 folds is too irregular to clearly establish their relationship to the macroscopic folds. In general the sense of deflection of S_1 in these folds is consistent with the larger fold geometry.

An exceptionally good example is present in the Big Narrows area where interlayered biotite gneisses in the Mt. McConnel layer of the microcline-quartz-plagioclase-biotite gneiss are folded about the main axial trace of the Little South fold structure. Drag or parasitic folds are developed on both limbs of the larger structure. See figure 25.

Large macroscopic F_2 structures are developed throughout the mapped area. Plate 4 is an index sheet which shows the location and the name of these structures. It also shows the subareas from which the structural data was compiled and the names of the large shear-zone and fault structures.

Figure 25: Mesoscopic F_2 folds developed in the southeast limb of the Little South antiform. Hammer in foreground gives scale.

Figure 26: Mesoscopic F_2 chevron fold developed in quartzofeldspathic mica schist.

The Poverty Flats, Diamond Rock and Sheets folds are all synformal structures. The Little South, Little Narrows, and Pendergrass folds are antiformal structures. The Dutch George, Lookout Mine and Falls Gulch fold complexes are areas of more complicated macroscopic F_2 structures. The Mishawaka and Pamige Ranch structures are very poorly defined.

Plate 3 is a generalized foliation map illustrating the form and trend of the macroscopic F_2 folds, the regional foliation S_1 and other structural elements. Specific subareas of the geologic map were chosen on the basis of the distribution of these structures for detailed analysis using π diagram techniques. All of the π diagrams are lower hemisphere projections showing the distributions of poles to S_1 and selected data for associated lineations, L_2, L_U, from the subareas. These π diagrams are all illustrated on plate 5.

A number of the subareas will be discussed in detail because they illustrate the geometry of the F_2 folding.

Subarea (2) includes the Dutch George fold complex which consists of an antiform and a synform whose axial traces trend E to ENE. These are disharmonic structures with a style transitional between that of parallel and similar folds. The nature of the hinge region of the synform changes progressively along the axial trace from open to tight. The subarea (2) plot shows a moderately well defined π axis. Related L_2 and L_U data are also plotted and these coincide in general with the axis. The scatter of the linear data and the form of the S_1 surfaces suggest that the axes of these structures are not uniform in orientation and that they possibly

flatten to the west. The folds are non-cylindroidal on the largest scale. The π concentrations further suggest that the folding is more similar than parallel in style. The axial plane orientations are subvertical.

Subareas (3), (4) and (9) comprise the area occupied by the Little South structure, a doubly plunging antiformal structure whose axial trace trends NE and whose axial plane is probably inclined very steeply to the NW. The π diagrams contribute little to the overall picture for two reasons. The axis of this fold appears to change attitude very abruptly at both ends, steepening rapidly over a very short distance to a subvertical, or even inverted, orientation. The fold is developed in a microcline-quartz-plagioclase-biotite gneiss where the foliation is locally poorly defined and locally overturned. However the outcrop pattern clearly indicates that this structure closes both to the NE and the SW and the near vertical attitude of S_1 in these areas indicates that the axis of the Little South fold must be vertical. Unfortunately lineations of any kind are very rare within this unit; those available are plotted.

Subareas (5), (6) and (7) contain a number of structures plunging steeply to the northeast, of which the largest is the Poverty Flats fold. This synformal structure is separated from the Little South antiform by the Pendergrass antiform and a very tight unnamed synform. Exposure in this critical region is poor due to the generally north facing slopes.

Subarea (5) contains the Pendergrass fold structure, an antiformal non-planar, noncylindroidal steeply plunging structure

analogous in many ways to the synformal structure in subarea (2). This structure also shows the progressive change in form of the hinge region from very open to very tight. Lineations of any kind are rare except near the NE end of the structure where it has become highly elongated. Zones of mylonitic rock are developed parallel with the axial trace of this structure and the adjacent Little South structure and subvertical streaking lineations are present on these surfaces. The S_1 data plot confirms the existence of a steeply plunging fold but contributes no other pertinent information.

Subarea (6) contains the Poverty Flats fold structure, a steeply plunging synformal structure. This fold is probably structurally quite similar to the Pendergrass antiform although the hinge region is not quite as sharp. The π diagram gives a fairly well-defined π axis. Scattered throughout this area are rare mesoscopic folds with orientations compatible with the larger structure. The available L_2 and L_U data correspond well with the calculated π axis. However, as in the subarea (2) data, there is a tendency for these to have an elongated pattern on the plot suggesting a progressive change in the plunge of the axis of the Poverty Flats fold.

Subarea (7) contains the Lookout Mine fold complex; an antiform-synform pair with axial surfaces trending NNE and with axes plunging to the NE. These folds are developed on a smaller scale than the other macroscopic F_2 structures and are transitional between the macroscopic and mesoscopic F_2 folds. They do not appear to be doubly plunging structures and they have a consistent axial

trace orientation. Perhaps these structures are closely related to the larger Poverty Flats fold to the west and represent minor wrinkles on the bottom of that structure.

The Sheets fold (subarea 11 and 12) is a doubly plunging canoe-shaped fold whose axis probably steepens abruptly at both ends. The Diamond Rock synform (subarea 17 and 18) is bounded on the west by the Skin Gulch shear zone; its extension to the east is obscured by the effects of later faulting. It is possible that the large body of Boulder Creek Granodiorite may occupy the core of the fold in that region. The exposed geometry of the fold suggests that the hinge may be subhorizontal in the central part of the structure and steeply incline in the west. The available L_2 and L_U data are compatible with this observation. The π diagram shows a moderately well defined π axis for the western closure of the structure. The adjacent Little Narrows antiform (subarea 16) is similar to the subarea (2) structures and the Pendergrass fold in the regular change in form of the hinge region from very open to very tight with the axial trace eventually becoming subparallel to the regional foliation S_1. The orientation of the axial traces of the Diamond Rock and Little Narrows folds and their associated lineations suggests that the axial planes of these folds are inclined to the NNE.

The Falls Gulch fold complex (subarea 14) is important for three reasons. It is one of the better exposed small F_2 fold complexes. Phacolithic bodies of older (?) pegmatite are present in the hinge region. Lastly, the axial traces trend WNW-ESE which is different from that of the western fold structures but similar

to those to the east (W.A. Braddock, 1970, personal communication).

The fold axes plunge almost due east, and the axial planes dip to the northeast. The northeastern limbs of the synform and the southwestern limb of the antiform are locally overturned. The diagram shows both a well defined π axis and two π maxima corresponding to the limbs of the folds.

In the southern part of subarea 13 a large F_2 structure, the Pamige Ranch fold, may be present. In the core of what might be an isoclinal structure with a subhorizontal axis and an E-W axial trace are mesoscopic F_2 folds with a very open geometry and subhorizontal axes. If present the structure is cut off to the west by the Stove Prarie fault and no closure to the east is recognizable. Presumably this structure, like many of the other large F_2 folds, closes up tightly into the regional foliation.

The data from the preceeding group of subareas have some important common features. The majority of these folds show progressive changes in orientation of their axes (this is not well documented for the Pendergrass fold). The different axial planes complexely fan out to the SW and converge to the NE where they are subparallel. The folds developed in the migmatitic biotite schists and clinozoisite biotite schist show a progressive change in thickness perpendicular to their axial planes and paralleling this change there is a pronounced change in style of the hinge regions from very open to tight (this is not apparent in the Little South fold). There appears to be a correlation between rock lithology and response to deformation. The biotite schists behaved differently than the microcline gneiss.

Ramsay (1962) has proposed a mechanism for the development of similar type folds based on a process of differential flattening. It is possible that such a mechanism was responsible for the formation of the F_2 folds in the Big Narrows area.

Assume a rectangular parallelopiped with its long axis parallel to b and horizontal and the a axis is vertical where a, b and c are kinematic symmetry axes (Ramsay, 1967, p. 333). If this solid is deformed by differential flattening in the plane ab then the resulting folds will have the following geometry (Ramsay, 1962, p. 325):

1) The folds will have varying amplitudes and wavelengths parallel to both a and b.

2) The axes will vary as a function of the degree of flattening.

3) Where the rate of change of flattening in the ab plane is zero the fold axes will be parallel to b.

4) Axes of adjacent folds will only be parallel where the rate of change of the flattening is zero.

5) Axial planes will have a fan-shaped geometry approaching parallelism only at maximum flattening.

Comparing these results with the geometry of the Big Narrows structures one finds the similarities striking. Progressive changes in both axial plane and axis orientation are observed.

An important characteristic of these rocks which may support this thesis is the common occurrence of thin shear (slip) surfaces in the microcline gneiss subparallel with the axial plane of the Little South fold. In addition a narrow but distinctive zone of mylonitic gneiss is present parallel with the axial plane of the

Pendergrass fold near where it appears to pinch out in the southwest quarter of section 15. Such textures might have developed during deformation when shear was taking place parallel to the vertical ab plane. However, the age of these textures is a critical problem because mylonites from the Skin Gulch shear zone have an age of 1.2 b.y., considerably younger than the postulated age of the F_2 folding.

The available data are insufficient to demonstrate an origin for F_2 folds by differential flattening. An alternative to this hypothesis is that these structures may be the product of superposed folding. Ramsay (1967, p. 520) has discussed in detail the types of patterns which may result from the interference of successive folding and a systematic variation in fold geometry is an important result. It is possible that these macroscopic doubly plunging structures are the result of superposition of F_2 folds on F_1 folds.

Other examples of macroscopic doubly plunging structures exist in the northern Front Range (W.A. Braddock, 1970, personal communication) but as yet no consistent pattern has emerged which would permit systematic analysis of their relationship. The mechanism of this second period refolding is essentially unknown. The presence of both mesoscopic chevron and parallel folds suggests that flexural slip processes may have been of some importance.

Metamorphic recrystallization during the second period of deformation produced sillimanite needles parallel to F_2 fold axes and shingled biotite grains around F_2 fold hinges. Second-period deformation was syn-high grade metamorphism not pre-high grade metamorphism as in the area to the south (Braddock, 1970, p. 589).

In a number of probable F_2 mesoscopic folds in knotted mica schist, the knots are parallel to the axial planes (S_2). In other folds the knots are parallel to S_1. If many of the F_2 folds were produced by shear parallel to the axial plane then those folds with knots lying in S_2 are probably F_2 with the knots forming during synkinematic recrystallization. Those folds with knots lying in S_1 are possibly F_4 folds, or F_2 folds produced by flexural slip processes (facilitating recrystallization in S_1), or F_2 folds formed at a time slightly subsequent to the high-grade regional metamorphism.

The Sheets, Mishawaka, Little Narrows and Diamond Rock folds all have phacolithic bodies of Boulder Creek Granodiorite in the fold hinge regions. The gneissic foliation in the granodiorite is parallel to the foliation in the adjacent amphibolite or biotite schist suggesting synkinematic emplacement. This observation is of primary importance in establishing a relative chronology for Precambrian events in this area.

In summary the macroscopic fold structures of the Big Narrows-Poudre Park area are believed to be primarily of F_2 age, contemporaneous with the regional metamorphism and Boulder Creek plutonism. The original nucleus of some of these structures, particularly the Little South fold, may have developed during F_1 deformation, and been later modified during F_2 deformation.

The distinctive doubly plunging structures may have originated either by a process of differential flattening or the superposition of folds, possibly F_2 on F_1. At least some of the F_2 structures were generated by flexural slip processes.

F_4 structures

In the central and western parts of the Big Narrows quadrangle and more rarely within the western part of the Poudre Park quadrangle occasional mesoscopic crinkle folds are developed. These are small folds with amplitudes and wavelengths ranging from a few mm to a few cm (fig. 27 and 28). Usually they occur in the hinge regions of larger mesoscopic folds and the axial planes of both the small and the large folds are subparallel. They are only present in the mica-rich schists, particularly the migmatitic biotite schist unit.

In thin section in these small crinkle folds the micas are clearly bent and kinked and the sillimanite deformed. The kink bands are subparallel to the axial plane of the crinkle folds although locally their orientation may be much more irregular (fig. 29, 30 and 31).

To the south of the Poudre Park-Big Narrows area folds of this style and apparent age are absent. There, the porphyroblastic minerals of the high-grade regional metamorphism postdate all of the folding episodes. In the north biotite and sillimanite produced during the regional metamorphism are deformed in small folds which probably represent a previously unrecognized period of deformation which is here defined as F_4.

It is quite difficult to determine the orientation of the axes of these structures due to their small size. Consequently, only their axial planes were measured in the field. Figures 32 and 33 are projections of poles to S_4. In both cases there are excellent maxima indicating a strong preferred orientation which is about E-W to WNW and subvertical.

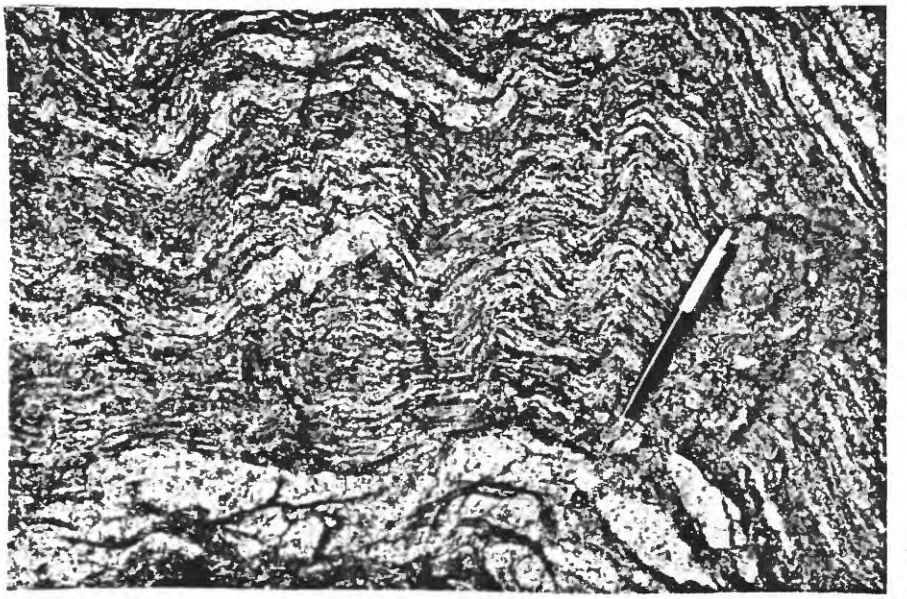

Figure 27: F_4 fold in migmatitic biotite schist. Note deformation of metasome lenses.

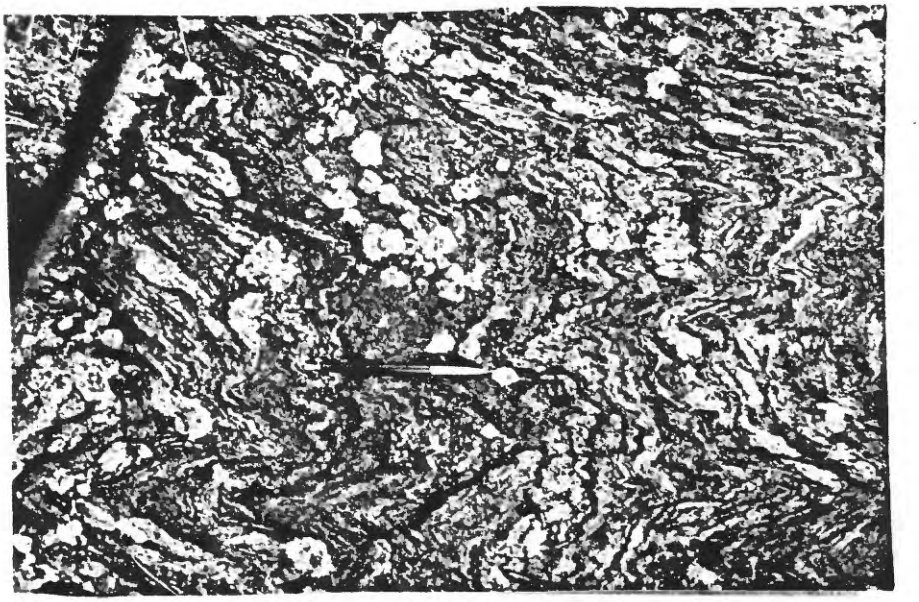

Figure 28: F_4 fold in migmatitic biotite schist. Note deformation of metasome lenses.

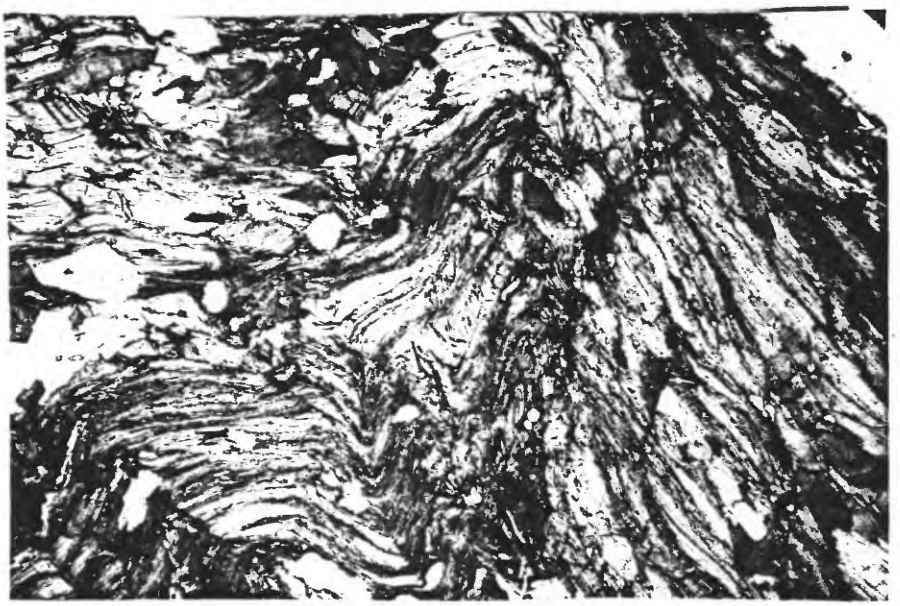

Figure 29: Photomicrograph of F_4 fold hinge in migmatitic biotite schist illustrating the deformation of the biotite in S_1. Sample 12-4-71. 9X. Uncrossed nicols.

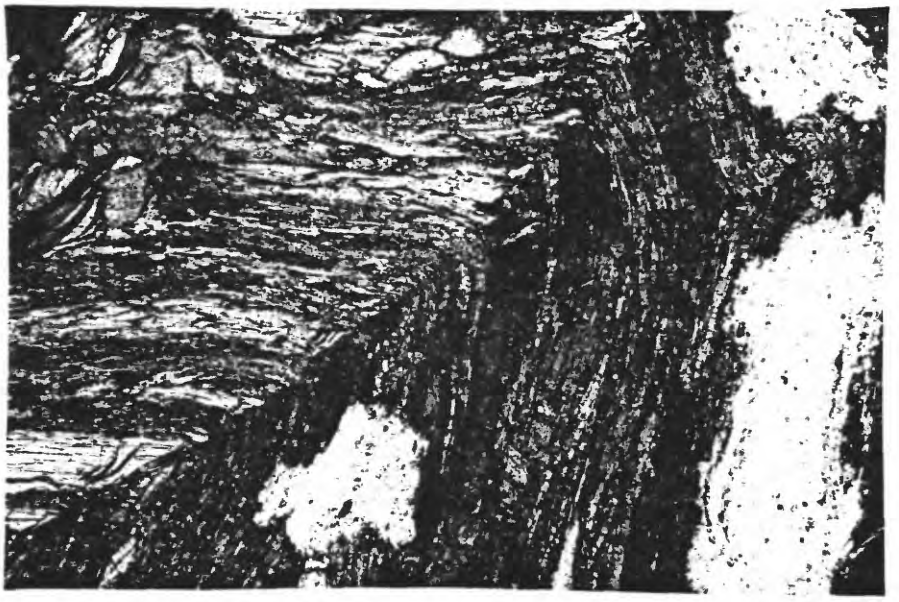

Figure 30: Photomicrograph of kinked biotite and deformed sillimanite within a F_4 fold hinge. Sample 12-4-71. Uncrossed nicols. 46X.

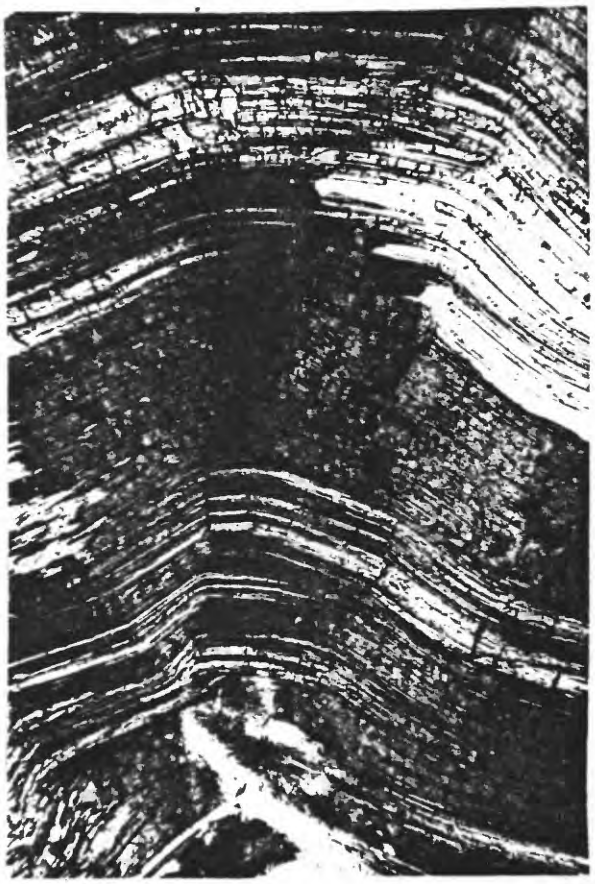

Figure 31: Photomicrograph of deformed sillimanite in kink-banded biotite in an F_4 fold. Sample 4-6-6A. Uncrossed nicols. 200X.

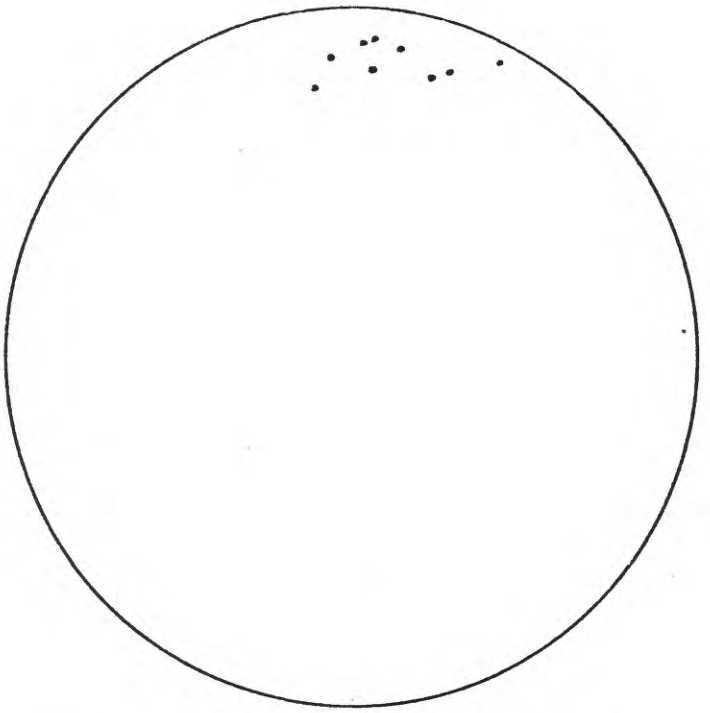

Figure 32: Poles to S_4. Subarea 2a

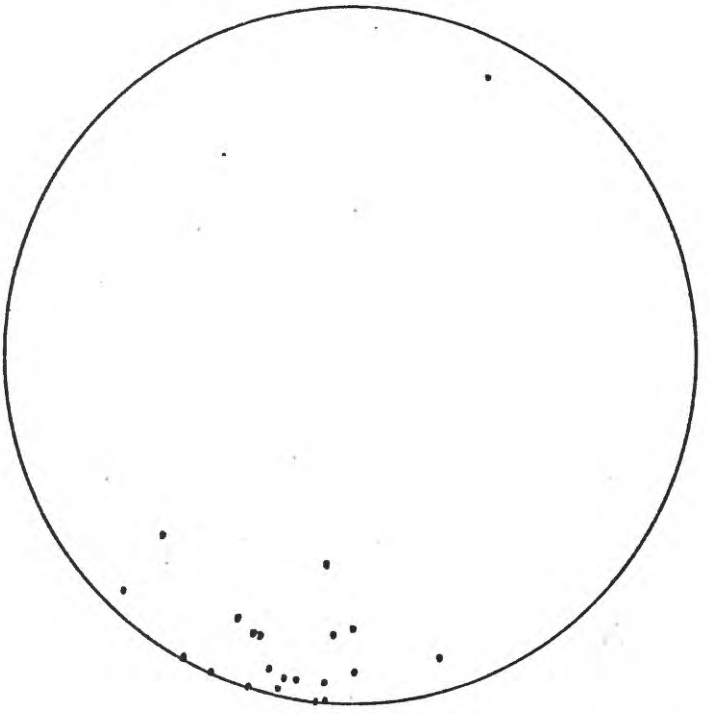

Figure 33: Poles to S_4. Subareas 3, 5, 6

Figure 34 is a projection of all available linear data attributable to F_4 folds in subarea two. Clearly there is considerable scatter suggesting either that the F_4 folding was non-cylindrical or that due to the orientation of the early fold limbs the F_4 fold axes have a low "axial direction stability". Too little is known of the geometry of the F_2 folds in this area to distinguish between these alternatives.

It is possible that F_4 folding does not represent a distinct period of deformation, but simply represents an extension of F_2 folding past the peak of regional metamorphism. The present author's opinion, however, is that these folds are related to the emplacement of the Log Cabin batholith, the southern boundary of which trends generally E-W in this area. During emplacement it may have exerted a N-S compressional stress on the rocks to the south.

Much of the mapped area consists of homoclinally dipping metasediments trending NE to E-W, so oriented that a weak compressive N-S stress might have little effect. However, wherever mesoscopic F_2 folds are present with nearly E-W trends the mesoscopic F_2 folds might close up and new F_4 folds might be developed in the hinge regions of the macroscopic folds. Crinkle folds would tend to be restricted to the hinge regions of these folds because here the micas and the foliation would be subparallel to the maximum compressive stress.

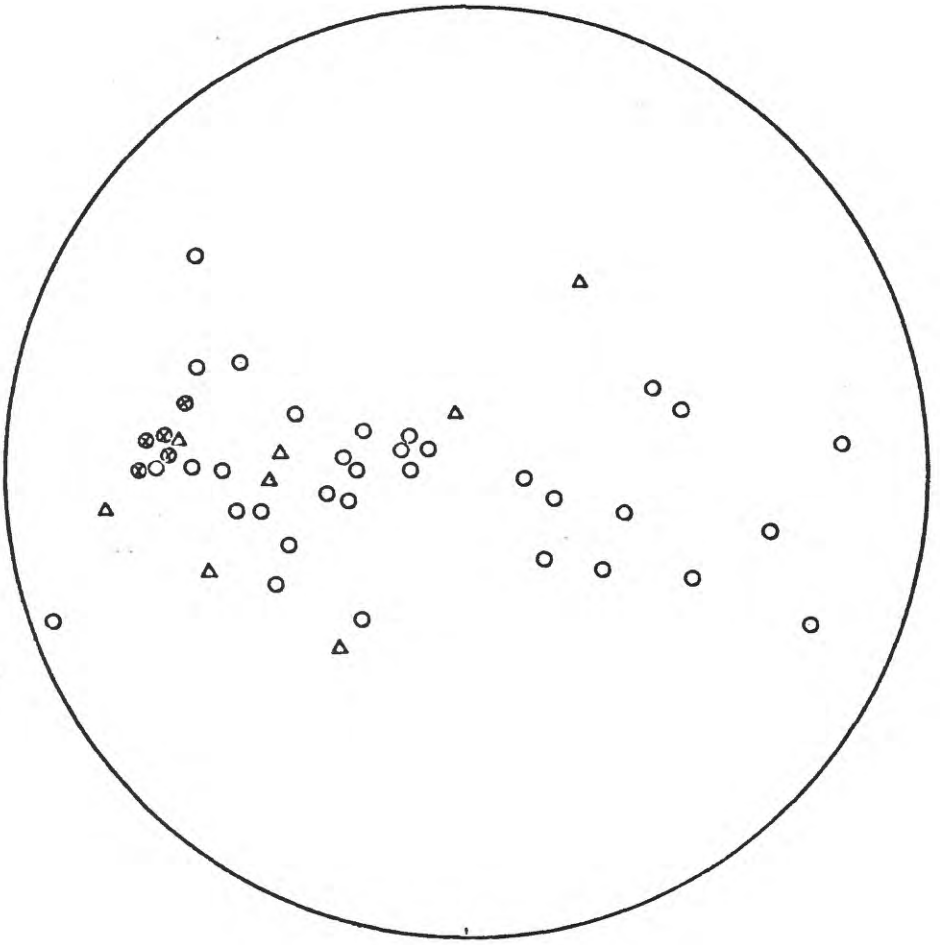

Figure 34: Fold axes and mineral streaking lineations from subarea 2a. It is difficult to distinguish L_2 from L_4. The following symbols are used:

- ○ L_2 or L_4
- ⊗ L_4
- △ Mineral streaking linear

Faults

Introduction

Throughout the Poudre Park-Big Narrows area there are numerous shear zones varying in width from a few centimeters to hundreds of meters. The nature of these shear zones is highly variable. They range from zones of massive, resistant ultramylonite to extensively fractured and altered fault breccia. Zones characterized primarily by mylonitic textures are referred to as shear zones and those by fault breccia and gouge as fault zones.

The shear zones trend NNE to ENE, the younger fault zones have N-S and E-W trends. The larger fault zones have associated strong topographic anomalies. The majority of the shear zones are steeply dipping, but a group in the west and north central portions of the area has a low dip to the northwest.

Evidence for weak cataclasis, although subtle, is widespread and the limits of the larger shear zones are quite gradational. A strong streaking lineation, L_s, is occasionally associated with the mylonitic rocks. The fault zones are prominent because of extensive red and yellow secondary hydrous iron oxides present in the zones.

Four (?) periods of shearing and faulting have been recognized ranging in age from middle Proterozoic to Tertiary. A detailed discussion of the isotopic evidence for the age of the initial period of shearing is presented in a following section.

Mylonitization

The earliest period of shearing produced extensive zones of flaser gneiss, augen gneiss, phyllonite, blastomylonite and ultramylonite. With minor emendations the terminology used in this report is that of Christie (1960). The terminology problem has been discussed at some length by numerous authors (see for example Christie, 1963; Hsu, 1955; Theodore, 1970; Watanabe, 1965). Recently, Dalziel and Bailey (1968) have proposed restricting the use of the term mylonite and using "mylonitic rock" as the descriptive term for all rocks with textures of varying degree of cataclasis and recrystallization but which are fine grained and well laminated. This useage has been adopted and accordingly all phyllonites, blastomylonites and ultramylonites are called mylonitic rocks. Flaser gneiss and augen gneiss are coarser-grained rocks with thin anastomosing seams of fine grained quartz, feldspar and secondary mica which are commonly derived from quartzofeldspathic meta-igneous and metasedimentary rocks. The augen gneisses, which grade into blastomylonites, have a higher proportion of fine-grained material and distinctive porphyroclasts of feldspar and quartz. It is often impossible to distinguish between relict microcline porphyroclasts and microcline "porphyroblasts" produced by recrystallization in the blastomylonites.

The largest NE-trending shear zone, the Skin Gulch shear zone, has a minimum exposed width of three meters and a maximum exposed width of approximately 400 meters. The dominant rock types affected by the shearing are biotite schists and gneisses. Subordinate amounts of pegmatite, amphibolite and quartz monzonite

are present. Within the zone are numerous well-laminated, multicolored bands of blastomylonite and ultramylonite up to a few meters across. Textures in the intervening portion of the shear zone range from near-mylonitic to those typical in the unsheared rock. Commonly, interlayered pegmatite most clearly shows the effects of cataclasis and recrystallization whereas the amphibolitic rocks only rarely show any macroscopic effects related to the shearing.

Within the limits of the Skin Gulch shear zone a number of folds of varying styles are developed ranging from mesoscopic chevron folds to microscopic isoclinal intrafolial folds. These fold structures are the products of the deformation which produced the cataclastic textures and recrystallization fabrics within the shear zones. Examples of some of these structures are shown in figures 35-40. The axial planes of the folds are parallel to the Skin Gulch shear zone and the well-developed shear foliation in the more intensely deformed blastomylonites and ultramylonites. The axial planes of these folds and the parallel shear foliation are termed S_5.

In the less-intensely deformed quartzofeldspathic schists irregular disharmonic folds are present which deform the pre-existing biotite. Associated quartz and feldspar show strong undulatory extinction. The elliptical quartz grains are flattened and elongated within the limbs of the early chevron folds parallel with the shear foliation S_5. There is abundant evidence of re-crystallization (polygonization) along quartz grain boundaries.

In the less-intensely deformed mica-rich units crenulation

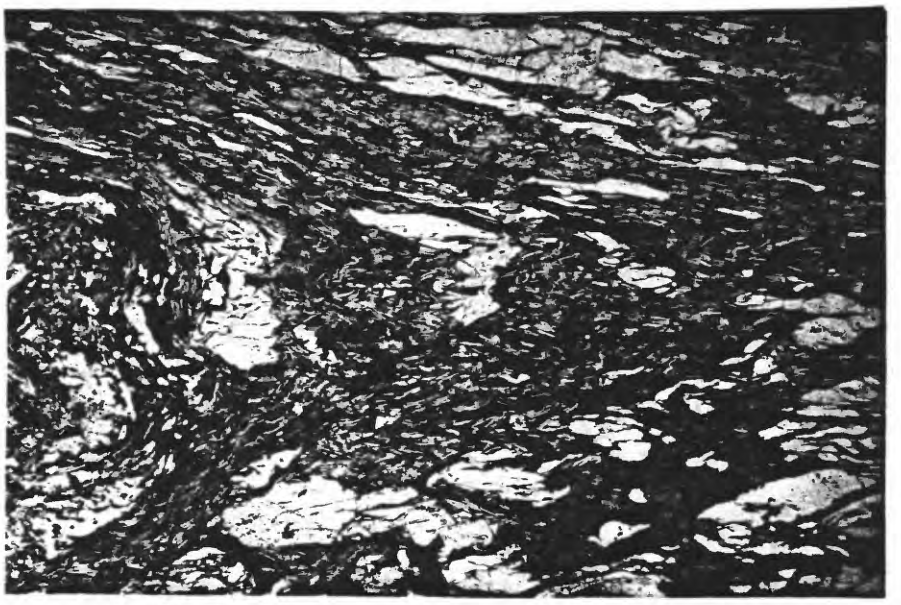

Figure 35: Photomicrograph of a disharmonic fold in a flaser gneiss. Note deformation of micas and quartz (Q). Sample 12-5-61G. Nicols uncrossed. 9X.

Figure 36: Photomicrograph of highly strained quartz fabric showing elongation of grains and sutured contacts. Sample 12-3-19D. Nicols crossed. 32X.

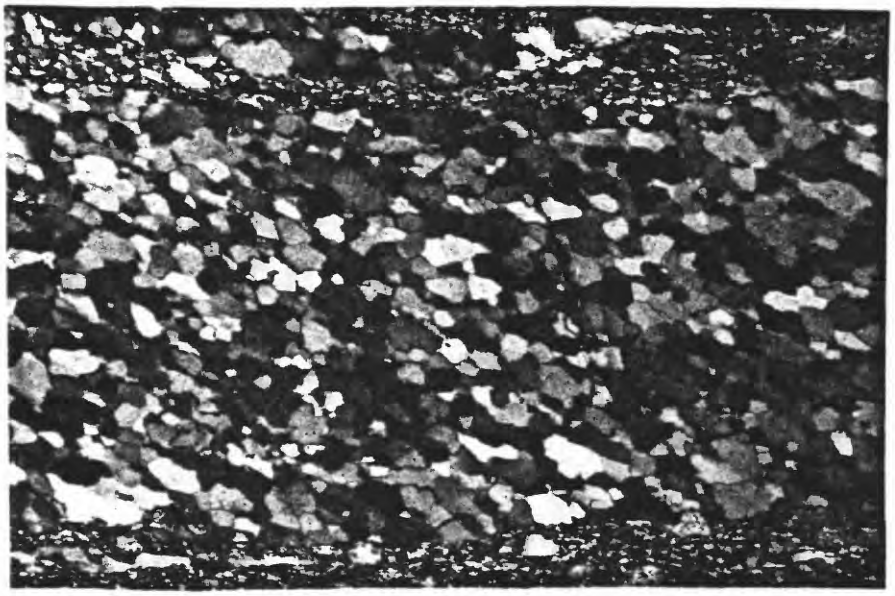

Figure 37: Photomicrograph of quartz fabric showing nearly complete recrystallization (polygonization). Sample 4-2-31B. Nicols crossed. 45X.

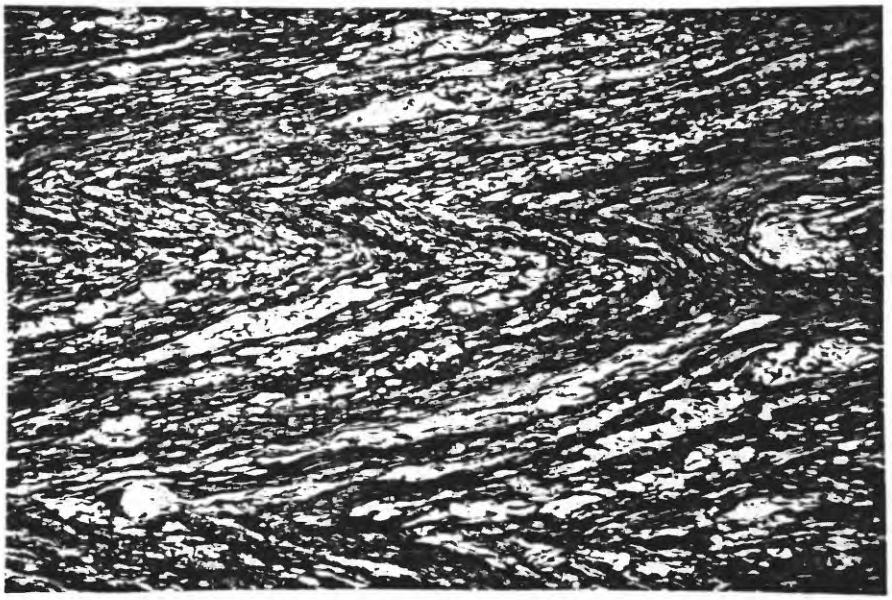

Figure 38: Photomicrograph of a chevron fold in phyllonite. Sample 12-5-61G. Nicols uncrossed. 9X.

Figure 39: Photomicrograph of blastomylonite-ultramylonite with extremely sheared out intrafolial fold hinges. Trace of S_1 (?) and S_5 are shown. Sample 12-5-58A. Nicols uncrossed. 9X.

Figure 40: Photomicrograph of blastomylonite-ultramylonite with intrafolial folds. Quartz within the fold hinges has completely recrystallized. Sample 12-5-68D. Nicols uncrossed. 9X.

folds with very tight hinge regions, locally true chevron folds, are present (fig. 38). Since these are slightly disharmonic and no detailed study of their geometry was carried out it is unclear whether they are really parallel or similar folds. The new lepidoblastic mica fabric indicates that extensive recrystallization was associated with the development of these folds: these are typical phyllonites. The lepidoblastic muscovite is bent and kinked indicating that recrystallization and deformation overlapped in time.

In the more-intensely deformed and recrystallized zones of blastomylonite and ultramylonite where tight intrafolial folds are found a prominent streaking linear is sometimes present. Too few folds of this type were observed to definitely establish the relationship between the streaking linear and the axes of the folds. No detailed petrofabric analyses were carried out to establish the orientation of the quartz and mica relative to the streaking linear.

These fold structures are correlated with this period of deformation for a number of reasons. The quartz, feldspar and mica subfabric is the product of a pervasive strain and recrystallization and has no counterpart outside the shear zone. It must have resulted from a thermal metamorphism associated with and presumably generated by the intense strain within this narrow zone.

In the Idaho Springs-Central City area of the Central Front Range detailed mapping by Moench and others (1962) established the existence of two phases of deformation. The younger deformation produced "terrace, monoclinal and chevron..." folds and was related

to a cataclastic deformation which produced a major northeast-trending shear zone--the Idaho Springs-Ralston shear zone. This zone has also been mapped in detail by Sheridan and others (1967) in the Ralston Buttes district; however, no folds similar to those recognized by Moench and others are reported.

The chevron folds recognized in the Skin Gulch shear zone and the folds in the Idaho Springs-Ralston shear zone are quite similar. The parallel trend of these two shear zones and their structural and textural similarities strongly suggests that they were produced by similar processes at similar times.

Intensive shearing and recrystallization produced the structures pictured in figures 35 and 36. The fold hinges (intrafolial folds) preserved in the very fine groundmass are presumed to be relicts of folds produced during earlier less-intense phases of the deformation. The average grain size of these rocks is less than 0.01 mm.

Figure 41 is a projection of the available data on the orientations of the streaking lineations (L_s) and clearly indicates the steep attitudes of these lineations. A small number of measurements of the fold axes (L_5) suggests that they may plunge 30 to 40° to the northeast. To the south in the Idaho Springs-Ralston shear zone the axes of the folds related to the younger cataclastic deformation are at a high angle to the prominent streaking lineations (Moench and others, 1962). If the Skin Gulch shear zone resulted from similar processes the same relationship between lineations may also hold.

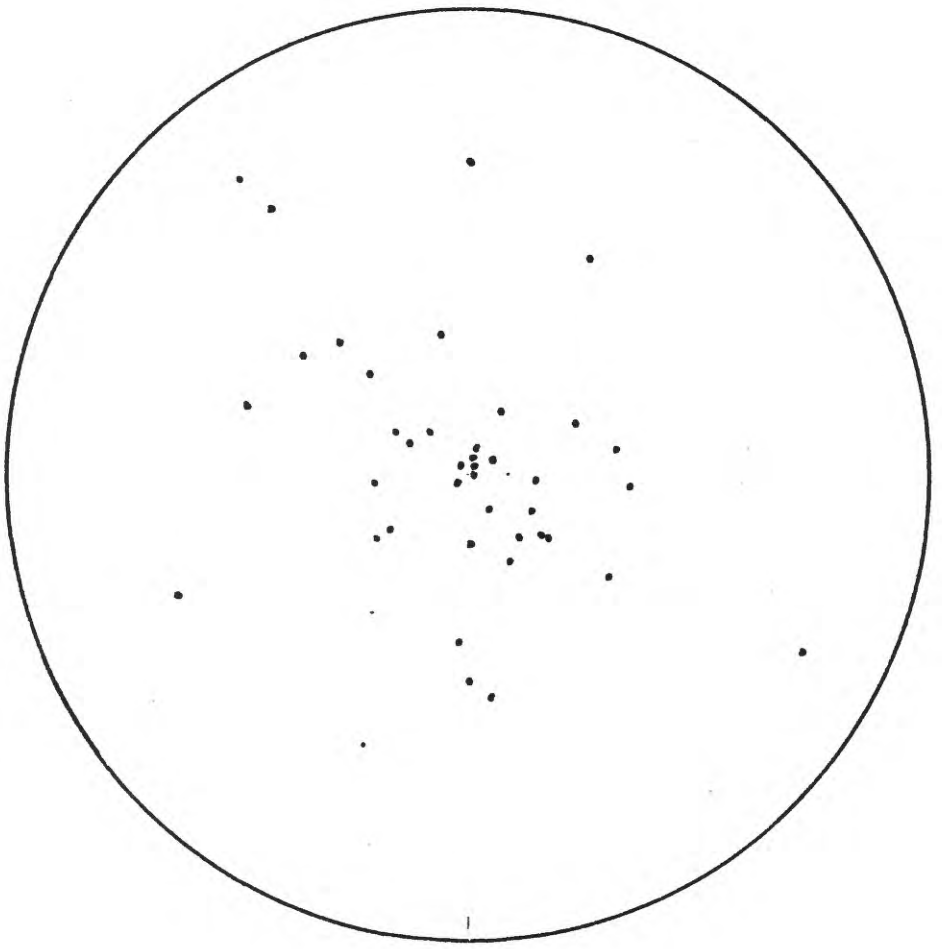

Figure 41: Cataclastic streaking lineations, L_s from the Skin Gulch shear zone and adjacent area

In classical analyses of deformed tectonites fold axes are termed b lineations and associated mineral streaking lineations (usually normal to b) are termed a. The related folds were thought to be the product of flexural slip and shear folding with movement taking place parallel with the steep streaking lineation.

Other major zones of dislocation in the earth's crust with abundant development of "mylonitic" textures include the Moine thrust (Christie, 1963), the Grenville front (Dalziel and Bailey, 1968) and the Brevard zone (Reed and Bryant, 1964; Reed, 1970). In both the Moine and Grenville zones intrafolial folds are present with their axes parallel to a steep, down-dip streaking lineation. Within the Brevard zone in the Grandfather mountain area the prominent streaking lineation is subhorizontal, parallel to the trend of the shear zone. The analysis of movement within the Brevard zone is complicated by the Linville Falls fault, a typical Appalachian thrust fault. The latest synthesis of the data suggests that movement took place simultaneously in both of these structures with a net diagonal slip component to the northwest (Reed, 1970, personal communication). Movement along the Brevard zone itself was predominantly strike-slip. Thus it appears that the lineation is parallel to the direction of tectonic transport.

There is some disagreement over the significance of the lineation in the Moine thrust. Christie (1963) suggests that the folds are flexural slip folds, that the sense of displacement is strike-slip and that the lineation is not a true a lineation in the direction of tectonic transport. Johnson (1965) believes that strike-slip displacement remains unproven and postulates an origin

by progressive flattening for most mylonitic zones.

Dalziel and Bailey (1968) after a detailed analysis of deformed garnets concluded that the mylonitic rocks within the Grenville front were deformed by a flattening process with extension parallel to the streaking lineation. The importance of flattening in the deformation process is emphasized by the common observation of an orthorhombic fabric developed within the mylonitic rocks (Christie, 1963; Dalziel and Bailey, 1968); however, the relationship of the flexural slip or shear folds to this movement picture remains unclear.

Within the Skin Gulch shear zone the textures, fold structures and lineations are assumed to be related. By analogy with other major shear zones the mylonitization within the Skin Gulch shear zone took place by progressive flattening with the maximum compression normal to the plane of shear (S_5). L_s lies in S_5, and may represent the direction of maximum elongation. There is no evidence of large-scale strike-slip displacement.

Brittle fracture

Subsequent to the mylonitization two (?) periods of brittle fracture resulted in the development of healed fault breccias.

Locally the early mylonites are strongly fractured and the fractures filled with quartz or quartz plus epidote (fig. 42). Movement during this event involved considerable dilation of the wall rocks since evidence for open-space filling is present (fig. 43). The quartz gangue is locally developed in layers more than a meter thick and forms prominent resistant ridges similar to the

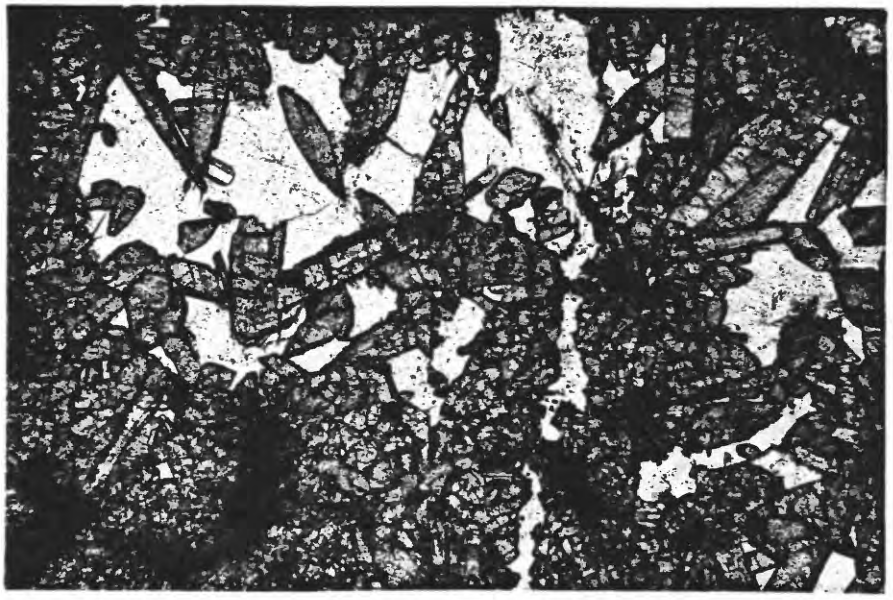

Figure 42: Photomicrograph of quartz and epidote gangue filling fractures in brecciated mylonite. Sample 12-3-23B. Nicols uncrossed. 36X.

Figure 43: Photomicrograph of quartz gangue showing outlines of quartz crystals suggesting growth in open fractures. Sample 12-5-73. Nicols crossed. 45X.

breccia reefs of the central Front Range.

Where healed fault breccias of this type were developed in blastomylonite and ultramylonite and the matrix is partly mylonitic rock flour, the resultant rock is kakirite in Christies' (1960) terminology (fig. 44, 45). These shear zones, the Skin Gulch shear zone in particular, have features in common with both the primary and secondary mylonites of the Moine thrust (Christie, 1963).

These healed fault breccias were in turn refractured and recemented by a quartz-epidote-calcite gangue. This event is distinguished from the first brittle fracturing on the basis of crosscutting relationships and the presence of calcite.

No definite estimate of age for this period of motion is possible. It must postdate the early mylonitization and predate the Laramide deformation. The possibility exists that it was associated with the pre-Pennsylvanian deformation of the central Rockies.

On a small scale map the outcrop pattern of the Skin Gulch shear zone, which has the most widespread evidence of 2nd-period motion, is that of a cymoid loop (McKinstry, 1948). Zones of abundant healed fault breccia and secondary quartz coincide with the central part of the shear zone. This and the outcrop pattern suggest extensive dilation produced by left-lateral strike-slip motion. Subhorizontal streaking lineations interpreted as slickensides are occasionally present. These may be related to the possible left-lateral motion of this period or they may be related to the Laramide faulting of the last period.

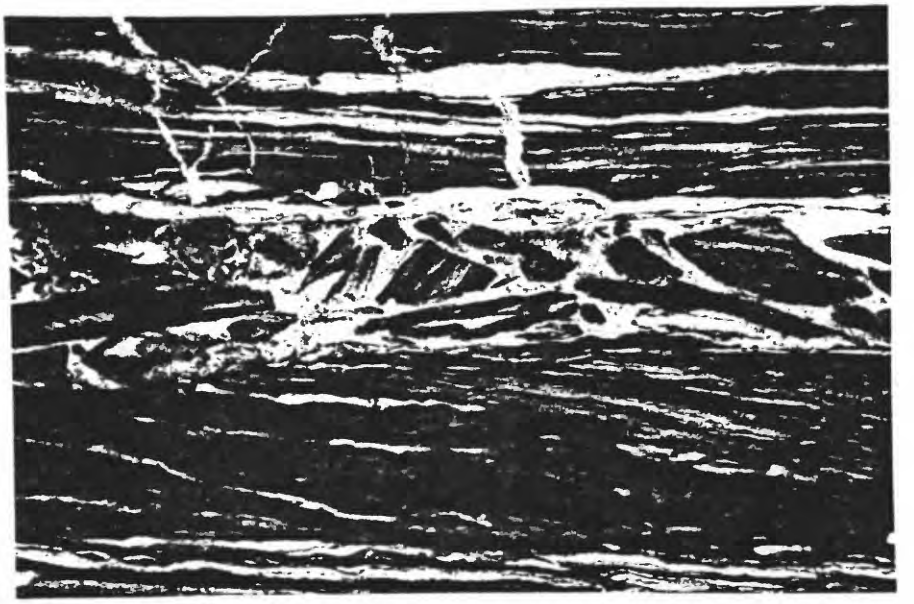

Figure 44: Photomicrograph of healed mylonite breccia. Sample 4-4-188. Nicols uncrossed. 25X.

Figure 45: Hand specimen of healed mylonite breccia. Roll of tape has a diameter of 12 cm.

No metalization was associated with this period of shearing.

Laramide faulting and brittle fracture

All of the structures formed during the earlier periods of shearing were in turn affected by the last, presumably Laramide, fracturing. This period of faulting produced wide zones of gouge and fault breccia. These are particularly well developed along the Poudre River fault at Dutch George Flats and Stove Prarie Landing.

Extensive alteration including oxidation of the mafic phases has taken place within these fault zones. The fault zones consist of pervasively fractured rock, thoroughly stained with secondary hydrous iron oxides (fig. 46). At Dutch John Flats and Stove Prarie Landing the Poudre River fault is intersected by other shear zones and unusually wide breccia zones are developed, hundreds of meters across. The Poudre River and the Stove Prarie fault display the most prominent third-period motion; both have topographic expression. By contrast many of the shear zones showing first or second period motion only have little or no topographic expression.

Evidence for a Laramide or Tertiary age for this period of faulting is only circumstantial. To the northeast, fault zones with similar characteristics clearly offset the Fountain Formation where the fault zones enter the Livermore embayment (Connor, 1962). The Cedar Gulch shear zone can be correlated with one of these faults. The extensive alteration and minor mineralization and metalization developed during this period of motion are similar to

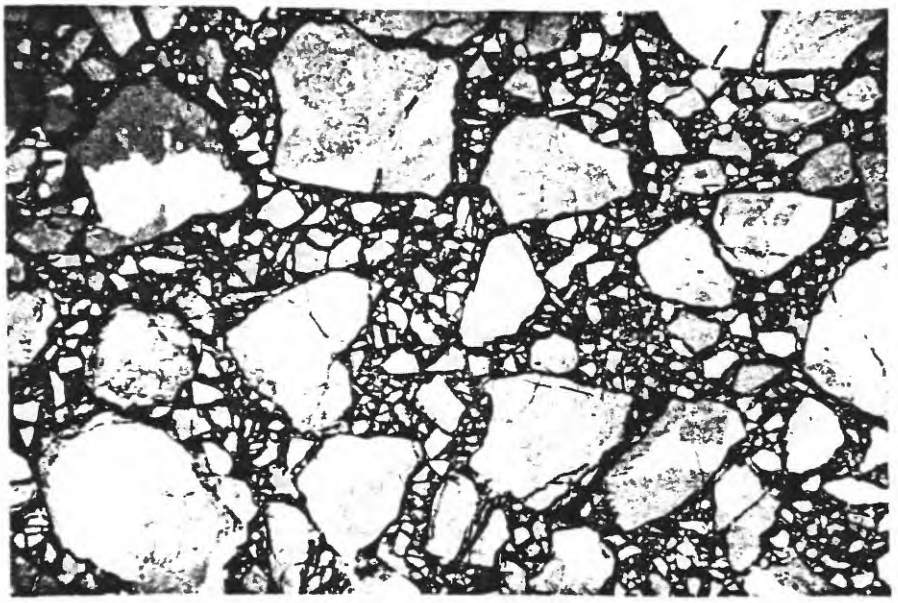

Figure 46: Photomicrograph of healed Laramide (?) fault breccia. Matrix between rock fragments is largely Fe-oxides. Slide has been stained for K feldspar. Sample 12-4-53. Nicols uncrossed. 10X.

that developed along definitely Laramide fault zones in the central Front Range.

The sense of displacement on these fault zones is unknown.

PETROLOGY OF METAMORPHIC ROCKS

Introduction

The petrology of the metasediments must be discussed within the framework of the entire northern Front Range because much pertinent data is contained within the lower-grade assemblages occurring to the south. Paragenetic relationships and field evidence for these other areas have been taken from Bucknam, 1969; Connor, 1962, Gawarecki, 1963; Nutalaya, 1966; Swann, 1962; Wohlford, 1965). The most comprehensive compilation of petrographic and petrologic data to date is that of Nutalaya.

The sequence of events that has been recognized in the Masonville and Drake quadrangles is (Braddock, 1970):

1. Early deformation and metamorphism producing greenschist facies rocks. The age of this event is not known.
2. Second period folding producing a crenulation cleavage.
3. Third period folding also producing a crenulation cleavage.
4. Second period regional metamorphism dated at about 1.75 b.y. which produced a zonal pattern of metamorphic assemblages. A small area within the Masonville quadrangle remained at greenschist facies; but to the south, west and north the rocks were metamorphosed to progressively higher grades. Biotite, garnet, staurolite, sillimanite + muscovite and sillimanite + microcline isograds have been mapped.

Distribution of metamorphic assemblages

The rocks within the Big Narrows-Poudre Park area have been metamorphosed to grade above the sillimanite-microcline isograd with the following exceptions:

1. An area in the south-central part (pl. 6) that lies between the sillimanite-muscovite and sillimanite-microcline isograds.
2. An area adjacent to the Skin Gulch shear zone which contains andalusite-cordierite assemblages which are interpreted to be the result of thermal metamorphism related to movement in this shear zone at about 1.2 b.y.

Other scattered occurrences of andalusite and cordierite are interpreted to be the relicts of earlier stages in the prograde 1.7 b.y. metamorphic episode.

Migmatites

Associated with the metamorphic rocks in the Big Narrows-Poudre Park area is abundant material in the form of migmatite. The degree of migmatization appears to increase with metamorphic grade to the north and is most intense in the more micaceous units. The thin, conformable, granitic pods, stringers and lenses parallel S_1, and locally phacolithic lenses are concentrated in the F_2 fold hinges. Two areas where the migmatization is particularly extensive are the southeast corner and the westcentral portions of the Big Narrows quadrangle.

With the possible exception of the Boulder Creek granodiorites the migmatitic rocks do not show any specific association with plutonic intrusive rocks.

The process of migmatization is largely conjectural. Some believe these leucocratic bodies are the result of partial anataxis of metasediments raised to the high temperatures of the upper amphibolite facies (Mehnert, 1968; Winkler, 1968). Others believe they are the product of metamorphic segregation phenomena taking place primarily in the solid state but possibly aided by intergranular fluids (White, 1966). This is an important distinction because the presence of migmatites has been traditionally the basis for utilizing the granite minima in estimating the temperature and pressure at which these assemblages equilibrated (see for example Lundgren, 1966).

Hedge (1969) studied the migmatites of the central Front Range in some detail utilizing the techniques of isotope geochemistry to establish the age and parentage of the metasome. He concluded that the metasome and the surrounding rocks were in isotopic equilibrium and were of the same age but was unable to establish definitely whether the metasome was the product of anataxis or of metamorphic differentiation. One of the key arguments used by both Hedge and White in support of metamorphic differentiation is that the composition of many metasomes does not fall anywhere near the minimum in the Ab-Or-Q ternary yet, the recent work of Luth and Tuttle (1969) on the hydrous vapor phase in equilibrium with granitic melts suggests that if there was a pervasive hydrous phase present, related to a deeper

anatectic melt, the crystalline products derived from it might have bulk compositions quite removed from the minimum. Thus the arguments of Hedge and White may not be valid and either process may have been active. No information was obtained during this study which would clarify this problem.

Microcline-sillimanite-muscovite assemblages

It is common to find the three phases-microcline, sillimanite and muscovite-"coexisting" in rocks in this area. On first thought this seems a somewhat anomalous situation since this area lies largely above the sillimanite-microcline isograd. In his analysis of the metamorphic history of the Glen Haven quadrangle Bucknam (1969) suggested that locally, primary muscovite coexists with microcline and sillimanite. This is also true for portions of the Big Narrows-Poudre Park area. Unfortunately, an accurate analysis of the distribution of these assemblages is hampered by the presence of the late muscovite, oftentimes difficult to distinguish from primary muscovite. A careful survey of the mineral assemblages in all of the pelite and psammitic units revealed four texturally distinct populations of muscovite only one of which is undoubtedly primary. These include medium-grained lepidoblastic primary muscovite, medium to coarse porphyroblastic muscovite, dense fine-to medium-grained seriate aggregates and medium-grained lepidoblastic secondary muscovite oriented at a high angle to S_1. These different types have already been discussed in the petrography section. Their distribution is shown on plate 6.

Evans and Guidotti (1966) recognized coexisting microcline, sillimanite and muscovite in Maine and concluded that the sillimanite-microcline isograd in that area was actually a zone within which this assemblage was found. It is not possible to delineate a zone within which these assemblages are found in the Big Narrows-Poudre Park area, however, their distribution may have resulted from processes similar to those described by Evans and Guidotti.

The formation of the assemblage microcline + sillimanite is governed by the reaction:

$$\text{muscovite-paragonite}_{ss} + SiO_2 + \text{plagioclase}_{ss} \rightleftharpoons \text{microcline} + Al_2SiO_5 + H_2O \qquad (1)$$

Theoretical analysis of phase relations in the system An-Ab-K-Sill (Evans and Guidotti, 1966) suggests that this reaction is discontinuous, and should occur over a small finite interval, ie. on an isogradic surface. However, field relationships in Maine (Evans and Guidotti, 1966) and perhaps in the northern Front Range suggest that this reaction is in fact continuous and that the assemblage represents divariant equilibrium.

Three explanations were proposed by Evans and Guidotti (1966):

1) "Isograd surfaces are parallel to the present land surface..." "In other words, P_{H_2O} and T varied together along the univariant curve for the breakdown of muscovite + quartz + plagioclase."

2) "Recrystallization and equilibration did not keep pace with the changing pressure-temperature conditions."

3) Rapid dehydration and low permeability might cause the local rock assemblages to buffer P_{H_2O}.

The authors consider the first unlikely, the second as inconsistent with observed textures and the third as most likely. In the northern Front Range isogradic surfaces are not parallel with the land surface and the first is unlikely. Textural evidence of disequilibrium or equilibrium is difficult to interpret and the second explanation may or may not be valid. The third explanation has the advantage of explaining the heterogeneity of assemblages in this area and is as plausible as the second.

The concept of buffered components in geologic systems has been discussed at length by Korzhinskii (1959), Zen (1961), Thompson (1965) and others. There are two types of buffering systems: those in which a component (such as H_2O is locally buffered (or inert in the terminology of Korzhinskii, 1959) and those in which a component is externally buffered (or perfectly mobile in the terminology of Korzhinskii, 1959). For a six-phase assemblage containing quartz, plagioclase, microcline, biotite, muscovite and sillimanite plus water we have a total of seven phases and seven components (SiO_2, Al_2O_3, K_2O, Na_2O, CaO, (MgFe)O, H_2O).

The analysis of variance of such system can be approached a number of ways. The Gibbs phase rule may be expressed as:

$$F = C-P + 2$$

and requires the knowledge of the parameters (P), the number of phases, and (C), the number of components. An alternative expression which can be used to analyze the variance of a system is:

$$F = \text{number of independent variable} - r$$

which requires knowledge of the number of intensive variables and the number of restrictions (r) (independent equations relating any of the phases). None of these factors are amenable to exact specification on the basis of petrographic description.

Utilizing expression (2) and assuming that the system is subject to the intensive variable P_t, T and μ_{H_2O}.

$$F = C-P + 3$$

however if μ_{H_2O} is locally buffered this reduces to:

$$F = C-P + 2$$

and for seven phases and seven components F=2 and this assemblage is divariant as the field data suggest.

Utilizing expression (3) and assuming the intensive variable P_t, T and μ_{H_2O} as well as the restriction that $\Delta\mu = 0$ for reaction (1) at equilibrium, we have:

$$F = 3-1 = 2$$

and the assemblage is again divariant. These results merely suggest that the interpretation of μ_{H_2O} as locally buffered and independent of P_t is correct: they do not prove it.

Local buffering of H_2O provides a reasonable explanation of the observed heterogeneity in five-and six-phase assemblages in the Big Narrows-Poudre Park area. It would be interesting to use the coexisting microcline-biotite-magnetite assemblages to determine the variation in μ_{H_2O}, if any. Unfortunately the chemical effects of the later retrograde metamorphism would probably prevent the use of the technique of Wones and Eugster (1965).

Microcline is not present in the metamorphic assemblages in

the south central portion of the area. Equivalent rock types to the east do contain microcline and sillimanite. A tentative position for the trace of the sillimanite + microcline isograd is indicated on plate 6. The large exposures of amphibolite in this area and the large bodies of Boulder Creek granodiorite (which are insensitive to this metamorphic isograd) impair the precision with which this isograd can be located.

The textures of the muscovite present an additional problem in the location and interpretation of this isograd. With only a few exceptions the muscovite textures in samples south of the isograd suggest that the muscovite is secondary, not primary. In many samples the porphyroblastic muscovite (Mu_2 on plate 6) is present throughout and is not restricted to areas rich in fibrolitic sillimanite. It is the author's opinion that this muscovite may represent primary muscovite recrystallized during the retrograde metamorphism associated with the emplacement of the Silver Plume granitic rocks.

Andalusite-sillimanite-cordierite assemblages

To the south, andalusite and cordierite occur widely in rocks above the staurolite isograd (Connor, 1962; Nutalaya, 1966; Bucknam, 1969; Punongbayen, personal communication) but their paragenetic relationship with the other index phases remains problematical. Nutalaya (1966) concluded that cordierite and andalusite formed during a third metamorphic event subsequent to the main regional metamorphism which produced staurolite and sillimanite and was unrelated to any period of deformation. He

cites abundant textural evidence he believes is in support of this conclusion including examples of corroded staurolite grains in andalusite, andalusite porphyroblasts enclosing fibrolitic sillimanite and cordierite replacing staurolite.

However, in the area analyzed by Nutalaya the porphyroblastic index minerals are superimposed on earlier microfolds developed in the metamorphic schistosity recognized in that area (S_2 of Nutalaya, 1966). These minerals are not rotated; indeed, there is no evidence other than reaction relationships which would indicate that andalusite and cordierite were not part of the main regional metamorphic event. As Bucknam (1966) has observed, perhaps we should consider biotite, garnet, staurolite, andalusite, cordierite, sillimanite and microcline as the product of a single prograde event.

Within the Big Narrows-Poudre Park area two different types of occurrences of andalusite and cordierite are recognized. Within the Poudre Park quadrangle scattered occurrences of andalusite and cordierite were noted. Andalusite occurs only as very small, highly corroded grains associated with fibrolitic sillimanite in some cases which appears to be later. Cordierite also occurs as highly corroded porphyroblast but no demonstrable paragenetic relationship with sillimanite was ever recognized.

Along the Skin Gulch shear zone in the adjacent migmatitic biotite schists large porphyroblasts of cordierite and andalusite are developed. Andalusite and sillimanite commonly occur in the same sample, andalusite always as poikiolitic lenticular porphyroblasts parallel with the foliation and sillimanite as

scattered needles or fibrolite aggregates parallel with the foliation. Andalusite-sillimanite textures are ambiguous. Cordierite may be later than sillimanite.

Recent experimental work on the stability of staurolite and cordierite as well as the aluminosilicates is extensive. Figure 47 summarizes the data of Richardson (1968) and Seifert (1970) on Fe cordierite and Mg cordierite respectively. Two reactions of particular importance are:

$$\text{Fe-cordierite} \rightleftarrows \text{almandine} + \text{sillimanite} + \text{quartz} \qquad (1)$$

(Richardson, 1968) which provides an estimate of the minimum pressure required for the breakdown of cordierite and

$$\text{Mg-cordierite} + \text{muscovite} \rightleftarrows \text{phlogopite} + \text{Al-silicate} + \text{quartz} + H_2O \qquad (2)$$

(Seifert, 1970) which establishes a maximum pressure for the stability of cordierite of 6.5 Kb.

Two additional reactions which may be of significance within the staurolite zone are:

$$\text{staurolite} + \text{quartz} \rightleftarrows \text{cordierite} + \text{Al-silicate} + H_2O \qquad (3)$$

$$\text{staurolite} + \text{quartz} \rightleftarrows \text{garnet} + \text{Al-silicate} + H_2O \qquad (4)$$

(Richardson, 1968) which might explain the observed staurolite-andalusite and staurolite-cordierite relationships.

If these reactions can be applied to rocks then the scattered occurrences outside of the Skin Gulch shear zone of andalusite and cordierite may actually be the product of prograde metamorphism synchronous with the production of the staurolite and sillimanite plus muscovite assemblages.

Staurolite and cordierite may have formed under approximately

similar P-T conditions (see figure 47); with increasing intensity of metamorphism some of the staurolite may have broken down to cordierite + Al-silicate assemblages (reaction 3) while finally within the sillimanite + muscovite zone both staurolite and cordierite became unstable (reactions 1, 2 and 4). This provides a tentative explanation for the considerably greater abundance of cordierite and andalusite between the staurolite and sillimanite-muscovite isograds than above the sillimanite-microcline isograd (Connor, 1962; this study).

The close proximity of the coarse porphyroblastic andalusite-cordierite assemblages with the Skin Gulch shear zone suggests that these assemblages are related to processes which produced the shear zone. They may have been produced during a local hornblende-hornfels facies metamorphism generated by the deformation within the shear zone.

Recrystallization within this zone has been extensive (see section on initial mylonitization) and X-ray analysis of the fine-grained blastomylonites indicates that they are mixtures of muscovite, biotite (?), chlorite (?), feldspar and quartz. In a number of places recrystallized calc-silicate gneisses are adjacent to the shear zone and the quartz + microcline + actinolite + clinozoisite-epidote could be the product of albite-epidote or hornblende hornfels facies metamorphism.

Other examples of low-to high-grade assemblages developed within large mylonitic shear zones are known. Theodore (1970) recognized upper amphibolite facies metamorphic assemblages associated with other mylonitic rocks in Southern California;

Sarker (1966) recognized the stability of kyanite in a Precambrian shear zone in India and Reed and Bryant (1964) recognized low-to medium-grade assemblages within the imbricate thrust structures in North Carolina.

An alternative explanation for these assemblages is that they represent a local region of lower-grade assemblages never raised completely to the level of the sillimanite-muscovite assemblages. If so the sillimanite must be interpreted as younger than either andalusite or cordierite. The author does not favor this interpretation because it leaves unexplained the anomalous association with the shear zone as well as what would be a singular occurrence of lower-grade rocks in an otherwise uniformly high-grade terrain.

Retrograde metamorphism

Abundant evidence of a period of retrograde metamorphism is present in the Front Range. Three types of evidence exist: corroded and altered garnet, oxidation of magnetite and ilmenite and secondary muscovite and chlorite.

Virtually all of the garnet porphyroblasts are partially altered to secondary biotite, chlorite, feldspar and quartz. The complete destruction of garnet in some samples suggests that the retrograde metamorphism was exceptionally efficient. Hsu (1968) clearly demonstrated the profound effect the variation of oxygen fugacity (fo_2) has on the stability of almandine. At 2 Kb, the stability field of almandine disappears at oxygen fugacities above those of the fayalite-magnetite-quartz buffer.

Almost all of the magnetite is either partially or completely oxidized to hematite and locally the ilmenite is also oxidized to amorphous iron-titanium oxides and possibly leucoxene. Pseudobrookite was tentatively identified in one sample of microcline gneiss from near the large pluton of mafic quartz monzonite. The development of hematite along cleavage planes in the biotite produced textures similar to those reported by Eggler and others (1969). These samples come from the southern edge of the mafic quartz monzonite body in the center of the Big Narrows quadrangle near both the Poudre River fault and the stock of biotite-muscovite granite. These samples and samples of the biotite-muscovite granite are quite red and on microscopic examination it is apparent that the K feldspars are rich in minute iron-oxide grains.

Eggler and others (1969) recognized the presence of hematite and pseudobrookite produced by a late stage alteration in the Sherman granite to the north. Pseudobrookite is not stable below 600°C (Lindsley, 1966) indicating that this alteration was a high-temperature phenomena. It is difficult, however, to clearly demonstrate a source for the fluid responsible for this alteration. The oxidation-alteration phenomena may have been related in time and space with the emplacement of the Silver Plume granite and the biotite-muscovite granite. Highly oxidizing fluids derived from Silver Plume-related magmas capable of producing hematite from magnetite are certainly capable of the destruction of almandine garnet.

The widespread porphyroblastic muscovite is the most obvious result of the retrograde metamorphism. The textures suggest that

muscovite grew at the expense of sillimanite but the source of potassium remains unknown. Some form of hydrous fluid must have been responsible for the introduction of water, and may also have transported potassium as an alkali chloride (Orville, 1963).

In addition to the large porphyroblasts of muscovite replacing sillimanite, fine-grained aggregates (shimmer aggregates) of muscovite and some lepidoblastic muscovite are developed (M_1, M_2 and M_3 on plate 6). The last type is important because it is sometimes associated with a secondary lepidoblastic biotite and both are strongly oriented at an angle to the earlier mica fabric, S_2. Apparently some of the rocks undergoing retrograde metamorphism were not in a hydrostatic stress field. This is consistent with the earlier observation that the emplacement of the Silver Plume granites may have been forcible producing a compressive stress in the rocks to the south of the Log Cabin batholith.

The retrograde metamorphism is considered approximately contemporaneous with the 1.4 b.y. plutonic event. As Peterman and others (1968, p. 2295) indicate this may be only a minimum age.

Conditions of metamorphism

Water pressure

Water pressure is presumed to have been equal to load pressure throughout most of the area most of the time. This is a commonly accepted approximation (Turner, 1968). It is reasonable because most of the prograde reactions taking place to the upper limit of the amphibolite facies are dehydration

reactions and the system is constantly flushed with water. A major exception to this generalization is in metasediments rich in interlayered carbonate-bearing units. In these, decarbonation reactions are as important as dehydration reactions and although P fluid may equal P total, P_{H_2O} must be considerably less than P total. However, carbonate-bearing units are quite rare in the northern Front Range. In addition the previously discussed microcline-sillimanite-muscovite assemblages may also represent evidence of local fluctuation in f_{H_2O}.

Oxygen fugacity

Oxygen fugacity is an important variable because it effects the stability of the iron oxides, biotite, cordierite, garnet and chlorite. In an earlier summary of metamorphic conditions in the northern Front Range Nutalaya (1966) assumed that the system was open to O_2 and that it was not locally buffered. He based his conclusions on the observation that the $Fe^{+++}/Fe^{++} + Fe^{+++}$ ratio in both biotite and hornblende increases systematically from low to high metamorphic grade. However, a large number of recent detailed chemical studies indicate that in regional metamorphic systems O_2 <u>is</u> locally buffered (Chinner, 1960; Albee, 1965; Klein, 1966; Himmelberg and Phinney, 1967; Butler, 1969). I feel that the present analytical data on compositions of co-existing phases in the Front Range is far too inadequate to demonstrate that the system was externally buffered with respect to O_2. It is more reasonable to adopt the more accepted view that O_2 is locally buffered until a detailed study of the distribution

of the iron-bearing phases has been completed.

In the opinion of many researchers the oxygen fugacity during metamorphism in common pelites is between that of the magnetite-hematite and fayalite-magnetite-quartz buffers (Buddington and Lindsley, 1964; Richardson, 1968). At 600° this places fo_2 from 10^{-20} to 10^{-14} bars (Eugster and Wones, 1962). Nutalaya (1966) used the techniques of Wones and Eugster (1965) to estimate the oxygen fugacity in biotite-microcline-magnetite assemblages in the sillimanite-microcline zone of the Front Range. He estimated 10^{-14} to 10^{-15} bars. On the basis of the recent data of Hsu (1968) on the stability of almandine garnet this now appears to be too high, at least for the garnet-bearing assemblages. A value of about 10^{-20} bars is a better estimate. It is assumed that an oxygen fugacity equivalent to the fayalite-magnetite-quartz buffer is a reasonable approximation for the Front Range metasediments during the regional high-grade metamorphism, recognizing that local buffering may cause considerable local variation in the equilibrium fo_2.

The oxygen fugacity during the retrograde metamorphism probably attained values of at least 10^{-15} bars.

Pressure and temperature during regional metamorphism

Our lack of chemical analyses of the chlorite produced during the early greenschist-facies metamorphic event, and the dearth of detailed experimental studies permits only the most general estimates of pressure and temperature within the chlorite

zone. Velde's work (1964) on the relative stability of clays, micas and chlorites suggests temperatures between 300 and 400°C at P_{H_2O} = 2Kb. The upper limit is defined by the appearance of biotite. No evidence is present in the Front Range assemblages for either lower-grade zeolitic assemblages or higher-grade amphibolite facies assemblages related to this early period of metamorphism.

During the main metamorphic event at 1.75 b.y. chlorite, biotite, garnet, staurolite, andalusite (?), cordierite (?), sillimanite + muscovite and sillimanite + microcline assemblages were successively developed. The first appearance of migmatite approximately corresponds with the microcline + sillimanite isograd.

Field relationships indicate that the garnet isograd is close to the biotite isograd (Nutalaya, 1966) and the garnet and staurolite isograds are separated by a much more considerable distance. This does not necessarily imply that the temperature difference between these different levels of metamorphism were comparable because nucleation and kinetic factors can have a sizeable effect on the first appearance of any phase. In addition, the work of Rutherford (1970) demonstrates that the first appearance of staurolite is essentially <u>independent</u> of fo_2 while Hsu (1968) demonstrates that the first appearance of garnet is strongly <u>dependent</u> on fo_2. Thus fo_2 may be as important as temperature in controlling the relative spatial position of these phases. Garnet probably first appears in the temperature range 450° to 550° at 3 to 4 Kb water pressure. The upper limit of the

garnet zone is fixed by the first appearance of staurolite which is now well known for Fe-staurolite (Richardson, 1968) and moderately well known for Fe-Mg staurolite (Hoschek, 1969). The different low-temperature phases in the studies appear to have little effect on the position of the univariant line representing the first appearance of staurolite. Fe-staurolite appears at 530-540° at P_{H_2O} = 3.5 to 4.5 Kb (fig. 47). The breakdown of staurolite to andalusite or cordierite plus other phases takes place at about 625-650° at H_2O = 4 to 4.5 Kb (Hoschek, 1969; Richardson, 1968; Seifert, 1970) (fig. 47).

These reactions should be closely followed by the first appearance of the assemblage muscovite + sillimanite since staurolite is observed to disappear at the muscovite + sillimanite isograd (W.A. Braddock, personal communication, 1970). The univariant curves representing these reactions intersect at 650° and 4.5 Kb (fig. 47). The field observation of staurolite-andalusite and staurolite-cordierite reaction pairs throughout the staurolite zone perhaps suggests some process is acting to cause these reactions to become divariant. Perhaps local variations in P_{H_2O} relative to P total are responsible or the solid solution of Mg-Fe is influencing the stability of these reactions.

The first appearance of migmatites occurs at about the microcline + sillimanite isograd. Figure 48 suggests that andalusite should be the stable Al_2SiO_5 polymorph in the migmatites. However, considering the uncertainties in both the position of the Al_2SO_5 triple point and in the minimum melting

FIGURE 47

Stability fields of metamorphic mineral assemblages containing staurolite and cordierite

This figure combines the data from a number of experimental studies in an effort to estimate plausible pressures and temperatures for the 1.7 b.y. regional metamorphism of the northern Front Range.

The three arrows represent postulated reaction paths for the following reactions:

- micas to staurolite
- staurolite to andalusite
- staurolite to cordierite

The experimentally determined mineral stability fields are based on the work of:

- Richardson and others, 1969
- Richardson, 1968
- Hoschek, 1969
- Seifert, 1970

The stippled area represents the stability field of staurolite-bearing assemblages. The following symbols are utilized:

B	biotite	St	staurolite
Mu	muscovite	M	microcline
Ch	chlorite	As	aluminum silicate
P	phlogopite	S	sillimanite
G	garnet	A	andalusite
Ct	chloritoid	K	kyanite
C	cordierite	Q	quartz

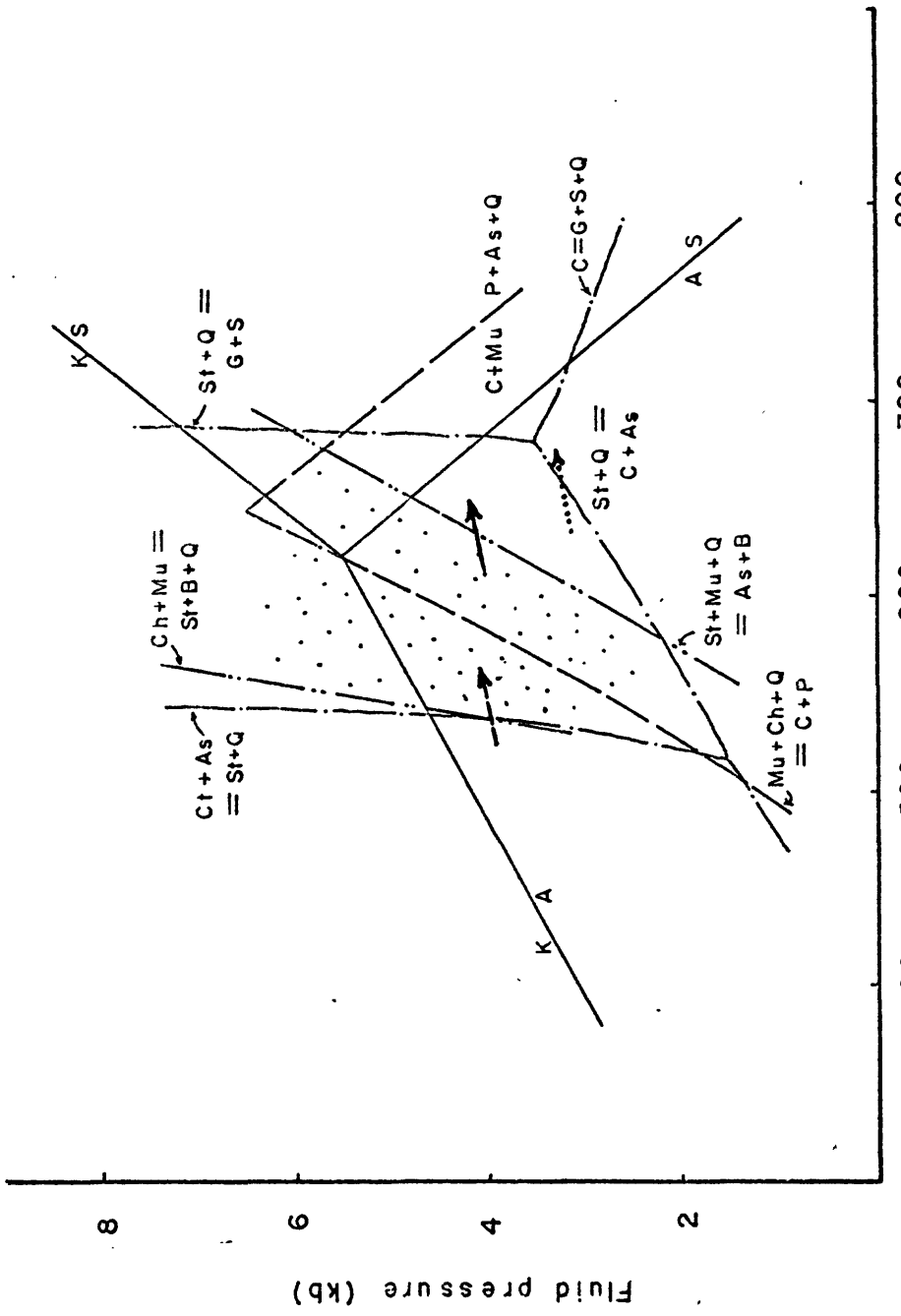
Fluid pressure (kb)
8
6
4
2
400
500
600
700
800
Temperature °C
K
A
K
S
St + Q ≡ G + S
Ch + Mu ≡ St + B + Q
Ct + As ≡ St + Q
C + Mu
P + As + Q
C = G + S + Q
St + Q ≡ C + As
A
S
St + Mu + Q ≡ As + B
Mu + Ch + Q ≡ C + P

Figure 47

FIGURE 48

Stability fields of metamorphic mineral assemblage containing the aluminum silicates and muscovite

This figure combines the data from a number of experimental studies in an effort to estimate plausible pressures and temperatures for the 1.7 b.y. regional metamorphism of the northern Front Range. This figure emphasizes reactions taking place at a slightly higher metamorphic intensity than those in figure 47.

The arrow represents a postulated generalized path for reactions taking place in the sillimanite + muscovite and sillimanite + microcline zones.

The experimentally determined mineral stability fields are based on the work of:

——————— Richardson and others, 1969

——— · ——— · ——— Evans, 1965

——— ·· ——— ·· ——— Luth and others, 1964. Minimum melting in the system $Ab-Or-SiO_2-H_2O$

The stippled area represents the stability field of sillimanite + microcline-bearing assemblages. Symbols are as in figure 47.

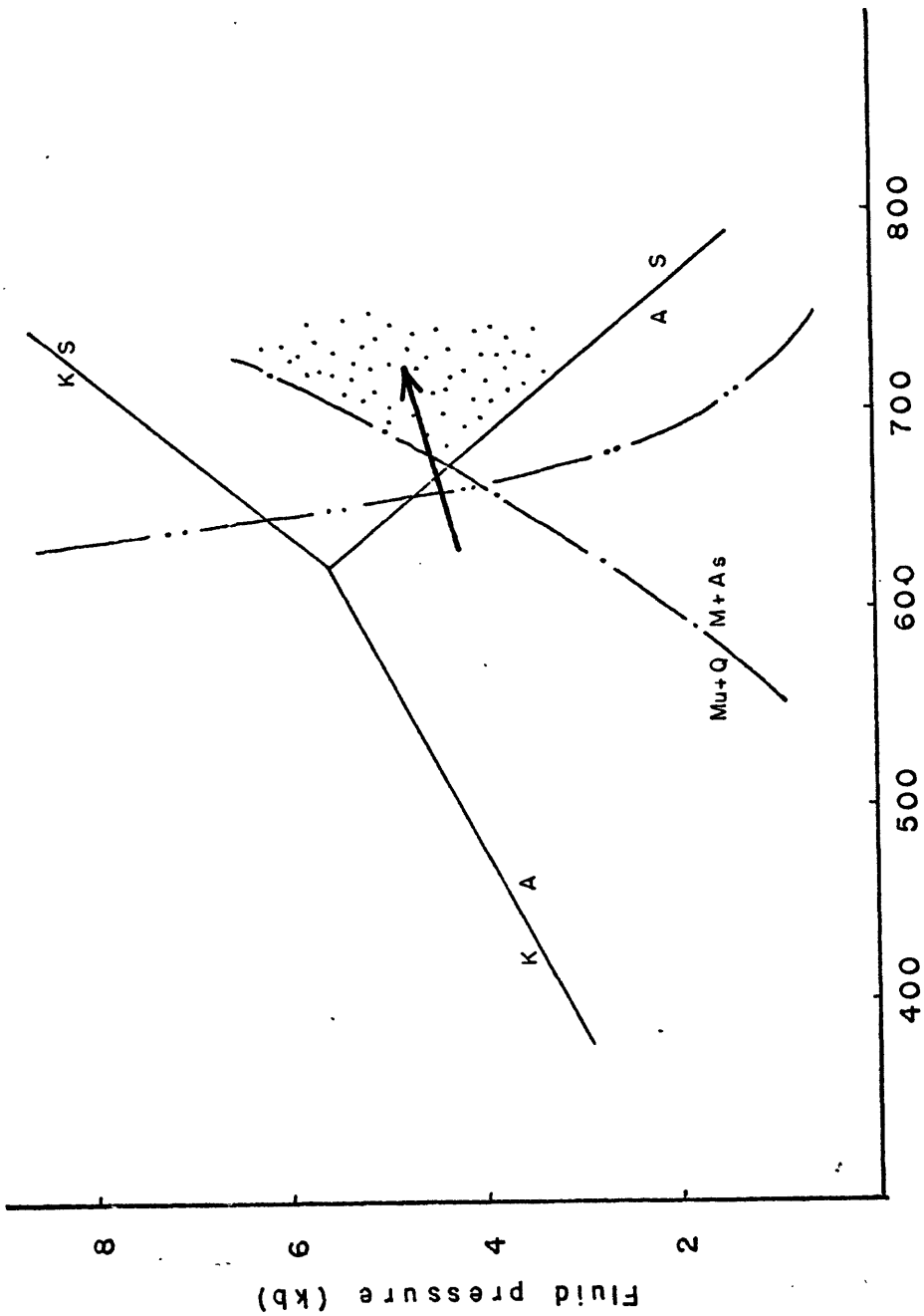
Fluid pressure (kb)
8
6
4
2
Temperature °C
400
500
600
700
800
K S
A S
K A
Mu+Q M+As

Figure 48

curve for pelitic rocks, this criticism is not significant because only a 20° rise in the minimum melting temperature would shift the intersection of muscovite + quartz ⇄ microcline + sillimanite reaction and the minimum melting curve into the sillimanite field. Considering the potential error in these boundaries an estimate of 670 to 680° and 4.5 Kb is reasonable.

How much higher the temperatures went above the microcline + sillimanite isograd is unknown. Orthopyroxene is absent from the amphibolitic units above that isograd in the Big Narrows-Poudre Park area. Apparently assemblages of the granulite facies did not appear.

Temperatures and pressures during the peak of regional metamorphism ranged from 530° and 4 Kb to perhaps 680°C and 4.5 Kb at the microcline-sillimanite isograd. The mineral assemblages developed in the progression of metamorphic facies are equivalent to those of the low-pressure intermediate or Buchan type of metamorphic facies series (Miyashiro, 1961). It is not directly comparable to the Bosost type of facies series which Winkler (1968) correlates with the Buchan type because of the absence of the assemblage sillimanite + cordierite + potassium feldspar. It is the author's opinion that such correlations have only limited value. As more and more metamorphic terrains are mapped in detail the differences become more apparent and we may yet see a retreat from the urge to name new facies series as we have seen a retreat from the habit of subdividing metamorphic facies (Fyfe and Turner, 1966).

NATURE OF THE PREMETAMORPHIC ROCKS

Introduction

The nature of the origin of the various rock units is greatly complicated by the high grade of metamorphism, the migmatization and the metamorphic differentiation processes; all of which have altered, perhaps drastically, the original character of these rocks.

Previous work in areas to the east and south by O'Connor (1961), Connor (1962), Swann (1962), Gawareckii (1963) and Wohlford (1965) has indicated that the metasediments were probably originally part of a thick sequence of eugeosynclinal graywackes, psammites and pelites. Only minor metaigneous rocks, many of the amphibolites, were recognized.

The two large bodies of microcline-quartz-plagioclase-biotite gneiss in the Big Narrows constitute a sizeable proportion of the metamorphic rocks in this area. The microcline-quartz-plagioclase-biotite gneiss was chosen for a detailed study because its origin is somewhat controversial, its structural setting is relatively well known, it is well exposed and it was thought to have a relatively uniform composition. This last supposition was proven strikingly incorrect by the trend-surface analysis whose results are applied in the following analysis and whose procedures are discussed in appendix 2.

A brief discussion of the ideas of previous workers in the northern Front Range on the origin of the other metamorphic rock units is presented.

Microcline-quartz-plagioclase-biotite gneiss

The bulk composition of the microcline-quartz-plagioclase-biotite gneiss is quartz monzonite. Braddock (1969) has calculated mesonorms for typical sedimentary rocks; arkoses plot in the quartz monzonite field on a quartz-plagioclase-microcline ternary diagram. Thus the rock could have initially been a quartz-monzonite intrusive, metamorphosed arkose or metamorphosed dacitic volcanics. These alternatives are discussed below.

Sedimentary origin

If this unit is the product of the metamorphism of sediments, the original sediments must have been of arkosic composition. A graywacke origin is ruled out by the excess of K_2O over Na_2O (graywackes are characterized by the excess of Na_2O over K_2O Pettijohn, 1963) and the consequent abundant potassium feldspar in this unit.

Arkosic sediments are the products of rapid erosion, transport, and deposition of material derived from igneous or metamorphic source rocks of intermediate to felsic compositions. If such a source area was a typical composite batholith analogous to the present-day Sierra Nevada and Coast Range batholiths the erosional products might be a heterogeneous mixture of fragments from many rock types. In addition many sequences of arkosic sediments include numerous thin lenses of pelite, psammite and other better-sorted sediments; lenses which might have locally homogeneous, but significantly different chemical compositions than the surrounding arkoses. Such a pile of sediments might have a heterogeneous

composition and when metamorphosed, a heterogeneous, near random, modal composition. The trend-surface results appear to be compatible with this model.

However, virtually all large bodies of arkosic sedimentary rock are closely associated with the basement source area from which they were derived (Walker, personal communication, 1970). The total lack of evidence in the northern Front Range for such a basement (the only exception being a possible 2.4 b.y. terrain in the Medicine Bow Range considerably to the north) strongly suggests that these are not meta-arkoses derived originally from an alluvial-fan environment.

Igneous intrusive origin

Evidence of crosscutting relationships was not found and interlayered metasediments are present suggesting that this is not an intrusive sill. However, this is not sufficient evidence to justify eliminating this origin as igneous sills with sheets of country rock are known.

The results of the trend-surface analysis on modal variation indicate a near random modal distribution. This would be unlikely in an igneous sill emplaced during a single magmatic event. The modal composition of such a sill should be quite uniform and a trend surface of low gradient but high significance might be expected.

Alternatively the igneous magma might be highly contaminated by assimilation of wall rock or the sill might be the product of multiple injection, both processes which would lead to a more

heterogeneous modal mineralogy.

An igneous intrusive origin is considered unlikely although possible.

Volcanic origin

Three alternative volcanic processes are possible: (1) rapid extrusion of thousands of feet of chemically uniform dacitic volcanics, (2) regular accumulation of progressively differentiated volcanics, and (3) accumulation of a chemically heterogeneous sequence of volcanics due to either rapid irregular changes in the physical parameters controlling differentiation in the source magma chamber or the irregular tapping of different magma sources due to tectonic activity.

If the gneiss was produced by a process similar to that in case one, variation in the mineral proportions would be small and a trend surface of very low gradient but high significance should be produced.

If the gneiss was produced by a process similar to that in case two, regular changes in the modal mineralogy might be expected between the top and the bottom of the unit. These would be indicated by trends or computed trend surfaces of high significance (high sum of squares explained).

Trend-surface results do not support either of these alternatives.

The third case represents a process capable of producing a heterogeneous mineralogy. The trend-surface results are compatible with these postulated processes, however, it is impossible to use

the trend-surface results alone to distinguish between this origin and a sedimentary origin.

The petrographic evidence cited earlier strongly supports a volcanic origin. The large relict bipyramidal quartz grains and the feldspar augen are probably remnants of an earlier porphyritic texture present in unmetamorphosed heterogeneous dacitic volcanics. Perhaps these were laid down in a tectonically active geosynclinal environment, locally reworked and interlayered with rare graywacke sediments adding to their heterogeneous character.

Biotite schist

There is abundant evidence of relict sedimentary textures in the lower-grade pelitic schists in the Drake and Masonville quadrangles to the south (Gawarecki, 1963). O'Connor (1961) and Gawarecki (1963) have discussed the chemistry of these rocks and concluded that they were shales, graywackes or subgraywackes. All discussion has been based on limited analytical data. A number of other authors have recalculated chemical analyses using modal and mineralogical data and arrived at similar conclusions (cf. Swann, 1962; Wohlford, 1965).

Braddock (1969), working in the central Front Range, has made a detailed comparison of calculated mesonorms of sedimentary rocks with the biotite gneiss of that area and also noted a similarity with shales and graywackes.

Amphibolite

The amphibolites of the Front Range have, as elsewhere, proved rather intractable objects of study. Comparison of their chemical analyses with those of average basalts has been made (O'Connor, 1961; Wohlford, 1965) and an origin as basalt flows or intrusive sills is possible. The common occurrence of amphibolites as massive concordant layers is compatible with such an origin. Many of the thin amphibolite lenses are associated with thin calc-silicate gneiss layers and interlayered with biotite schist suggesting that these rocks are derived from impure limestones (O'Connor, 1961, p. 59).

Recently L.J. LaFountain (personal communication, 1970) has compared large numbers of chemical analyses of amphibolites from elsewhere in the world with those available from the Front Range using discriminant-function analysis. He concludes that the majority of the Front Range amphibolites are orthoamphibolites. Clearly additional study is needed to clarify the origin of these rocks.

Boulder Creek Granodiorite

Mechanism of emplacement

Within the Front Range there is a general relationship between the sillimanite-microcline isograd, migmatization and Boulder Creek plutonism; however, this is not apparent on the scale of a single pluton of Boulder Creek Granodiorite. The field evidence within the Big Narrows-Poudre Park area strongly suggests that these plutons, particularly the phacolithic bodies, are syn-kinematic with the F_2 period of deformation.

Buddington (1959) lists the presence of phacolithic bodies and associated migmatities as two of the key indications of catazonal plutons and it is within this group of plutons that the best evidence for "granitization" or a chemical replacement origin is found. In the case of the Boulder Creek batholith and related plutons there is sufficient local evidence of sharp crosscutting contacts to necessitate the presence of a fluid (probably crystal rich) magma during part of the plutonic event. Lovering and Goddard (1950) have commented that the inclusions within the Boulder Creek show little evidence of assimilation, suggesting that they cannot be interpreted as remnants of an in situ granitization process.

Emplacement may have been by passive injection parallel to the foliation of the metasediments to form the lensoid bodies; injection into the hinge zones of folds to form the phacolithic bodies; and by large scale assimilation of the wall rocks to produce

the larger plutons. The abundance of inclusions is possible evidence of stoping and assimilation.

Chemical and experimental data

The application of experimental results to these rocks involves the greatest approximations of any of the applications discussed in the section on igneous petrology. The chemical composition of these rocks is the farthest removed from the Ab-An-Or or Ab-Or-Q ternary of any of the plutonic rocks because of the large percentage of Mg, Fe and Ca.

Norms have been computed for the four new analyses reported in table 12. These are combined with four prevously obtained norms from Boulder Creek Granodiorite bodies in the northern Front Range (Braddock, personal communication) on figure 49. Two results are apparent: considerable deviation from the position of the cotectic in the Ab-An-Or system at 5 Kb P_{H_2O} and considerable scatter in the plotted points.

The deviation from the cotectic is due to the bulk composition of the system which does not lie in the Ab-An-Or system. The scatter of the points might be due to local heterogeneities caused by assimilation of different materials. The majority of these assimilated rocks would have been biotite schists and gneisses since these constitute the majority of the wall rocks. Unfortunately no chemical analyses of the metasediments in the northern Front Range are available but mesonorms calculated by Braddock (1969) suggest compositions in the range quartz diorite to quartz monzonite.

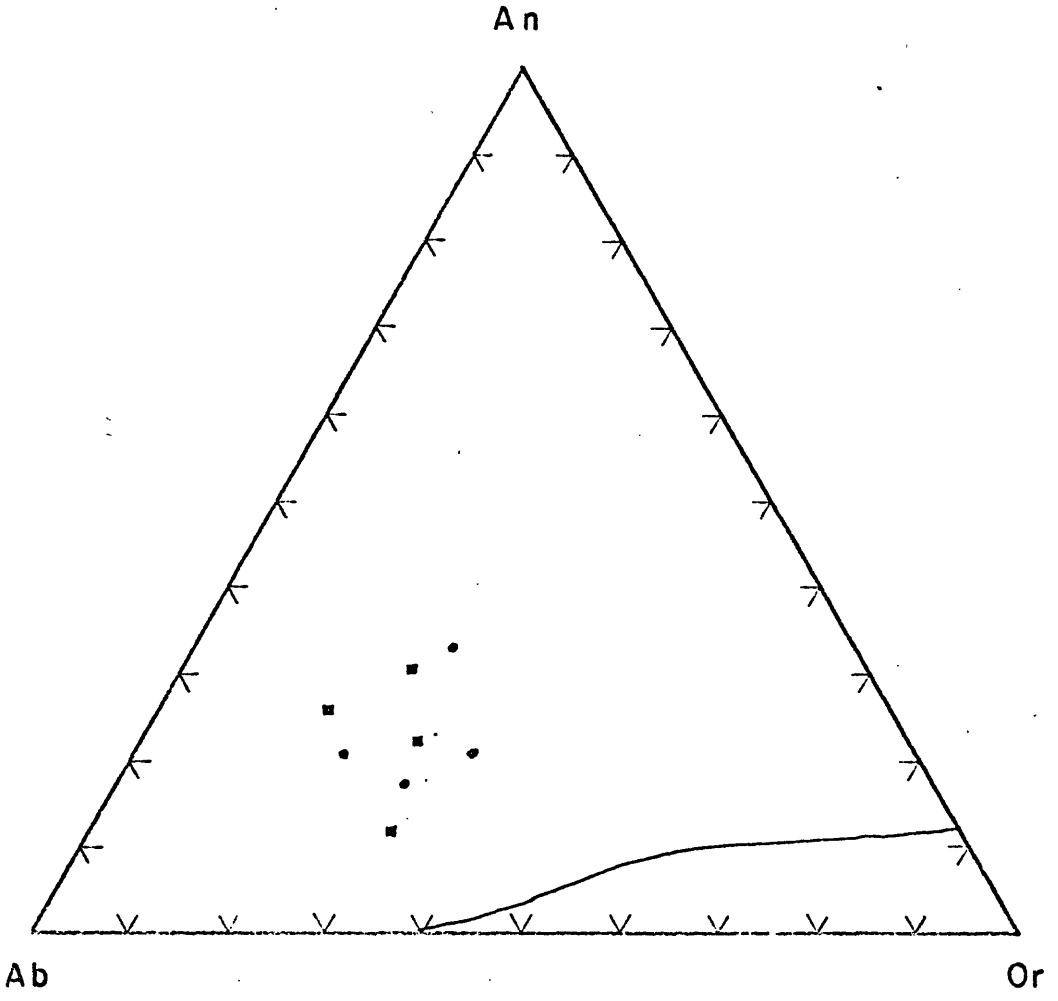

Figure 49: Ternary plot of CIPW norms of Boulder Creek Granodiorite with the 5 Kb cotectic from Yoder and others (1957).

- • data from this study
- ■ data from W.A. Braddock, 1969, personal communication

Assuming that all of these rocks were derived by magmatic crystallization, as the field evidence suggests, the variation in bulk composition may represent the contamination by assimilation or hybridization of a parent quartz-dioritic magma. Progressive differentiation in the source area may also be responsible for some of the variation. Such contamination by crustal rocks would shift the bulk composition in the Ab-An-Or ternary away from the Ab-An side.

Experimental work on rocks of directly comparable plutonic setting is not available. However, Piwinskii (1968) has studied the melting behavior of dioritic and granodioritic rocks from the Sierra Nevada batholith. Estimates of pressure at the site of emplacement for these rocks by Bateman and others (1963) are comparable to those estimated in an earlier section for the high-grade regional metamorphism which was contemporaneous with Boulder Creek plutonism in the Front Range.

Piwinskii (1968) has demonstrated that the Sierra Nevada rocks could have been produced by the hybridization of upper mantle or lower crustal derived gabbroic magma by a melt derived from the partial melting of felsic to intermediate crustal rocks. The melting data obtained from H_2O-saturated systems indicates that temperatures of at least 740°C at 4 Kb are required to produce significant melting. The coexistence of biotite, hornblende and calcic plagioclase with a melt to much higher temperatures indicates that emplacement was most probably as a liquid-crystal mush. Such a model is probably also applicable to the origin of the Boulder Creek Granodiorite.

The initial Sr^{87}/Sr^{86} ratio of the Boulder Creek granodiorites is 0.7035 and for the high-grade metamorphic rocks of the same age it is 0.7079 (Peterman and others, 1968). 0.7035 is greater than the Sr^{87}/Sr^{86} ratio of upper mantle material at 1.7 b.y. (0.7015, based on the Sr^{87}/Sr^{86} evolution diagram of Hamilton and Meyer, 1967) and less than that of the high-grade metamorphic rocks. Thus these data are consistent with a mixed source of both upper mantle or lower crustal material and upper crustal material for the Boulder Creek granodiorite magmas.

In addition the uniform isochron plot obtained by Peterman and others (1968) demonstrates that the magma which formed the Boulder Creek plutons, although perhaps substantially contaminated by assimilation processes, did homogenize Sr^{87}/Sr^{86} presumably at the site of partial melting, assimilation and magma hybridization. Therefore the close association of migmatites is due only to the fact that a catazonal regime is favorable for the formation of migmatites and the emplacement of phacolithic gneissic granitic bodies. The lack of zoning in the plagioclase feldspars suggests that the emplacement into a high-metamorphic-grade catazonal environment permitted the homogenization of these feldspars. Quite probably some chemical exchange between host rocks and the Boulder Creek magmas did take place at the site of emplacement but this must have been a minor process serving only to blur the intrusive contact.

Silver Plume Granite

Mechanism of emplacement

The mechanism of emplacement of these rocks is largely unknown. The locally gradational contacts indicate the possibility of minor chemical homogenization although the chemical similarity of the wall rocks (granitic gneisses, migmatitic biotite schist and quartzofeldspathic schists) with the melt indicates that large-scale assimilation might be difficult to recognize. The absence of small inclusions over large areas of these intrusives and the uniformity of the composition of these granitic rocks indicates that assimilation probably was not extensive.

There are a numer of medium-to large-sized xenoliths ten's of meters to kilometers across and these may represent either roof pendants or large stoped blocks. Their uniform orientation (particularly in the north central portion of the Big Narrows quadrangle) and their increasing abundance to the southeast suggests that at least locally the roof of the batholith has been only partly dissected. Perhaps stoping with associated minor assimilation has been responsible for the present map pattern. Since the stoped blocks are now largely dropped out of view over large areas this remains a plausible but unsubstantiated hypothesis.

Immediately to the south of the batholith there are a number of small folds (F_4)which are interpreted to have been produced by the forcible emplacement of the Silver Plume. They are the only evidence for this type of emplacement of any Silver Plume body in the northern Front Range. Cataclastic textures are abundant within the porphyritic quartz monzonite and the mafic quartz monzonite

facies. The age of cataclasis is probably post Silver Plume, but some of the cataclasis might be due to the emplacement mechanism.

Chemical and experimental data

The chemical analyses and the computed norms in table 12 all indicate that these rocks are corundum normative-peraluminous granitic rocks. Luth and others (1964) argued that peraluminous subsolvus granites are indicative of relatively high water pressures, perhaps water saturated systems. This is an important distinction because all of the available experimental work was done under water saturated conditions and, thus, is theoretically only applicable to natural rocks crystallizing in a similar environment. In the Front Range pegmatites are locally associated with the Silver Plume granitic rocks and these suggest relatively high water pressures during part of the history of these plutonic rocks.

The mineralogical, chemical and field evidence strongly supports a magmatic origin for the Silver Plume granitic rocks. Figures 50 through 53 summarize the normative and mineralogical data on the Silver Plume of the Big Narrows-Poudre Park area. Data projected onto the An-Ab-Or ternary is a more accurate portrayal of the bulk chemistry than data projected onto the Q-Ab-Or ternary because the critical relationships of the feldspars are better illustrated. Figure 51 clearly indicates the close association of the bulk chemistry of these rocks with the ternary cotectic. In addition the feldspar pairs plotted on figure 52 have tie lines consistent with the tie lines determined by Yoder and others (1957).

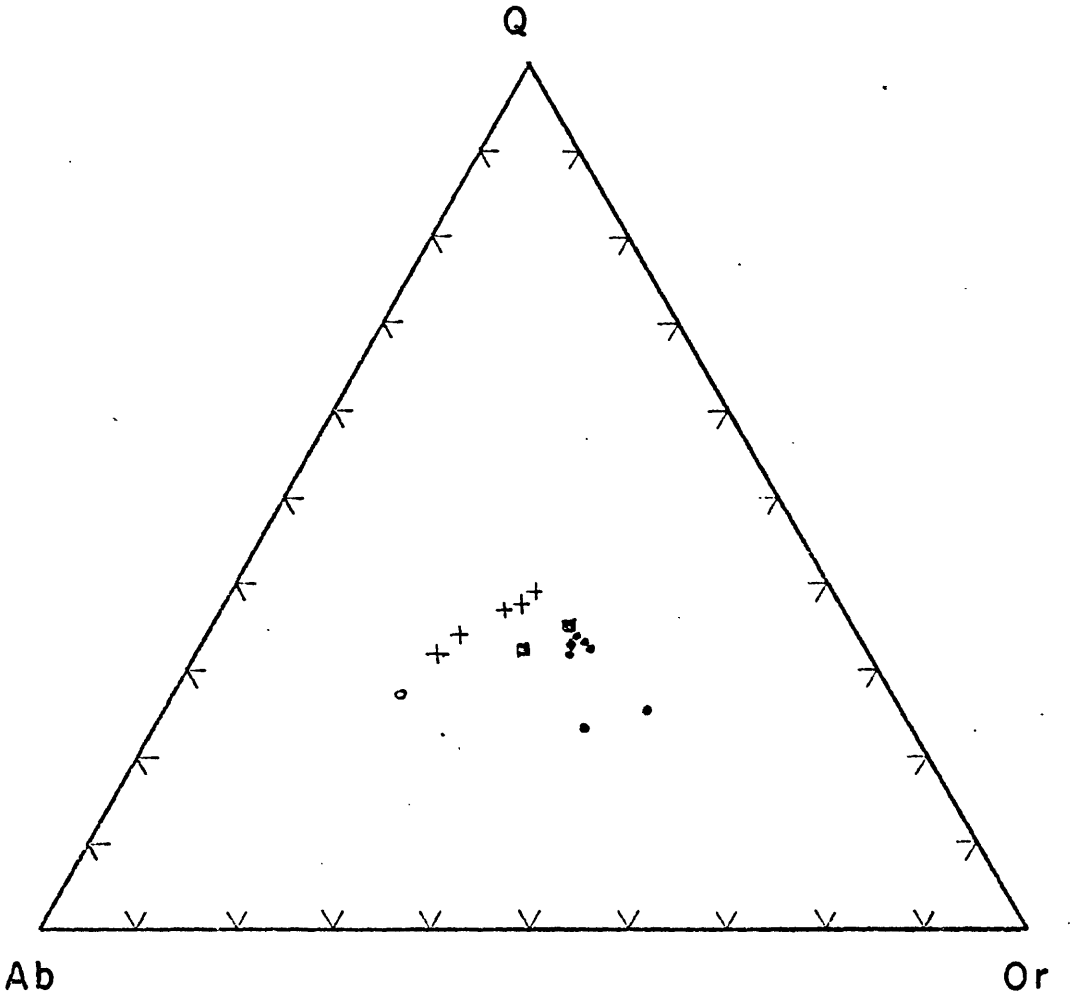

Figure 50: Q-Ab-Or ternary with CIPW norms of Silver Plume Granite and the isobaric minima and eutectic for the H_2O saturated Q-Ab-Or system from Luth and others (1964).

▪ porphyritic quartz monzonite

◆ mafic quartz monzonite

• quartz monzonite

+ o data from Luth and others (1964)

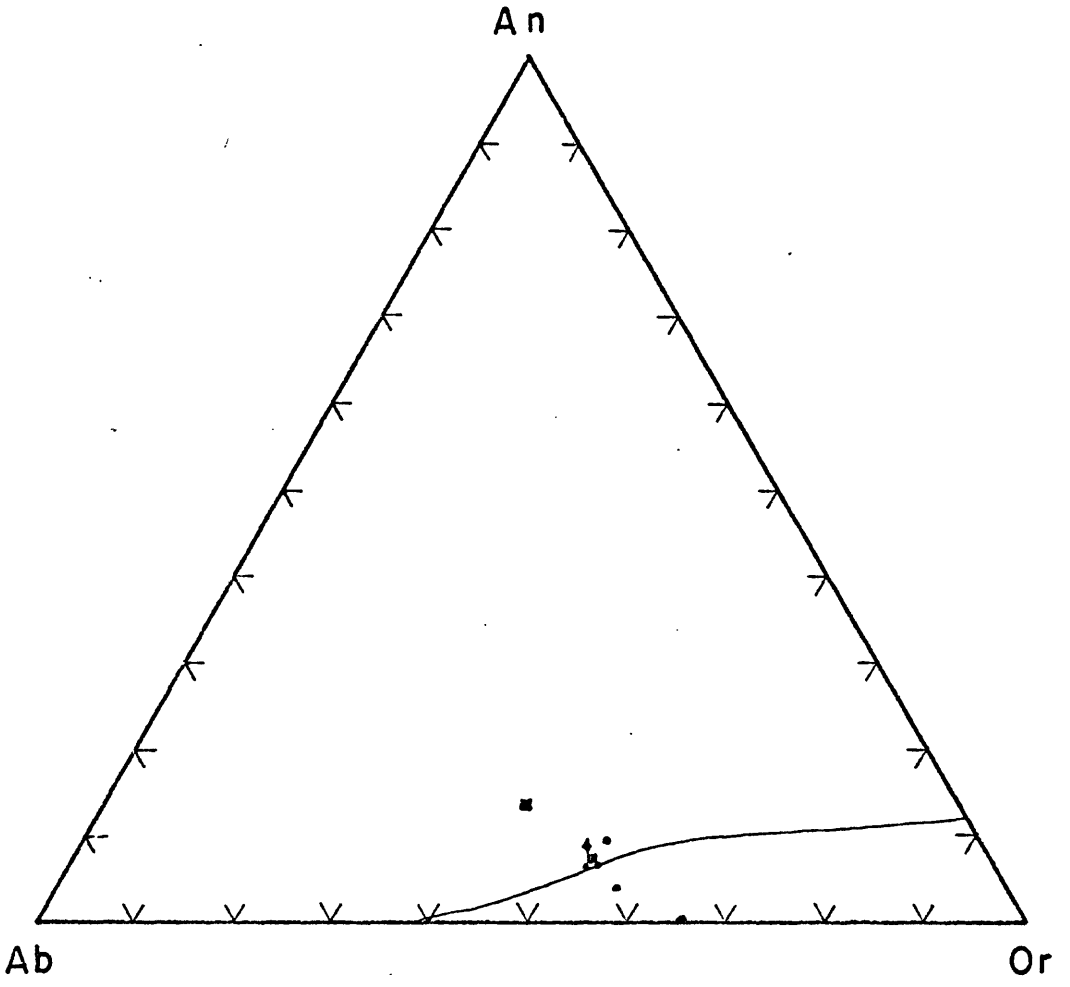

Figure 51: Ab-An-Or ternary with CIPW norms of Silver Plume Granite and the 5000 bar cotectic from Yoder and others (1957).

- ■ porphyritic quartz monzonite
- ♦ mafic quartz monzonite
- • quartz monzonite

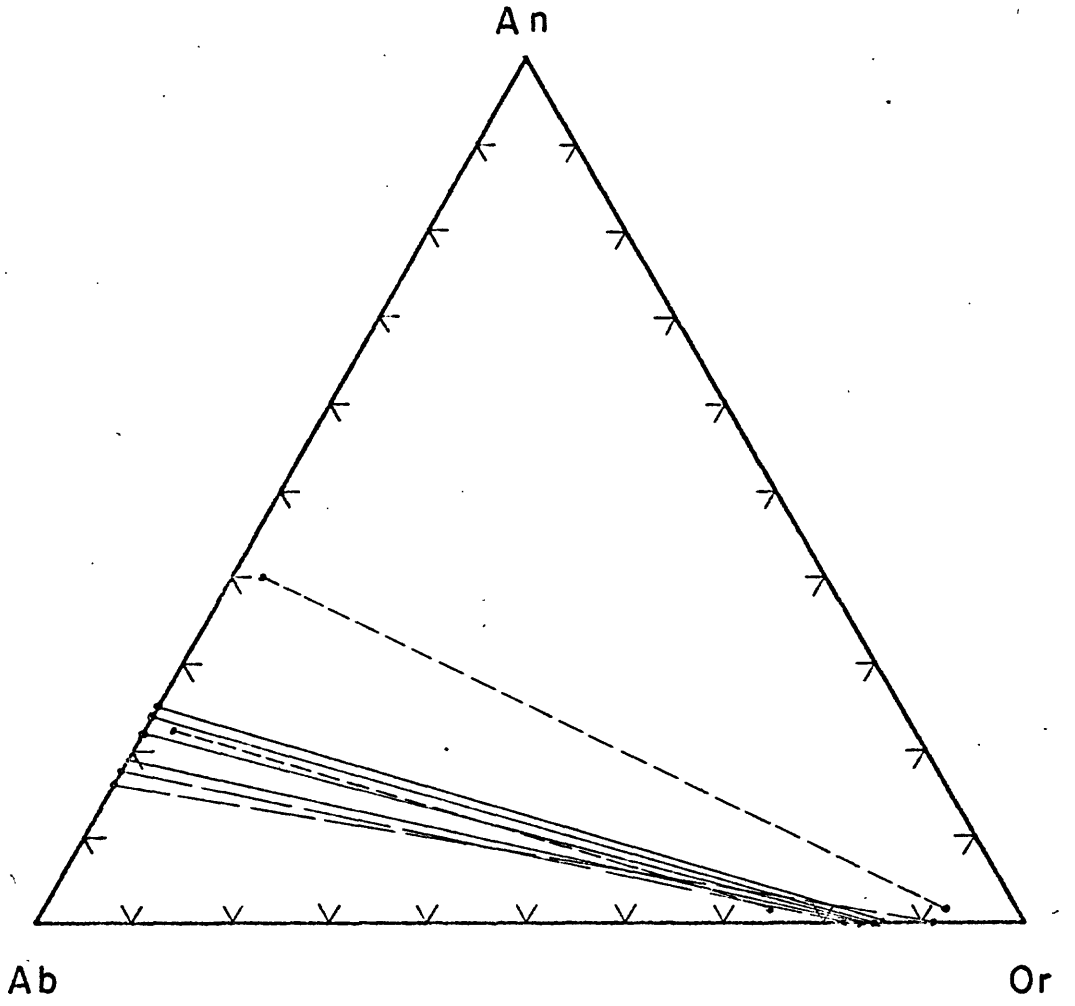

Figure 52: Ab-An-Or ternary with coexisting feldspar tielines from:

experimental work of Yoder and others (1957)
mafic quartz monzonite
porphyritic quartz monzonite

Until recently no experimental results were available on the liquidus relationships in An-bearing granitic systems and petrogenetic arguments based on analogy with only the Q-Ab-Or or An-Ab-Or ternaries have suffered from this deficiency.

Figure 53 shows the isobaric liquidus (1 Kb) at a constant An content of 5 weight percent determined by James and Hamilton (1969). Although it is improbable that phases within the Silver Plume granitic rocks equilibrated at pressures of only 1 Kb, the close association of the normative compositions with the ternary cotectic indicates that crystal-liquid equilibrium crystallization was probably important in the evolution of these rocks.

A number of theories have been proposed to explain the genesis of batholithic igneous rocks. These include:

a) Magma derived by partial fusion of upper crustal material.

b) Magma derived by partial fusion of crustal material and contamination of the melt with mafic material derived from the upper mantle.

c) Differentiation of magmas produced by partial melting within the upper mantle to produce granitic magmas which rise to the crust.

d) Magma derived by partial fusion of the upper mantle which moves up to the crust and is contaminated by crustal materials.

e) Granitization

Of these processes the last, granitization, is considered the most improbable. One of, or some combination of the first four processes was responsible for the generation of the Silver Plume

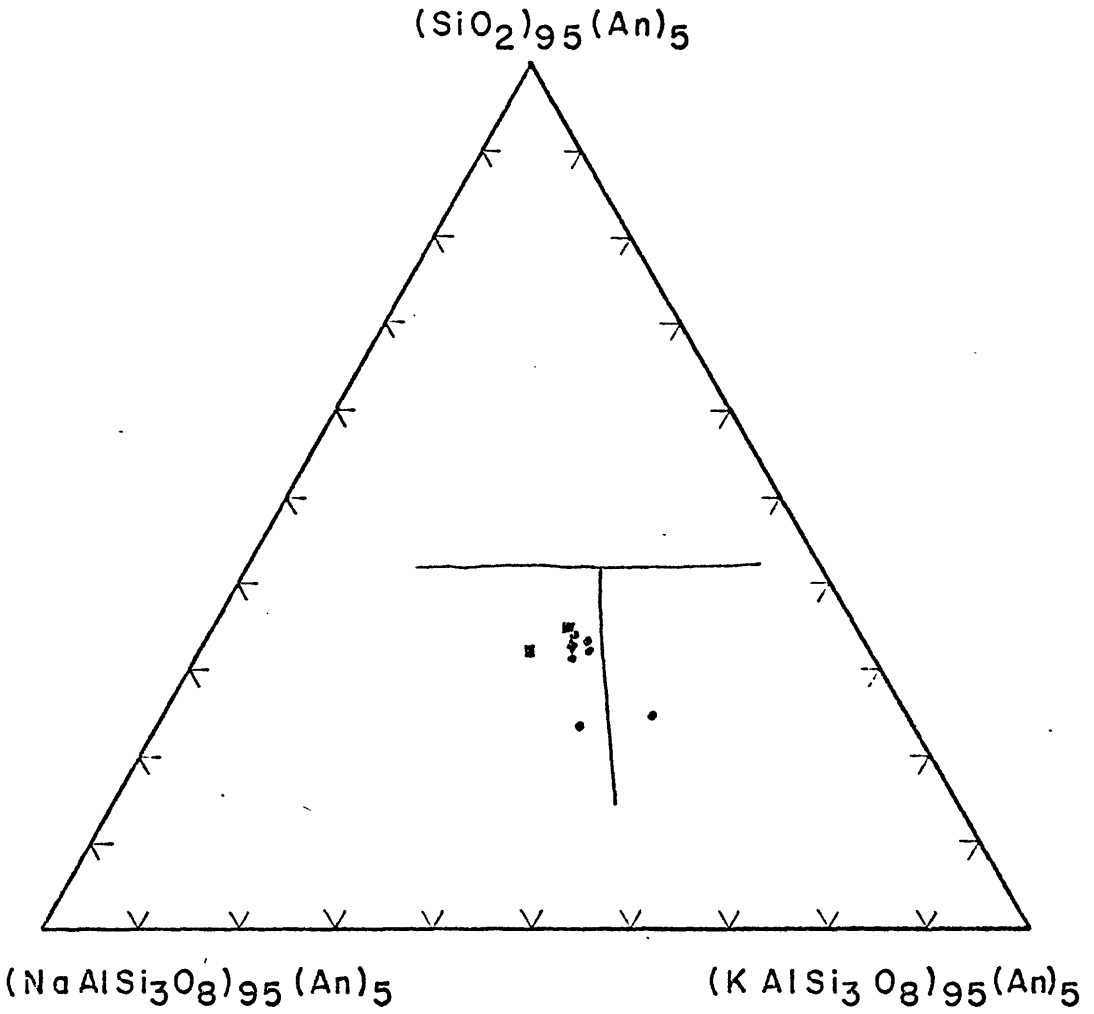

Figure 53: Section through the H_2O saturated Q-Ab-An-Or quaternary at An_5 for P_{H_2O} = 1kb. Traces of the univariant boundary curves are shown. CIPW norms of Silver Plume Granite are plotted. Experimental data is from James and Hamilton (1969). Symbols are as in figure 50.

magmas.

Isotopic evidence provides the key to the interpretation of the relative roles of mantle and crustal materials in the partial melting process. Hurley and others (1965) demonstrated that the initial Sr^{87}/Sr^{86} ratios of the Sierra Nevada granitic rocks were too high for these magmas to have been derived from the mantle directly and too low to have been derived only from crustal materials. The work of Peterman and others (1968) indicates that somewhat similar conclusions are valid for the 1.4 b.y. Silver Plume intrusives of the Front Range. Sr^{87}/Sr^{86} initial ratios range from 0.7025 to 0.7031 for the different Silver Plume batholiths. These values are well below Sr^{87}/Sr^{86} ratios for the upper crustal metamorphic wall rocks at the time of emplacement (0.710-0.730, based on analysis of data presented in Peterman and others, 1968) and slightly above the probable Sr^{87}/Sr^{86} value for mantle derived basaltic rocks at that time (0.7015, based on consideration of the Sr^{87}/Sr^{86} evolution diagram of Hamilton and Meyer, 1967). These data indicate:

a) the Silver Plume granitic magmas must have had a sizeable component of upper mantle or lower crustal derived material mixed through contamination by assimilation or hybridization processes.

b) they cannot have been derived entirely from mantle material by partial melting; at least some crustal material was involved in the melt.

Of the four postulated processes of magma generation it is now possible to eliminate the first, magma derived by partial fusion of

upper crustal material, as being incompatible with the isotopic data. Some combination of upper mantle, lower crustal and upper crustal partial melting with subsequent hybridization is the most plausible mechanism. Whatever the mechanism, it has produced a series of plutons of generally quartz monzonitic composition. Extensive partial melting and subsequent differentiation of the upper mantle might be expected to produce large quantities of relatively more mafic magma. There is no evidence for such magma in the Front Range basement. Clearly further work is needed to clarify these problems.

Recent experimental work on granitic rocks of the Sierra Nevada batholith (Piwinskii and Wyllie; 1968, 1970) demonstrates that temperatures of at least 700°C are required to produce melting and extensive melting is required to produce a liquid of intermediate composition. Since the presumed water-undersaturated conditions in the middle or lower crust would further increase the temperatures required for melting, partial fusion must have taken place at great depths; most probably considerably deeper than the site of emplacement.

The strongly porphyritic facies of some of the Silver Plume rocks are compatible with initial formation of magma at depth, consolidation of that magma in a chamber, partial crystallization at depth (forming the large phenocrysts) and finally emplacement as a crystal-liquid mush in the upper crust. The flow layering observed in these rocks could have been developed during this final event.

Insufficient data is available to estimate the depth of emplacement of the Silver Plume plutons. One can only safely say that their petrology and structure are compatible with the mesozonal plutons of Buddington (1959).

The close relationship in time and space of the Silver Plume in the Log Cabin batholith and the Sherman Granite suggests that their petrogenesis was similar. The presence of hornblende is characteristic of some of the Sherman Granite but too little experimental work is available to evaluate the significance of this with regard to the petrogenesis of the Sherman and Silver Plume rocks.

Biotite-muscovite granite

Mechanism of emplacement

The lack of xenoliths suggests that assimilation was of little or no importance in the emplacement of this unit. The xenomorphic-granular texture and the absence of a flow foliation indicate that crystallization must have occurred from a magma in situ at the present structural level. The complexity of the local structure and in particular the effects of the later shearing prevented the recognition of any structures related to a process of forcible intrusion. It seems likely, however, that such a process was largely responsible for the emplacement of this unit. If stoping was the dominant process all stoped blocks have been conveniently eliminated from view.

Chemical and experimental data

These rocks are peraluminous, subsolvus two-mica granitic rocks. A chemical analysis and calculated CIPW norm are given in table 12. Other workers have referred to the Silver Plume rocks as two-mica granites (Lovering and Goddard, 1950; Eggler, 1967); however, in this area the muscovite content of the Silver Plume rocks is quite low and it is in the biotite-muscovite granites that muscovite constitutes a significant fraction of the mode. Also in contrast with the Silver Plume rocks the differentiation index (Thornton and Tuttle, 1960) is higher--93.4 versus 87.2 (mean of eight values).

The abundant micas and fluorite associated with this rock type suggest a high water and volatile content in the melt from which these rocks crystallized. Luth and others (1964) consider the association of pegmatites and aplites plus the subsolvus peraluminous character of the rock as evidence of high water pressures in the magma system at the time of emplacement. Of all the granitic rock types studied, this one is most likely to have crystallized under $P_T = P_{H_2O}$ conditions similar to those of the recent experimental studies.

The norms of the biotite-muscovite granite from table 12 plus the norms of three other samples collected from the Big Thompson canyon area (Braddock, personal communication, 1969) are plotted on the Q-Ab-Or ternary in figure 54. The positions of the boundary curves and ternary minimum for $\{Ab\text{-}Or\text{-}Q\}_{97}\ An_3$ at P_{H_2O} = 1 Kb (James and Hamilton, 1969, p. 118) are also shown. There is a good correlation of the minimum in this experimental system with the norms.

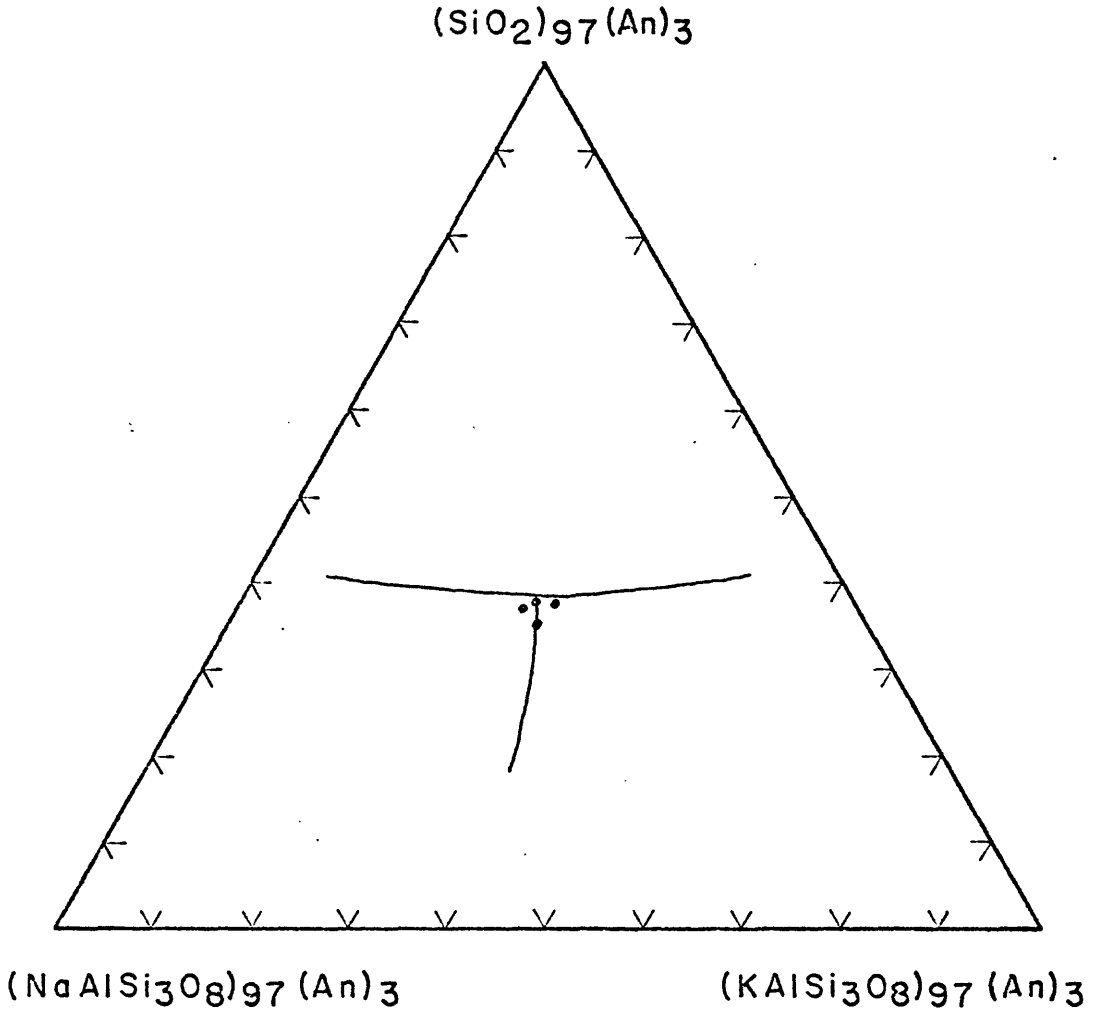

Figure 54: Section through the H_2O saturated Q-Ab-An-Or quaternary at An_3 for P_{H_2O} = 1kb. Traces of the univariant boundary curves are shown. CIPW norms of biotite-muscovite granite are plotted. Experimental data is from James and Hamilton (1969).

The results of James and Hamilton were obtained at P_{H_2O} = 1 Kb. For a number of reasons this value is too low. The abundance of primary muscovite indicates that it was probably a stable phase on the liquidus. The data of Evans (1965) on the stability of muscovite provides a lower limit on the pressure at which crystallization took place. The upper stability limit of muscovite plus quartz and the quaternary minimum of Luth and others (1965) intersect at about 3.5 Kb. This intersection plus the melting data of Piwinskii (1968) and Piwinskii and Wyllie (1970) suggest that equilibrium crystallization took place at about 4 Kb P_{H_2O} and over a temperature interval of 700 to 650° C.

The biotite-muscovite granites have an unusually high initial Sr^{87}/Sr^{86} ratio of 0.721 (Peterman and others, 1968). Peterman and others suggested that this may have resulted from the production of a melt by partial melting of crustal rocks with unusually high Sr^{87}/Sr^{86} ratio or by contamination of a melt with older metamorphic rocks. Whichever origin is correct the large difference between the initial ratio of the Silver Plume granitic rocks and the biotite-muscovite granite demonstrates that different processes were important for their respective petrogenesis.

CHRONOLOGY OF GEOLOGIC EVENTS

Sedimentation, early deformation and greenschist facies metamorphism

At some time prior to the high-grade regional metamorphism a thick sequence of graywackes, psammites and pelites were laid down, possibly in a geosynclinal environment, on a basement as yet unrecognized in the Front Range. Interlayered with these sediments were basaltic and dacitic volcanics. Shortly after, or during, sedimentation an early schistosity was developed by intergranular movement in compacting sediments and was followed by a low-grade greenschist facies metamorphism (Braddock, 1970). These processes are only recognizable in a limited area to the south of this mapped area. There is no reason to suppose similar processes did not take place in the Poudre Park-Big Narrows area. The rare F_1 folds there may be related to the process which produced the early schistosity and isoclinal folds in the south.

No accurate estimates of the age of these events in the Front Range are available. However the recent work in the Precambrian of the Needle Mountains and related isotopic ages does provide some interesting data (Barker, 1969; Barker and others, 1969; Silver and Barker, 1968). In that area initial sedimentation and volcanism produced a sequence of conglomerates, basic and acidic volcanics and minor graywackes. These rocks were isoclinally folded and metamorphosed at about 1.8 b.y. Both the U-Pb data on zircons from the metavolcanics and whole rock Rb-Sr data on these rocks give similar results. This and the low Sr^{87}/Sr^{86} initial ratios for the Twilight gneiss suggest a small time interval between sedimentation,

volcanism and metamorphism (Barker and others, 1969). Although an early period of deformation, pre-amphibolite facies metamorphism, has not been recognized in the Needle Mountains area the similarity in ages of the whole rock Rb-Sr data for this area and the Front Range suggests that these events may be part of a large Precambrian orogenic event at 1.8 - 1.7 b.y. The early events in the Front Range Precambrian rocks may also have taken place over a short time interval. Similar studies on U-Pb zircon systems are needed since Rb-Sr whole rock studies have proven to be useless in determining ages of these early events in the Front Range (Peterman and others, 1968).

F_2 folding, high grade metamorphism and Boulder Creek plutonism

At approximately 1.75 b.y. a regional metamorphism was superimposed on these rocks producing sillimanite + muscovite and sillimanite + microcline assemblages over a wide region in the northern Front Range (Peterman and others, 1968). Only in a small area within the Drake and Masonville quadrangles was this metamorphism of lower grade (biotite, garnet and staurolite isograde were developed). Much of the metasediments in the Poudre Park-Big Narrows area are highly migmatitic and this area was affected by the greatest intensity of metamorphism of this period. The F_2 folding developed synchronously with the high-grade metamorphism producing macroscopic and mesoscopic structures, the latter containing small folds with synkinematically recrystallized minerals. Contemporaneous with, or shortly following the metamorphism, migmatization and folding the emplacement of large phacolithic bodies of Boulder Creek

granodiorite occurred.

At approximately the same time in the Drake-Masonville area deformation and plutonism was also occurring except that there the style and timing of the deformation was distinctively different. Two sets of slip cleavages (one trending NE and one NW) were produced, both forming slightly before the growth of the porphyroblastic index minerals of the high-grade metamorphism (Nutalaya, 1966). Thus, in the southern area deformation reached maximum intensity somewhat earlier than metamorphism whereas in the north they appear to have been synchronous. Perhaps the heat source was closer to the northern area permitting the maximum temperatures to be reached earlier there while essentially the entire area was simultaneously under stress. The disappearance of the slip cleavages to the north may be due to the different rhealogical behavior of similar rocks at different metamorphic grade. The rocks in the north were at second sillimanite isograde conditions and highly migmatitic whereas those to the south were still at a lower grade.

Plutonic activity in the southern area was approximately synchronous with the deformation. However, the picture is complicated by the presence of a second group of intrusives of tonalitic composition varying relationships with the slip cleavage deformation (Nutalaya, 1966).

F_4 folding and Silver Plume plutonism

At some time after the 1.7 b.y. events a northwest-trending

swarm of andesite dikes was emplaced, some of which extend into the Poudre Park-Big Narrows area. They are found as inclusions within the 1.4 b.y. old Silver Plume intrusives. Eggler's (1967) mapping to the north indicated two ages of andesite dikes; some cut Sherman Granite, some do not, none of the dikes cut the Silver Plume intrusives. The radiometric ages of the Sherman and Silver Plume intrusives are essentially identical; field relations indicate that the Sherman is older (Eggler, 1967).

In the Poudre Park-Big Narrows area andesite dikes were emplaced either before, during or following the emplacement of Sherman Granite; no crosscutting relationships were observed. After the emplacement of a small stock of Sherman, extensive plutonism resulted in the formation of the Log Cabin batholith, which was probably a composite batholith composed of at least three facies: quartz monzonite, mafic quartz monzonite and porphyritic quartz monzonite. Age relations of these different facies are unknown precisely but their emplacement probably overlaps in time. Emplacement appears to have been by a combination of forcible intrusion, stoping and assimilation.

A widespread retrograde metamorphism indicated by late muscovite after sillimanite, sericitized plagioclase and altered garnets is correlated with the emplacement of the Silver Plume plutonic rocks.

Intrusion of the plutonic rocks and a resulting N-S compressive stress produced a new set of small crinkle folds, F_4, primarily in the hinge regions of older F_2 folds by the tightening up of these folds under renewed stress.

Mylonitization

At about 1.2 b.y. ago numerous northeast trending mylonitic shear zones developed including a particularly prominent zone, the Skin Gulch shear zone. The dominant process in the development of the mylonitic textures was probably progressive flattening. Strike-slip displacement was probably negligible.

Heat generated by the deformation within the shear zone may have produced a suite of anomalous andalusite-cordierite assemblages adjacent to the shear zone. Extensive recrystallization took place within the shear zone as indicated by a new mica microfabric.

Chevron and isoclinal intrafolial folds within the shear zone, F_5, were produced during the formation of the shear zone. Their exact relationship with the postulated movement picture for the shear zone remains an enigma.

Subsequent deformation and other Tertiary events

Two (?) later periods of brittle deformation resulted in the fracturing and rehealing of the early mylonitic shear zones with a quartz, epidote and calcite gangue. Displacement during one of these events probably involved left-lateral strike-slip displacement on NE trending faults.

Extensive brittle fracture, alteration, oxidation and minor metalization occurred during Laramide faulting. The nature of fault displacements are almost unknown but possibly high-angle normal or reverse. Metalization is probably non-economic.

Small porphyry dikes and one rhyolite porphyry plug were

emplaced at some time during the Tertiary. Original exposures may have been more extensive as porphyry cobbles are more common in Miocene-Pliocene gravels developed along an old course of the Cache La Poudre River than in present river gravels. Laramide deformation may have extended into the late Tertiary as these gravels may be displaced along high-angle faults.

Rb-Sr WHOLE ROCK STUDY OF THE SKIN GULCH SHEAR ZONE

Introduction

The age of the northeast-trending, mylonite-bearing shear zones constitutes a major remaining deficiency in our knowledge of the age of Precambrian tectonic events in the Front Range. Prior to this study the age of the initial movement on these zones could only be said to be younger than Silver Plume plutonism (1.4 b.y.) and older than Pennsylvanian sedimentation (Fountain Formation).

The widespread development of "mylonitic" textures within these zones is indicative of extensive cataclasis and recrystallization. The efficiency of chemical differentiation processes in metamorphic terrains is well known (Turner and Verhoogen, 1960, p. 581-586). A number of authors have discussed the origin of mylonites through mechanical processes and the possibility of an origin through chemical processes and Prinz and Poldervaart (1964) and Sclar (1965) concluded that the primary agent was mechanically induced strain. However, recent work has also indicated the common association of low-to-high-grade mineral assemblages with mylonitic rock fabrics (Hsu, 1955; Christie, 1960; Sarkar, 1966; Theodore, 1970 and this work). This evidence indicates that medium to high temperatures are characteristic of some mylonite-bearing shear zones and the presence of recrystallization fabrics (blastomylonites) are evidence of chemical reorganization.

The northeast-trending Skin Gulch shear zone crops out over

a distance of at least fifteen kilometers. The shear zone varies in width from three meters to four hundred meters. The entire gamut of cataclastic rock types are represented within the zone with local development of blastomylonite and ultramylonite in bands up to a meter thick. Rock types involved in the shearing include amphibolite, biotite schist and calc-silicate gneiss approximately 1.7-1.8 b.y. in age and pegmatite and Silver Plume quartz monzonite, approximately 1.4 b.y. in age. Locally, adjacent to and within the shear zone, andalusite-cordierite-bearing assemblages are developed in the migmatitic biotite schists. Field relationships strongly suggest that these metamorphic assemblages are the product of processes within the shear zone.

The microscopic textures in the cataclastic rocks indicate extensive recrystallization. The phyllonites show development of medium-grained lepidoblastic muscovite and chlorite. In the very-fine-grained blastomylonites and ultramylonites the micaceous minerals have a strong preferred orientation.

The development of layered mylonites suggests transport of material, the development of secondary muscovite and chlorite indicates extensive recrystallization and neomineralization and the thermal aureole suggests temperatures characteristic of hornfels-facies metamorphism.

It is postulated that, if chemical transport and recrystallization are significant processes within these zones, homogenization (partial or complete) of the strontium isotope distribution will have taken place, and dating the time of mylonitization may be

possible. If this hypothesis is correct then over what volumes has the Sr^{87}/Sr^{86} ratio been homogenized? Over what distance has transport of Sr and possibly Rb been effective?

This study was undertaken to attempt to answer these questions.

Specific Sample Suites

Three different suites of samples were collected, each representing a different scale of observation within the shear zone. These three suites represent respectively the hand-specimen scale, the outcrop scale and the geologic-unit scale. Analysis at these various levels should permit estimation of the scale of Sr isotope homogenization.

The first suite of six samples (group I) was taken from a single 10-cm-wide band of layered blastomylonite by sampling six discrete layers within the band. The host rock was probably a biotite schist, perhaps slightly migmatitic. The individual samples were cut from the band using a diamond saw.

The second suite of four samples (group II) was taken from across the face of an outcrop exposing approximately three meters of mylonitic rocks ranging in texture from augen gneiss to ultramylonite. The mylonites were strongly color banded and each sample included a number of bands. The host rock was probably a combination of pegmatite, Silver Plume quartz monzonite, biotite schist and amphibolite (?).

Three additional samples were taken, one each from three other outcrops of mylonitic rocks within the shear zone. These three

samples were from rocks with textures ranging from that of phyllonite to that of ultramylonite. Host rocks were probably pegmatite and biotite schist. These samples combined with the samples of group I and II constitute group III.

All of the sample sites are shown on figure 55. The central portion of the Skin Gulch Shear zone was profoundly brecciated and altered by the crosscutting Poudre River fault zones during the Laramide orogeny. Outside of this zone evidence for later hydrothermal alteration, metasomatism and brecciation is minimal to non-existent. No sampling of the central zone was attempted.

Analytical Methods

Whole rock Rb-Sr analysis techniques were used in this study. The experimental and theoretical aspects of these techniques are now firmly established (Fairbairn, 1961; Nicolaysen, 1961; Riley and Compston, 1962; Lanphere, et al., 1964). X-ray fluorescence and isotope-dilution procedures were used.

X-ray fluorescence analysis

All samples were initially analyzed using X-ray fluorescence techniques to provide information for the selection of samples for isotope-dilution analysis and for the selection of proper spike proportions. Direct determinations for Rb/Sr ratios using X-ray fluorescence techniques were not made. Measurements were made on a General Electric unit, model XRD-6S, with a molybdenum target and a LIF crystal. Procedures were those of Peterman, et al., (1968) and Doering (1968). Powdered rock samples (-200

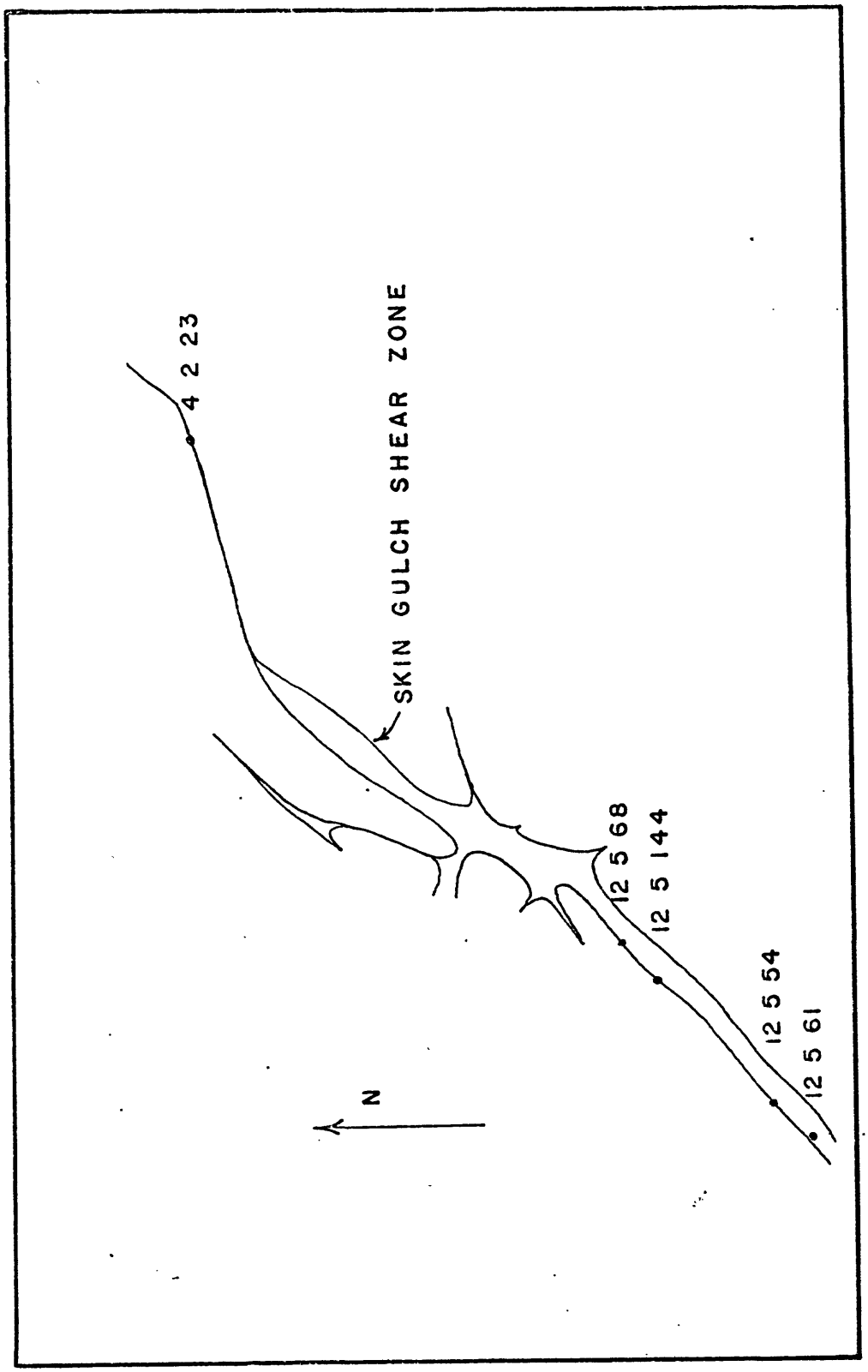

Figure 55: Sample locations for isotope study.

mesh) were ground in a Specs ballmill for approximately eight minutes. Analyses were made on the powdered rock samples which had been loaded directly into nylon sample planchettes.

Rb content, Sr content and the Rb/Sr ratio of each sample were determined. The sample runs were alternated with runs made on standards chosen for similarity in rock type and composition. The Rb/Sr ratio was corrected against the Rb/Sr ratios determined by isotope-dilution techniques using the previously determined procedures of Doering (1968). This procedure should guarantee a precision in the determination of Rb/Sr of 3 percent. The precision of the determination of Rb and Sr contents is lower but still high enough to permit use of the data for estimation of spike proportions in the isotope-dilution runs.

Isotope-dilution analysis

The sample dissolution and spiking techniques are those of Peterman, et al., (1967). Spike compositions were chosen on the basis of the X-ray fluorescence data. Runs were made on 6-inch, 60°, single-focusing mass spectrometers using triple-filament techniques. Unspiked runs made for the determination of Sr^{87}/Sr^{86} and spiked runs made for Rb and Sr compositions were made on separate mass spectrometers.

All Sr isotopic data are normalized to $Sr^{86}/Sr^{88} = 0.1194$. In the Rb-Sr calculations the constants used were:

$$Rb^{87}\lambda_{\beta} = 1.39 \times 10^{-11}/\text{yr}.$$

Normal Rb isotopic composition: $(Rb^{85}/Rb^{87}) = 2.591$

The estimated precision of determination of individual points

on the isochrons are: Rb^{87}/Sr^{86} - $\pm$ 1.25 percent of the value give; and Sr^{87}/Sr^{86} - $\pm 0.0002_5$.

Results

The isotope-dilution and X-ray fluorescence determinations are presented in table 14. The data are plotted on isochron or strontium-evolution diagrams (Lamphere and others, 1964). The results from the group I samples are plotted in figure 56, the results from the group II samples in figure 57 and the results from group III samples (all points) in figure 58. The isochrons were fitted to the data using the least-squares refinement technique of McIntyre and others (1966). All ages determined from the isochrons are tabulated in table 13.

From figures 56-58 it is clear that the fit of all points to a unique isochron is far from possible. The considerable discordance of a few of the points was considered in the calculation of the isochrons in the following manner. One point (12-5-144-68) in group I is considerably discordant. This point was redone and essentially the same results were obtained. Therefore, because of the ambiguous nature of this point, two isochrons were calculated for the group I data: one including all the points and one excluding the discordant point. Both are tabulated in table 13, only the latter is plotted in figure 56. All group II points were used to compute the group II isochron. For the group III data two isochrons were computed: one utilizing all points except 12-5-144-6B and one utilizing all points except 12-5-144-6B, 12-5-54D and 12-5-68D, the most discordant points.

TABLE 13

Summary of Radiometric Ages Determined

from the Isochron Plots in figures 56, 57, and 58

	Age in 10^6 years	Initial Sr^{87}/Sr^{86}
Group I Data: Hand Specimen Scale		
Including all six points	1445 ± 517	0.7268
Excluding point 12-5-144-6B	1056± 320	0.7469
Group II Data: Outcrop Scale		
Including all points	1210 ± 244	0.7336
Group III Data: Shear Zone Scale		
Including all data points (Groups I, II, III) except 12-5-144-6B	1193± 90	0.7391
Including all points but 12-5-144-6B 12-5-54D 12-5-68D	1180 ± 64	0.7385

TABLE 14

Rb-Sr Data for the Mylonitic Rocks from the Skin Gulch Shear Zone

	X-Ray Fluorescence			Isotope Dilution			
Sample	Rb,ppm	Sr,ppm	Rb/Sr*	Rb,ppm	Sr,ppm	Rb^{87}/Sr^{86}	Sr^{87}/Sr^{86}
			GROUP I				
12-5-144-1B	83.7	74.9	1.12	90.1	81.7	3.22	0.7943
12-5-144-2B	103	72.7	1.42	118	86.4	3.98	0.8084
12-5-144-3B	114	77.5	1.47	119	84.4	4.12	0.8070
12-5-144-4B	120	69.1	1.74	139	81.6	4.97	0.8192
12-5-144-5B	81.6	68.8	1.19	83.1	70.5	3.44	0.7969
12-4-144-6B	103	47.8	2.16	108	51.9	6.10	0.8598
			GROUP II				
4-2-23E	231	130	1.78	197	114	5.05	0.8216
4-2-23F	350	127	2.76	431	154	8.21	0.8718
4-2-23G	291	137	2.12	259	124	6.12	0.8379
4-2-23M	254	179	1.42	237	170	4.07	0.8008
			GROUP III				
12-5-54D	133	109	1.22	127	106	3.49	0.8021
12-5-61G	219	47.3	4.62	229	50.4	13.46	0.9643
12-5-68D	197	81.8	2.41	199	83.7	6.98	0.8675

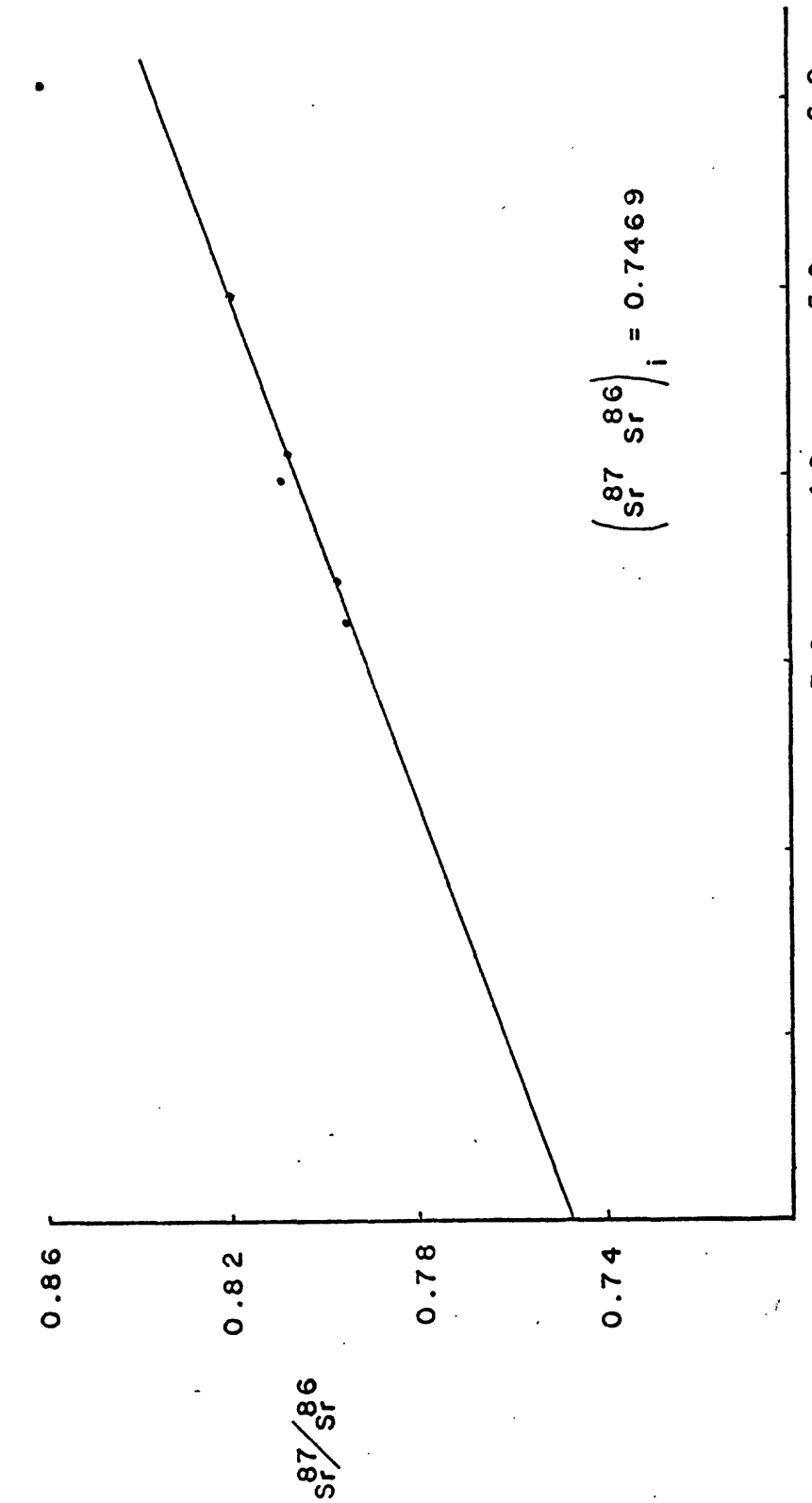

Figure 56: Rb^{87}/Sr^{86} - Sr^{87}/Sr^{86} plot of group I data

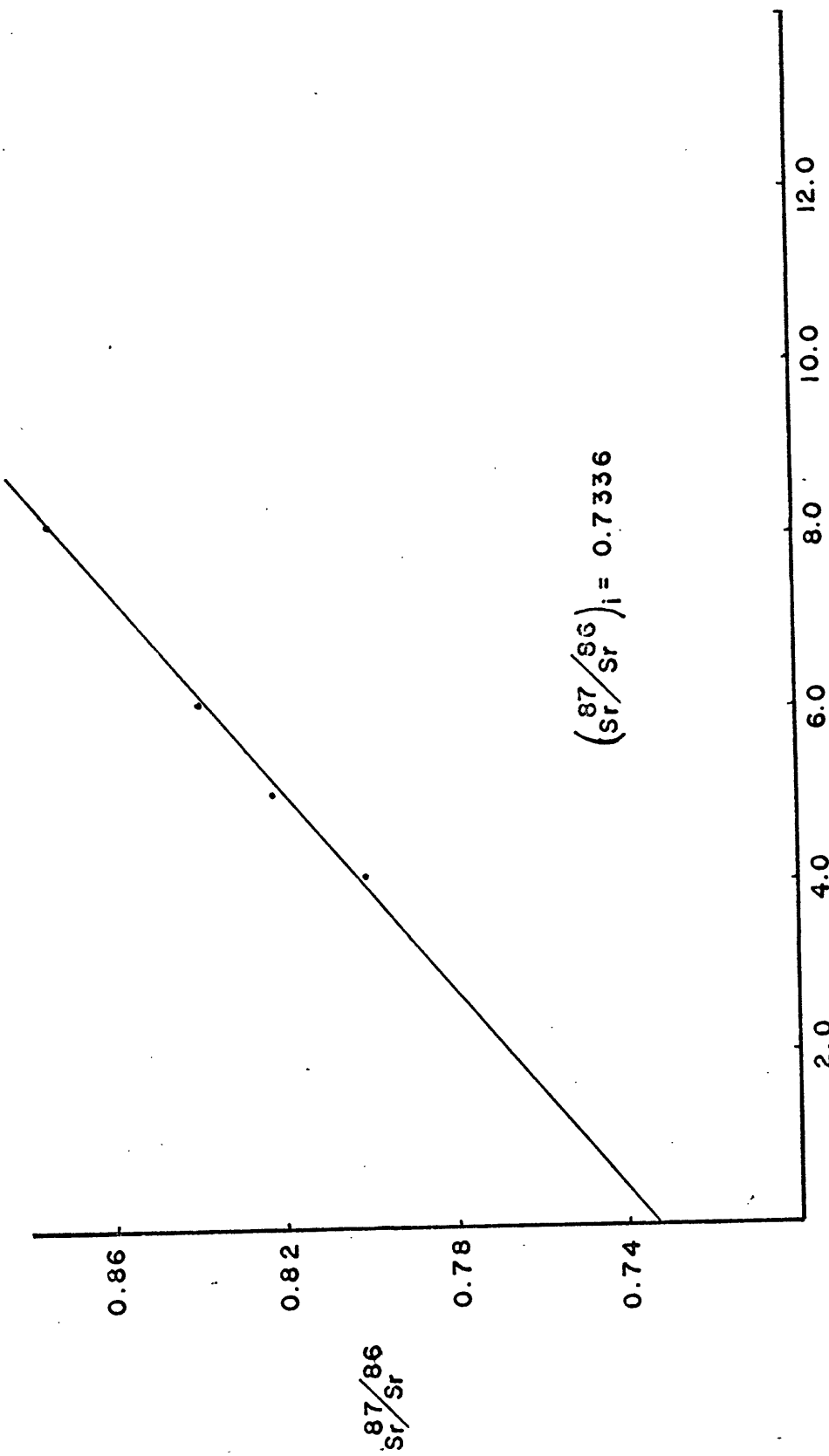

Figure 57: $Rb^{87}/Sr^{86} - Sr^{87}/Sr^{86}$ plot of group II data.

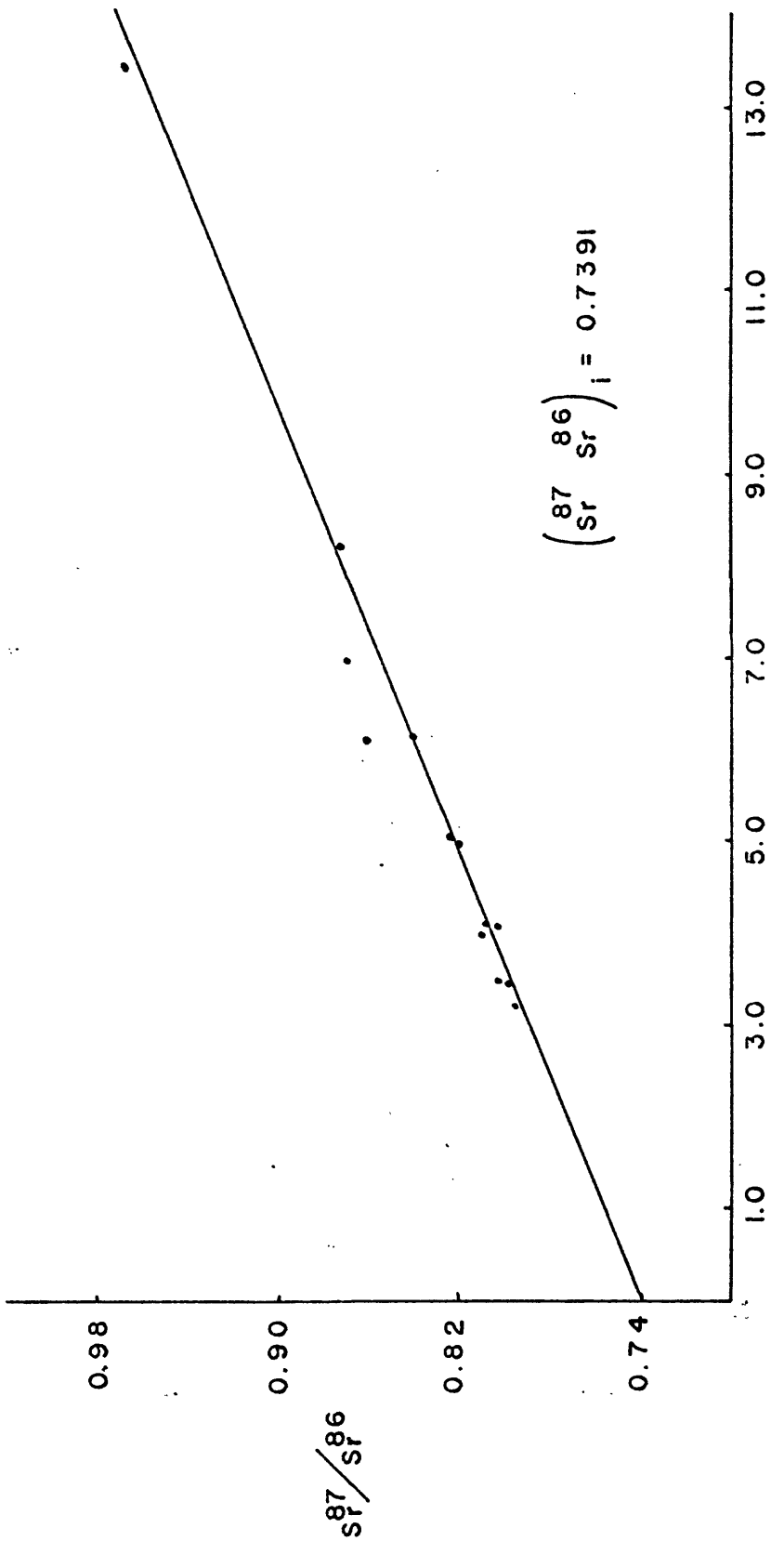

Figure 58: Rb^{87}/Sr^{86} - Sr^{87}/Sr^{86} plot of group III data

Since both isochrons give approximately the same age only the first is plotted on figure 58.

Discussion

There is a wide scatter in the tabulated ages ranging from 1.06 b.y. to 1.45 b.y. All of the ages have some significance as indicators of the redistribution of Sr^{87}, not all of them are significant with regard to the real age of the deformation. The initial assumption of redistribution of Sr^{87} resulting from stress-induced recrystallization is verified. Rocks with an initial age of 1.75 b.y. have been substantially reset. The important question is whether the data supply a real estimate of the age of the shearing, and whether they provide a meaningful estimate of the degree of homogenization and chemical equilibrium in this system.

The group I data, although decidedly scattered, define a recognizable isochron of about 1.06 b.y. excluding the one discordant point. These samples from a layered blastomylonite zone eight cm wide were selected to represent a minimum possible volume of chemical redistribution. The discordant sample is from the outer layer of this suite.

The group II data define a good isochron with an age of 1.21 b.y. Although this is based on only four points the spread in the Rb^{87}/Sr^{86} values is greater than in the group I data. Both group III isochrons give ages of about 1.185 b.y. and due to the larger number of points the error limits at the 95 percent confidence level are considerably less (see table 13). The exclusion of

points 12-5-54D and 12-5-68D has no significant effect on the age although these points are certainly more discordant than might be explained simply by analytical error.

Assuming either complete or incomplete homogenization and a subsequently open or closed system there are four possible processes which might affect an array of whole rock data points.

1) Complete homogenization followed by closed system evolution to the present.
2) Complete homogenization followed by open system evolution to the present.
3) Incomplete homogenization followed by closed system evolution to the present.
4) Incomplete homogenization followed by open system evolution to the present.

In the general case only process (1) will produce a linear array of whole-rock data points. Under special circumstances process (3) might also; however this is unlikely enough to justify neglecting it as an alternative. Processes (2), (3) and (4) will produce a scattered array of whole-rock data points on an isochron plot.

Previous work on Precambrian rocks of the northern Front Range (Hedge and others, 1967; Peterman and others, 1968) indicates that whole rock Rb/Sr systems behaved as closed systems subsequent to the 1.75 b.y. high-grade metamorphism and subsequent to the 1.4 b.y. plutonic event. Thus it is possible that these rocks also behaved as closed systems subsequent to the cataclastic deformation. Incomplete homogenization of Sr^{87}/Sr^{86} is the most reasonable

explanation of the scatter in these isochrons.

Since the shear zone was undoubtedly a pathway for hydrothermal fluids during late Proterozoic times it may also have been a pathway during more recent events (particularly Laramide events), perhaps leading to open-system conditions. This is considered unlikely for these samples because they were collected where evidence of Laramide reactivation of the shear zone was nonexistent.

The good group II isochron indicates that equilibration (homogenization) of the Sr^{87}/Sr^{86} took place locally over dimensions of at least three meters. It further suggests that transport of Sr perpendicular to the cataclastic foliation must have taken place to permit homogenization even though the mineralogical layering indicates pronounced variations in the bulk chemistry.

Since these data indicate transport of Sr over outcrop wide dimensions the group I hand-specimen data are anomalous. Apparently the homogenization processes were not equally effective throughout the shear zone. Perhaps the group I specimens were collected from a part of the shear zone which was dryer during cataclasis and recrystallization with an associated hydrous intergranular fluid was less pervasive. The fact that the outer layer (the layer of the blastomylonite immediately adjacent to the less sheared well rocks) is the most discordant is compatible with this hypothesis and further suggests that the effectiveness of this process changed abruptly over very short distances. Mixing was presumably less than perfect at the edge of that zone.

The overall scatter between outcrops indicated by the group

III data indicates that homogenization was probably not a shear-zone-wide phenomenon. However the reasonable agreement of the group II and group III isochrons suggests strongly that this event took place about 1.2 b.y. ago.

A large amount of isotopic data is available on the Precambrian rocks of the northern Front Range (Peterman and others, 1968).

It is possible to utilize this data to construct a diagram which crudely illustrates the nature and amount of isotopic exchange necessary within the rocks in the shear zone to homogenize Sr^{87}/Sr^{86}.

Two isochrons are shown on figure 59; the 1.2 b.y. isochron from the group III data and a 500 m.y. isochron calculated from the data of Peterman and others (1968). The former illustrates the present distribution of isotopic ratios and the latter illustrates the distribution of isotopic ratios in the unsheared wall rocks as they would appear 1.2 b.y. ago just prior to mylonitization (500 m.y. after the beginning of closed system evolution). The data of Peterman and others (1968) were obtained from medium to high grade metamorphic rocks and igneous rocks within the northeastern Front Range. Thus they should provide an acceptable estimate of the isotopic ratios in the vicinity of the Skin Gulch shear zone at the time of mylonitization.

Assuming that complete homogenization did take place within the Skin Gulch shear zone at least over small volumes, the distribution of isotopic ratios indicated by the 500 m.y. isochron must have been reset to the 0.739 initial of the group III isochron. Since the 500 m.y. data points are distributed both above and

Figure 59

Comparison of isochrons for Skin Gulch shear zones with isochrons for unsheared igneous and metamorphic rock

———————— 1.2 b.y. group III isochron determined in this study

— — — — — — 500 m.y. isochron as it would appear at 1.2 b.y. for rocks originally isotopically homogenized at 1.75 b.y.

The data points utilized in the calculation of the 500 m.y. isochron are from Peterman and others (1968).

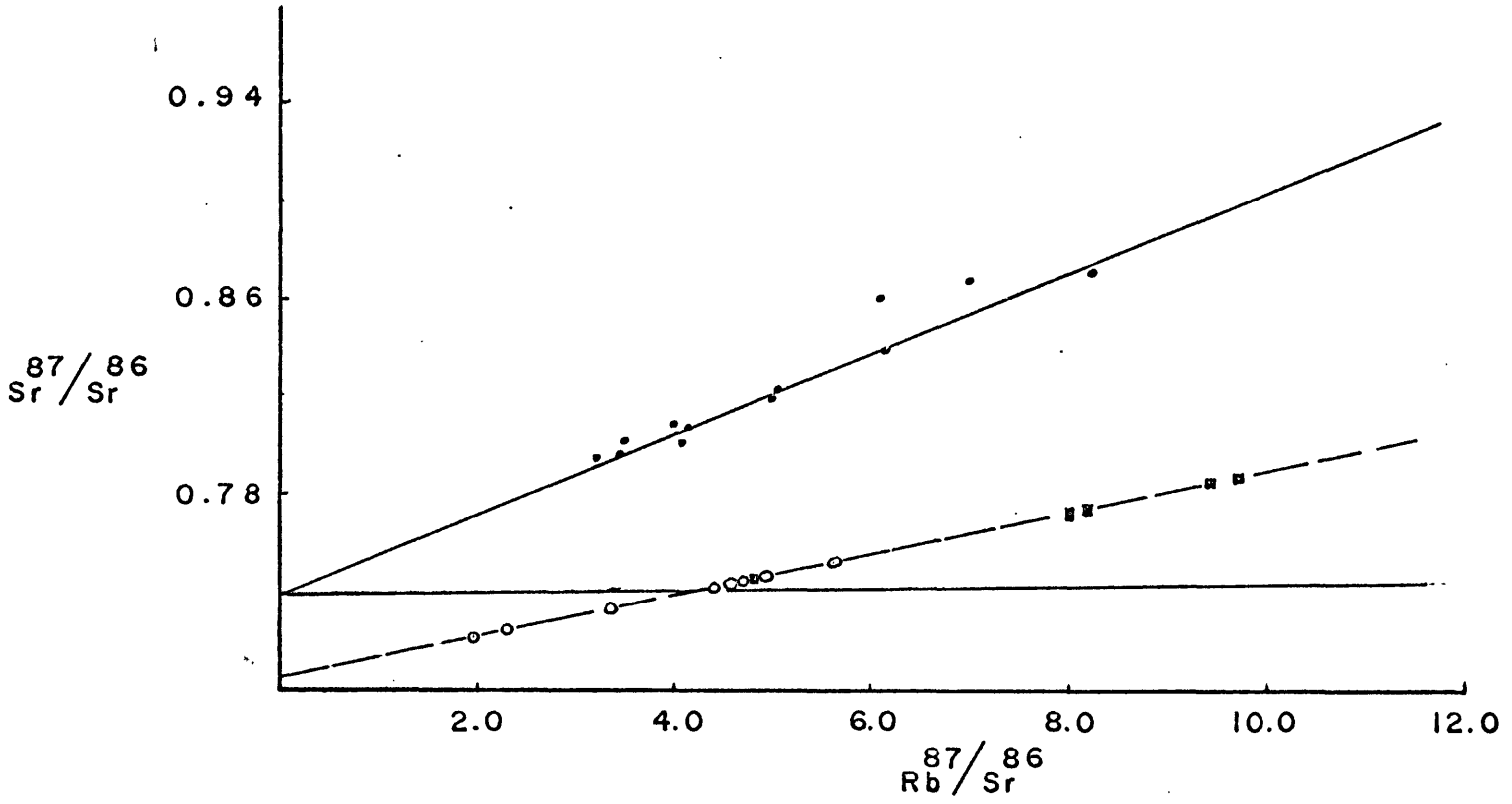

Figure 59: Comparison of isochron for Skin Gulch shear zone with isochron for unsheared igneous and metamorphic rock

below this initial ratio, simple exchange of radiogenic strontium could have been the dominant mechanism of homogenization.

In order to accurately plot exchange paths and to determine the extent of transport of Rb the precise original isotopic ratios within the unsheared rocks must be known. Unfortunately these are unknown.

In summary this whole rock Rb-Sr study has established that partial to complete homogenization may occur in zones of intense strain and recrystallization and that the whole rock Rb-Sr technique may be used to obtain the ages of these shear zones. These studies provide further and more detailed support for this application of the whole rock Rb-Sr technique originally suggested by Dietrich and others (1969). Further studies are needed on mylonitic zones cutting isotopically homogeneous rocks of known composition to determine to what extent both Sr and Rb are mobilized by stress-induced recrystallization.

TERTIARY AND QUATERNARY DEPOSITS

Late Tertiary Gravels

There are extensive deposits of high-level sand and gravel extending northeast from the west-central boundary of the Big Narrows quadrangle into the Livermore embayment area. These deposits are restricted to a narrow band from one to two kilometers wide and now lie from 400 to 800 feet above the present channel of the Cache La Poudre River. They consist of sand and gravel locally poorly sorted, with large boulders in excess of one meter in diameter. Exposures within the Big Narrows and Poudre Park quadrangles are poor; the gravel-covered areas are masked by a boulder-studded colluvial cover and form smoothly rounded hills (fig. 60). The only good cross section of the deposits occurs in section 3, R71W, T9N in the Livermore Mountain quadrangle where a roadcut has exposed a fifty foot section of gravel and interbedded sands and silts.

The cobbles consist primarily of granitic rocks derived from the Log Cabin batholith, granitic gneiss derived from layers of microcline-quartz-plagioclase-biotite gneiss and minor amounts of metasediments and Tertiary intrusive (?) igneous rocks. These latter rocks are more abundant in these gravels than in the low-level terrace gravels and alluvium of the present channel of the Cache La Poudre River. The distribution of rock types in both types of deposits is otherwise quite similar. The rocks within the high-level gravels are more weathered than those present in the low-level terraces.

Figure 60: View of Late Tertiary gravels forming gravel-covered bench (grassy ridge in middle of photograph). View is to the northeast.

A detailed analysis of the thickness and distribution of the gravels is hampered because of extensive dissection and extensive transport of gravels downslope as colluvial debris. The latter process has blurred the bedrock-gravel contacts. The deposits vary in thickness, being as much as 200 feet thick in the vicinity of Green Mountain and possibly even thicker farther to the northeast. In many places later dissection has so modified the deposits that only remnants remain as small caps on ridges, hilltops or valley-sides.

Farther to the north in the Prairie Divide area, extensive gravels similar to these have been recognized (Bryan and Ray, 1940). Recent work in this area by Denson (referred to by Richmond, 1965, p. 218) established a possible Miocene-Pliocene age for these deposits on the basis of a correlation with the Ogallala Formation. If the gravels in the Poudre Park-Big Narrows are correlative, as seems possible (W.C. Bradley, 1969, personal communication), they may also be of Miocene-Pliocene age.

The linear distribution of these deposits and the presence of stratification and sorting suggests that these are fluvial deposits originally laid down in a late-Tertiary stream channel. The trend of these deposits coincides at the western border of the Big Narrows quadrangle with the present channel of the Cache La Poudre River. No similar deposits to the west are known. Apparently in the late Tertiary the Cache La Poudre river drained to the northeast into the Livermore embayment rather than due east as it does now. The gradient of the late Tertiary stream channel can only be crudely estimated. It appears to be less

than that of the present river (old channel--8 feet/mile; new channel--15 feet/mile).

These observations raise some interesting questions. Why are there no gravel deposits to the west? Possible explanations include a lack of aggradation to the west and/or later dissection. More-detailed work on the surficial deposits to the west is needed in order to answer this question. Dissection cannot be the whole answer because then the downstream deposits must still be explained.

Assuming that a stream diversion did take place in the latest Tertiary, why did it take place? Possible explanations include structural diversion, stream piracy and aggradation leading to the spill-over of a divide (W.C. Bradley, 1970, personal communication). Again too little data are available to choose between these alternatives.

There is a possibility that in the Livermore Mountain quadrangle the gravels are displaced by high-angle faults of unknown throw, presumably related to the uplift of the present mountain range (W.A. Braddock, 1970, personal communication). The stream diversion may be related to the uplift and rotation (?) of the northern Front Range crustal block in late-Tertiary times.

Stream piracy is a possibility. Assuming an elevation of about 7000 feet for the late-Tertiary valley at the westernmost exposure of gravels and no structural disturbance, the relative gradients of the old channel draining out to Livermore and the present channel draining to La Porte can be estimated. The present channel has a gradient perhaps twice as great as the

postulated late Tertiary stream channel. If such a difference also existed at the time of stream diversion it may have been largely responsible for the more rapid headward erosion of the present channel resulting in eventual stream piracy.

The locally thick sequences of gravels particularly in the south-central portion of the Livermore Mountain quadrangle and the north-central portion of the Poudre Park quadrangle indicates that extensive aggradation took place. Whether or not such a process led to complete valley filling and spill-over into an adjacent drainage at the present junction of these systems it may have been a contributing factor in a complicated process involving structural disturbance and stream piracy.

The present channel of the Cache La Poudre River merits some additional comment. The mapping within the Poudre Park and Big Narrows quadrangles established the existence of a large east-west fault zone, the Poudre River fault. Within the Poudre Park quadrangle the river channel corresponds closely with this fault. However, within the Big Narrows quadrangle the river diverges markedly from the trace of the fault zone. No obvious explanation is apparent. Two minor NNE trending shear zones which bound the Big Narrows region may be of some significance but both have less-well-developed breccia zones than the Poudre River fault.

Quaternary Terrace Gravels

Scattered along the Cache La Poudre River are occasional gravel terraces. These vary from a few feet to as much as eighty feet above the present river level. In some, the bedrock surface

is only thinly veneered with gravels (Narrows picnic-area site) and in others the gravels are from 10 to 40 feet thick. Most of the smaller terraces appear to be perched on the sides of gently to steeply inclined hillsides and assignment of an elevation to either the underlying bedrock surface or the upper gravel surface is an arbitrary decision. Their upper surfaces are now much modified by both dissection and the addition of colluvium. The largest and best-defined terrace surface is Dutch George Flats, which is at an elevation of 20-25 feet above present river level.

Early work (Bryan and Ray, 1940) established a detailed sequence of terraces which were correlated with specific glacial advances in the mountains to the west. The glacial terminology of Bryan and Ray (1940) has been much modified since the time of their work (see Richmond, 1965). No attempt was made to differentiate between different terrace levels on the map; only the larger gravel deposits are shown. The highest gravels may be related to the fifth terrace of Bryan and Ray (1940) which they correlated with the Home moraine some twelve miles to the west of the Big Narrows quadrangle. The Home moraine is now correlated with the late stade of the Bull Lake glaciation (Richmond, 1965). The well-defined Dutch George Flats terrace may be correlative with the second terrace of Bryan and Ray (1940) and the Temple Lake stade of the recent Neoglaciation.

Colluvium and Alluvium

Most hillsides, particularly the lower ones, are covered with scattered patches of colluvium. Talus is developed sporadically on the steepest north-facing hillsides in the Cache La Poudre River Canyon. Neither of these types of deposits were mapped.

Most of the larger streams have associated alluvial deposits. These and some of the larger meadows in the upland areas are mapped as Quaternary alluvium.

In a few places large arcuate blocks (composed largely of gravels) a few hundred meters across with irregular topography are found within the Tertiary gravels. These are mapped as landslide debris. They may actually have moved as large slump blocks. It is not clear whether the underlying bedrock was also involved.

ECONOMIC GEOLOGY

Introduction

A number of prospects are scattered throughout the area mapped. Few encountered anything but narrow discontinuous zones of barren oxidation and gouge along Laramide fault zones or pyrite within some of the amphibolites. Exceptions include some rare scheelite-bearing calc-silicate gneisses and some strongly hydrothermally altered calc-silicate gneisses with minor sulfide mineralization. Preliminary results of a petrographic examination of the largest of these latter two types of deposits are presented as well as some brief comments on the economic potential of the gravels.

Tungsten prospects

At least three tungsten prospects have been located within the Big Narrows-Poudre Park area although only one of them has any record of production (Belser, 1956). Two of these were definitely located by the author, the third was only tentatively identified. No development or assessment work of any kind appears to have been made on these prospects in a number of years and none of the prospects are now under claim. These prospects are located on plate 6 and the names used by Belser (1956) have also been utilized here.

The largest of these three prospects is the Lookout Mine located in Section 23, T8N, R72W accessible by unimproved road from Stove Prairie. Production of 100 tons of 2 percent WO_3 is

reported for 1954 (Belser, 1956). The development consists of a number of large trenches five to eight meters wide, two to four meters deep and up to fifty meters long. The longest trench parallels the regional foliation. The prospect is located within the large calc-silicate gneiss unit lying northwest of the Skin Gulch shear zone.

The rock lithology at the Lookout Mine is primarily calc-silicate gneiss with minor interlayered migmatitic biotite schist and quartzofeldspathic mica schist. A few crosscutting pegmatites up to four meters in width are present. The mineralogy of the calc-silicate gneiss is relatively simple. Calcite-rich bands are interlayered with calcite-free bands and the scheelite appears to be restricted to the latter. The calcite-rich bands are composed of quartz, calcite, clinozoisite and clinopyroxene with minor garnet. The calcite-free bands are composed of quartz, clinozoisite, garnet, clinopyroxene, an unidentified completely altered phase that was possibly pyroxene or amphibole, minor sphene and, locally, scheelite. The unidentified phase occurs as a mixture of clay and hydrous Fe oxide. Scheelite occurs as large, irregular, lenticular grains with some inclusions of pyroxene. No powellite was recognized and the chemical analyses indicate very little Mo. The scheelite fluoresces a bluish-white. Idocrase was not recognized in the deposit although it was present in other prospects.

The gneiss has minor thin mylonitic zones parallel with the gneissic banding and in thin section evidence of cataclasis and recrystallization is common. The quartz shows evidence of being

highly strained, with development of sutured contacts and a polygonal fabric. The garnet, some of the clinozoisite and the scheelite is fractured and the fractures are filled with quartz or clinozoisite. The scheelite also shows strong undulatory extinction.

The mineralized zone is three to four meters wide, however, individual scheelite-bearing bands were not observed to exceed thirty centimeters in width. Sampling was carried out using an ultraviolet lamp. Table 15 lists chemical analyses for WO_3 and Mo while table 16 lists semiquantitative spectrographic analyses.

TABLE 15

Quantitative analyses of Tungsten-bearing Calc-silicate gneisses

Lab No.	Field No.	WO_3%	Mo(ppm)
D140519	12-6-155A	1.3	15
D140520	12-6-155B	2.0	17
D140521	12-6-155C	3.0	30
D140522	12-6-155D	4.7	31
Technique		Gravimetry	Colorimetry

Analysts: V.E. Shaw (WO_3) and C. Huffman, Jr. (Mo), U.S. Geological Survey, 1969

Samples 155A and 155B were taken across typical 10-cm-wide scheelite-bearing bands, sample 155D from a 30-cm-wide band and sample 155C is a composite sample of scheelite-bearing calc-silicate gneiss. Field observations suggest that these bands are quite discontinuous and that they are quite uncommon even within the mine area. The ore shipped was no doubt hand cobbed.

Two features which are perhaps characteristic of the scheelite-

TABLE 16

Semiquantitative Spectrographic Analyses of Calc-silicate Gneisses

Lab. No.	D140519	D140520	D140521	D140522
Field No.	12-6-155A	12-6-155B	12-6-155C	12-6-155D
Fe (%)	5.	5.	3.	3.
Mg (%)	0.7	1.5	1.	0.7
Ca (%)	G	G	G	G
Ti (%)	0.15	0.15	0.15	0.1
Si (%)	G	G	G	G
Al (%)	7.	10.	7.	7.
Na (%)	L	0.5	0.1	0.05
K (%)	N	N	N	N
P (%)	N	0.5	N	N
Mn (ppm)	5000	1000	1500	1500
Ba (ppm)	100	150	100	70
Be (ppm)	70	300	30	50
Co (ppm)	7	N	10	7
Cr (ppm)	10	20	15	15
Cu (ppm)	20	20	10	2
La (ppm)	30	30	N	30
Mo (ppm)	15	N	30	20
Nb (ppm)	50	100	100	70
Ni (ppm)	15	15	15	10
Sn (ppm)	70	N	N	N
Sr (ppm)	150	300	100	150
V (ppm)	100	100	100	100
W (ppm)	10000	20000	30000	70000
Y (ppm)	50	70	50	20
Zr (ppm)	100	100	100	50
Ga (ppm)	50	50	30	30
Yb (ppm)	5	7	7	3

Looked for in all samples but not found: Ag, As, Au, B, Bi, Cd, Pb, Pd, Pt, Sb, Sc, Te, U, Ce, Ge, Hf, In, Li, Re, Ta, Th, Tl, Eu.

Looked for in 12-6-155A, 12-6-155B, 12-6-155D but not found: Pr, Nd, and Sm.

Looked for in 12-6-155B but not found: Gd, Tb, Dy, Ho, Er, Tm, Lu.

Analyst: L. A. Bradley, U. S. Geological Survey, 1969.

G = Greater than 10%

N = Not detected or at limit of detection

L = Detected, but below limit of determination

bearing lenses in this area are the absence of calcite and the presence of garnet. Whether these may be usefully applied in prospecting throughout the outcrop of this gneiss would require additional work to establish. This unit crops out over an area of about 3 km^2 to the north and east of the property.

The origin of these deposits remains somewhat obscure. Tweto (1960) has reviewed the various tungsten-bearing deposits in the Precambrian gneisses of Colorado and has concluded that they must have resulted from the chemical redistribution of tungsten originally present in the sediments from which these metasediments were derived. This process may have been metamorphic differentiation and recrystallization associated with the major regional metamorphism. The superposition of cataclastic textures on the scheelite-bearing assemblages in the Lookout Mine indicates that they must be pre 1.2 b.y. shearing in origin although, perhaps, somewhat modified at that time. There is no evidence in this area that these assemblages are related to the 1.4 b.y. Silver Plume plutonism. However, as Tweto has observed, this may be a possibility for some of the Colorado deposits.

Base-metal sulfide prospects

Within the Skin Gulch shear zone where it is intersected by the Poudre River fault a number of prospects are located on small intensely hydrothermally altered zones. In some of these, copper mineralization was dominant; in others, lead and zinc mineralization was dominant. All of the mineralized zones are quite small. Development is generally limited to scattered prospect pits.

The largest of these prospects is located in the southeast quarter of section 6, T8N, R71W on the north side of the Cache La Poudre river. Workings include a number of adits and a shaft of unknown depth, probably caved. The dumps from these workings are composed of highly oxidized, sulfide-rich interlayered calc-silicate gneiss and biotite schist. Surface exposure of the hydrothermally altered zone is quite limited, less than 150 meters along strike.

Preliminary studies of thin sections and polished sections of highly oxidized, sulfide-bearing material from the zone exposed in the shaft indicate complete alteration of the rock to calcite and clay mixtures with distinctive veins of antigorite asbestos. These veins are from less than one mm. to four mm. in width and quite discontinuous. They appear to be restricted to the bands of altered rock.

Sulfide mineralization consists of pyrite and galena plus some very small unidentified phases. A semiquantitative spectrographic analysis of a composite sample from the mineralized zone is reported in table 17.

The very limited areal extent of these zones of alteration suggests that further development is probably not warranted.

Tertiary and Quaternary gravel deposits

Potentially valuable gravel deposits of two types are present within the area studied: high-level late-Tertiary gravels located in the northern portions of the Big Narrows and Poudre Park quadrangles and the southern portion of the Livermore

Mountain quadrangle and Quaternary terrace gravels present along the present course of the Cache La Poudre river.

These deposits have been described in an earlier section. The late Tertiary gravels are presently being exploited for road aggregate on the Livermore-Red Feather lakes road. These deposits are thick and there are large reserves available for this use.

The deposits along the Cache La Poudre River are much thinner and less extensive. No attempt has been made to critically analyze any of these deposits as potential sources of clean sand and gravel. At present the larger deposits probably lie too far from potential consumers for their economic exploitation.

TABLE 17

Semiquantitative spectrographic analysis of hydrothermally altered Calc-silicate gneiss

Lab No. D139925

Field No. 12-3-276B

Fe (%)	G	Al (%)	0.3
Mg (%)	5.0	Na (%)	0.05
Ca (%)	10.0	K (%)	N
Ti (%)	0.005	P (%)	N
Si (%)	G		
Mn (ppm)	15,000	La (ppm)	30
Ag (ppm)	15	Mo (ppm)	15
Ba (ppm)	7	Ni (ppm)	7
Be (ppm)	2	Pb (ppm)	15000
Bi (ppm)	30	Sr (ppm)	20
Cd (ppm)	150	Y (ppm)	20
Co (ppm)	150	Zn (ppm)	100000
Cr (ppm)	2	Yb (ppm)	2
Cu (ppm)	700		

Looked for but not found: As, An, B, Nb, Pd, Pt, Sb, Se, Sn, Te, U, V, W, Zr, Ce, Ga, Ge, Hf, In, Li, Re, Ta, Th, Tl, Pr, Nd, Sm, Eu.

Analyst: B.W. Lanthorne, U.S. Geological Survey, 1970

G = greater than 10%

N = not detected or at limit of detection

LITERATURE CITED

Albee, A. L., 1965, Phase equilibrium in three assemblages of kyanite-zone pelitic schists, Lincoln Mountain Quadrangle, Central, Vermont: Jour. Petrol., v. 6, p. 246-301.

Baird, A. K., D. B. McIntyre, E. E. Welday and D. M. Morton, 1967. A test of chemical variability and field sampling methods, Lakeview Mountain Tonalite, Lakeview Mountains, southern California batholith: California Div. Mines and Geology Spec. Rept. 92, p. 11-19.

Barker, F., 1969, Precambrian geology of the Needle Mountains, southwestern Colorado: U. S. Geol. Survey Prof. Paper 644-A, p. A1-A33.

Barker, F., Z. E. Peterman and R. A. Hildreth, 1969, A rubidium-strontium study of the Twilight gneiss, West Needle Mountains, Colorado: Contr. Mineral. and Petrol., v. 23, p. 271-282.

Bateman, P. C., L. D. Clark, N. King Huber, J. E. Moore and C. D. Rinehart, 1963, The Sierra Nevada batholith - a synthesis of recent work across the central part: U. S. Geol. Survey Prof. Paper 414-D, p D1-D46.

Belser, C., 1956, Tungsten potential in Chaffee, Fremont, Gunnison, Lake, Larimer, Park and Summit Counties, Colorado: Bureau of Mines Inf. Circ. 7748, 31 p.

Boos, M. F. and Boos, C. M., 1934, Granites of the Front Range - the Longs Peak - St. Vrain batholith: Geol. Soc. America Bull., v. 45, p. 303-322.

Braddock, W. A., 1969, Geology of the Empire Quadrangle,Grand, Gilpin and Clear Creek Counties, Colorado: U. S. Geol. Survey Prof. Paper 616, 56 p.

Bryan, K. and Ray, L. L., 1940, Geologic Antiquity of the Lindenmeier site in Colorado: Smithsonian Misc. Coll., v. 99, #2, 76 p.

Bucknam, R. C., 1969, Structure and petrology of Precambrian rocks in part of the Glen Haven quadrangle, Larimer County, Colorado: Colo. Univ., unpub. Ph.D. thesis, 92 p.

Buddington, A. F., 1959, Granite emplacement with special reference to North America: Geol. Soc. America Bull., v. 70, p. 671-747.

Buddington, A. F. and Lindsley, D. H., 1964, Iron-titanium oxide minerals and synthetic equivalents: Jour. Petrol., v. 5, p. 310-357.

Butler, P., 1969, Mineral compositions and equilibrium in the metamorphosed iron formations of the Gagnon Region, Quebec, Canada: Jour. Petrol., v. 10, p. 56-101.

Chayes, F., 1956, Petrographic Modal Analysis: Wiley, New York, 113 p.

Chayes, F., 1970, On deciding whether trend surfaces of progressively higher order are meaningful: Geol. Soc. America Bull., v. 81, p. 1273-1278.

Chinner, G. A., 1960, Pelitic gneisses with varying ferrous/ferric ratios from Glen Clova, Angus, Scotland: Jour. Petrol., v. 1, p. 178-217.

Christie, J. M., 1960, Mylonitic rocks of the Moine Thrust Zone in the Assynt Region, North West Scotland: Geol. Soc. Edin. Trans., v. 18, p. 79-93.

Christie, J. M., 1963, The Moine Thrust Zone in the Assynt Region, Northwest Scotland: U. of Col. Pub. in Geol. Sci., v. 40, p. 345-440.

Connor, J. J., 1962, Precambrian petrology and structural geology of the Cray Rock - Livermore Mountain area, Larimer County, Colorado: Colo. Univ., unpub. Ph.D. thesis, 132 p.

Dalziel, I. W. D. and S. W. Bailey, 1968, Deformed garnets in a mylonitic rock from the Grenville front and their tectonic significances, Am. Jour. Sci., v. 266, p. 542-562.

Darton, N. H., E. Blackwelder and C. E. Siebenthal, 1910, Laramie-Sherman folio, Wyo.: U. S. Geol. Survey Folio no. 173, 17 p.

Dietrich, R. V., P. D. Fullagar and M. L. Bottino, 1969, K/AR and Rb/Sr rating of tectonic events in the Appalachians of Southwestern Virginia: Geol. Soc. America Bull., v. 80, p. 307-314.

Doering, W. P., 1968, A rapid method for measuring the Rb/Sr ratio in silicate rocks: U. S. Geological Survey Prof. Paper 600-C, p. C164-C168.

Eggler, D., 1967, Structure and petrology of the Virginia Dale ring dike complex, Colorado-Wyoming Front Range: Colo. Univ., unpub. Ph.D. thesis, 154 p.

Eggler, D., 1968, Virginia Dale Precambrian ring-dike complex, Colorado-Wyoming: Geol. Soc. America Bull., v. 79, p. 1545-1564.

Eggler, D. H., E. E. Larson and W. C. Bradley, 1969, Granites, gneisses, and the Sherman erosion surface, southern Laramie Range, Colorado-Wyoming: Am. Jour. Sci., v. 267, p. 510-522.

Eslen, J. E., P. F. Smith and J. C. Davis, 1968, KWIKR8, A fortran IV program for multiple regression and geologic trend analysis: Computer Contribution 28, State Geological Survey, Kansas.

Engster, H. P., and Wones, D. R., 1962, Stability relations of the ferruginous biotite, annite: Jour. Petrology, v. 3, p. 85-125.

Evans, B. W., 1965, Application of a reaction rate method to the breakdown equilibria of muscovite and muscovite plus quartz: Am. Jour. Sci, v. 263, pp. 647-667.

Evans, B. W., and Guidotti, C. V., 1966, The sillimanite-potash feldspar isograd in western Maine, U.S.A.: Contr. Mineral. and Petrol., v. 12, p. 25-62.

Fairbairn, H. W., P. M. Hurley and W. H. Pinson, 1961, The relation of discordant Rb-Sr mineral and whole rock ages in an igneous rock to its time of subsequent Sr^{87}/Sr^{86} metamorphism: Geochim. Cosmochim. Acta, v. 23, p. 135-144.

Fuller, M. B., 1924, General features of Precambrian structure along the Big Thompson River in Colorado: Jour. Geology, v. 32, p. 49-63.

Fyfe, W. S., and Turner, F. J., 1966, Reappraisal of the metamorphic facies concept: Contr. Mineral. and Petrol., v. 12, p. 354-364.

Gawarecki, S. J., 1963, Geology of the Front Range foothills in the Palisade Mountain-Masonville area, Larimer County, Colorado: Colo. Univ., unpub. Ph.D. thesis, 185 p.

Hall, A., 1969, Regional variation in the composition of British Caledonian Granites: Jour. Geology, v. 77, p. 466-481.

Hamilton, W. and Myers, W. B., 1967, The nature of batholiths: U. S. Geol. Survey Prof. Paper 554-C, p. C1-C30.

Hedge, C. E., 1969, A petrogenetic and geochronologic study of migmatites and pegmatites in the Central Front Range: Colorado School of Mines, unpub. Ph.D. thesis, 169 p.

Hedge, C. E., Z. E. Peterman and W. A. Braddock, 1967, Age of the major Precambrian regional metamorphism in the northern Front Range, Colorado: Geol. Soc. America Bull., v. 78, p. 551-557.

Hepp, M. M., 1966, A Precambrian andesite dike swarm in the northeastern Front Range, Larimer County, Colorado: Colo. Univ., unpub. M.S. thesis, 75 p.

Himmelberg, G. R. and Phinney, W. C., 1967, Granulite-facies metamorphism, Granite Falls-Montevideo Area, Minnesota: Jour. Petrol., v. 8, p. 325-348.

Hoschek, G., 1969, The stability of staurolite and chloritoid their significance in metamorphism of pelitic rocks: Contr. Mineral. and Petrol., v. 22, p. 208-232.

Howarth, R. J., 1967, Trend-surface fitting to random data - an experimental test: Am. Jour. Sci., v. 265, p. 619-625.

Hsü, K. J., 1955, Granulites and mylonites of the region about Cucamonga and San Antonio Canyons, San Gabriel Mountains, California: California Univ. Pubs. Geol. Sci., v. 30, p. 223-352.

Hsü, L. C., 1968, Selected phase relationships in the system Al-Mn-Fe-Si-O-H: A model for garnet equilibrium: Jour. Petrol., v. 9, p. 40-83.

Hurley, P. M., P. C. Bateman, H. W. Fairbairn and W. H. Pinson, Jr., 1965, Investigation of initial Sr^{87}/Sr^{86} ratios in the Sierra Nevada plutonic province: Geol. Soc. America Bull., v. 76, p. 165-179.

James, R. S. and D. L. Hamilton, 1969, Phase relations in the system $NaAlSi_3O_8$ - $KAlSi_3O_8$-$CaAl_2Si_2O_8$ - SiO_2 at 1 kg water vapour pressure: Contrib. Mineral. and Petrol., v. 21, p. 111-141.

Klein, C., Jr., 1966, Mineralogy and petrology of the metamorphosed Wabush Iron formation, Southwestern Labrador, Jour. Petrol., v. 7, p. 246-305.

Korzhinskii, D. S., 1959, Physicochemical basis of the analysis of the paragenesis of minerals: New York, Consultants Bureau, 142 p.

Krumbein, W. C., 1959, Trend surface analysis of contour-type maps with irregular control-point spacing: Jour. Geophys. Research, v. 64, p. 823-834.

Krumbein, W. C. and Graybill, F. A., 1965, An introduction to statistical models in geology: New York, McGraw-Hill, 475 p.

Lanphere, M. A., G. J. Wasserburg and A. L. Albee, 1964, Redistribution of strontium and rubidium during metamorphism, World Beater Complex, Panamint Range, California: in Isotopic and cosmic chemistry, ed. by H. Craig, S. L. Miller and G. J. Wasserburg, p. 269-320, Amsterdam, North Holland Pub. Co.

Lindsley, D. H., 1966, Lower-thermal stability of $FeTi_2O_5$ - Fe_2TiO_5 (pseudobrookite) solid-solution series (obs.): Geol. Soc. American Spec. Paper 87, p. 97.

Lovering, T. S. and Goddard, E. N., 1950, Geology and ore deposits of the Front Range, Colorado: U. S. Geol. Survey Prof. Paper, 319 p.

Lundgren, L. W., Jr., 1966, Muscovite reactions and partial melting in southeastern Connecticut: Jour. Petrol., v. 7, p. 421-453.

Luth, W. C., R. H. Jahns and O. F. Tuttle, 1964, The granite system at pressures of 4 to 10 kilobars: Jour. Geophys. Research, v. 69, p. 759-773.

Luth, W. C. and Tuttle, O. F., 1969, The hydrous vapor phase in equilibrium with granite and granite magmas: Geol. Soc. America Memoir 115, p. 513-548.

Mandelbaum, H., 1963, Statistical and geological implications of trend mapping with non-orthogonal polynomials: Jour. Geophys. Research, v. 68, p. 505-519.

McKinstry, H. E., 1949, Mining geology: New York, Prentice-Hall, 680 p.

Mehnert, K. R., 1968, Migmatites and the origin of granitic rocks: New York, Elsevier Publ. Co., 393 p.

Miyashiro, A., 1961, Evolution of metamorphic belts: Jour. Petrol., v. 2, p. 277-311.

Moench, R. H., 1964, Geology of Precambrian rocks, Idaho Springs District, Colorado: U. S. Geol. Survey Bull. 1182-A, 70 p.

Moench, R. H., J. E. Harrison and P. K. Sims, 1962, Precambrian folding in the Idaho Springs-Central City area, Front Range, Colorado: Geol. Soc. American Bull., v. 73, p. 35-58.

Morton, D. M., A. K. Baird and K. W. Baird, 1969, The Lakeview Mountains Pluton, Southern California Batholith Part II: Chemical composition and variance: Geol. Soc. America Bull., v. 80, p. 1553-1564.

Nicolaysen, L. O., 1961, Graphic interpretation of discordent age measurements on metamorphic rocks: Ann. N. Y. Acad. Sci., v. 91, p. 198.

Nutalaya, P., 1966, Metamorphic petrology of a part of the northeastern Front Range, Larimer County, Colorado: Colo. Univ., unpub. Ph.D. thesis, 149 p.

O'Connor, J. T., 1961, The structural geology and Precambrian petrology of the Horsetooth Mountain area, Larimer County, Colorado: Colo. Univ., unpub. Ph.D. thesis, 129 p.

Orville, P. M., 1963, Alkali ion exchange between vapor and feldspar phases: Am. Jour. Sci., v. 261, p. 201-237.

Orville, P. M., 1967, Unit cell parameters of the microcline - low albite and the sanidine - high albite solid solution series: Am. Mineralogist, v. 52, p. 55-86.

Peikert, E. W., 1965, Model for three-dimensional mineralogical variation in granitic plutons based on the Glen Alpine Stock, Sierra Nevada, Cal., Geol. Soc. America Bull., v. 76, pp. 331-348.

Peterman, Z. E., B. R. Doe and A. Bartel, 1967, Data on the rock GSP-1 (granodionite) and the isotope-dilution method of analysis for Rb and Sr: U. S. Geol. Survey Prof. Paper 575-B, p. B181-B186.

Peterman, Z. E., C. E. Hedge and W. A. Braddock, 1968, Age of Precambrian events in the northeastern Front Range, Colorado, Jour. Geophys. Research, v. 73, p. 2277-2296.

Pettijohn, F. J., 1963, Data of Geochemistry - chemical composition of sandstones - excluding carbonate and volcanic sands: U. S. Geol. Survey Prof. Paper 440-S, p. 51-521.

Piwinskii,A. J., 1968, Experimental studies of igneous rock series, Central Sierra Nevada Batholith, California: Jour. Geology, v. 76, p. 548-570.

Piwinskii, A. J., and Wyllie, P. J., 1968, Experimental studies of igneous rock series: a zoned pluton in the Wallowa batholith, Oregon: Jour. Geology, v. 76, p. 205-234.

Piwinskii, A. J. and Wyllie, P. J., 1970, Experimental studies of igneous rock series: Felsic body suite from the Needle Point pluton, Wallowa batholith, Oregon: Jour. Geology, v. 78, p. 52-76.

Plas, L. van der, 1966, The Identification of Detrital Feldspars Elsevien, New York, 305 p.

Plas, L. van der and Tobi, A. C., 1965, A chart for judging the reliability of point counting results: Am. Jour. Sci., v. 263, p. 87-90.

Prinz, M. and A. Poldervaart, 1964, Layered mylonite from Beartooth Mountains, Montana: Geol. Soc. America Bull., v. 75, p. 741-744.

Ramsay, J. G., 1962, The geometry and mechanics of formation of "similar" type folds: Jour. Geology, v. 70, p. 309-327.

Ramsay, J. G., 1967, Folding and Fracturing of Rocks: New York, McGraw Hill, 568 p.

Reed, J. C., Jr. and Bryant, B., 1964, Evidence for strike-slip faulting along the Brevard zone in North Carolina: Geol. Soc. American Bull., v. 75, p. 1177-1196.

Richardson, S. W., 1968, Staurolite stability in a part of the system Fe-Al-Si-O-H: Jour. Petrol., v. 9, p. 467-488.

Richardson, S. W., M. C. Gilbert and P. M. Bell, 1969, Experimental determination of kyanite-andalusite and andalusite-sillimanite equilibria; the aluminum silicate triple point: Am. Jour. Sci., v. 267, p. 259-273.

Richmond, G. M., 1965, Glaciation of the Rocky Mountains, in The Quaternary of the United States: Princeton, N.J., Princeton University Press, p. 217-230.

Riley, G. H. and Compston, W., 1962, Theoretical and technical aspects of Rb-Sr geochronology: Geochim Cosmochim Acta, v. 26, p. 1255-1281.

Rutherford, M., 1970, Phase relations in the system $Al_2O_5SiO_2$ - Fe - O - H at P_{fluid} = 2kb (abs.): Trans., Am. Geophys. Univ., v. 51, p. 437.

Sarkar, A. N., 1966, A study of kyanite fabric in a thrust zone: Neues. Jahb. Mineralogie Monatsh., No. 2, p. 59-65.

Sclar, C. B., 1965, Layered mylonites and the Processes of Metamorphic differentiation: Geol. Soc. America Bull., v. 76, p. 611-612.

Seifert, F., 1970, Low-temperature compatibility relations of condierite in haplopelites of the system K_2O-MgO - Al_2O_3 - SiO_2 - H_2O: Jour. Petrol., v. 11, p. 73-99.

Sheridan, D. M., C. H. Maxwell and A. L. Albee, 1967, Geology and uranium deposits of the Ralston Buttes district, Jefferson County, Colorado: U. S. Geol. Survey Prof. Paper 520, 121 p.

Silver, L. J., and Barker, F., 1968, Geochronology of Precambrian rocks of the Needle Mountains, southwestern Colorado, Part 1, U-Pb zircon results (abs.): Geol. Soc. America Spec. Paper 115, p. 204.

Solomon, M., 1963, Counting and sampling errors in modal analysis by point counter: Jour. Petrol., v. 14, p. 367-382.

Swann, G. A., 1962, Structure and petrology of Precambrian rocks in the Cache La Poudre - Rist Canyon area, Larimer County, Colorado: Colo. Univ., unpub. Ph.D. thesis, 97 p.

Spurr, J. E. and Garrey, G. H., 1908, Economic geology of the Georgetown quadrangle, Colorado, with a section on general geology, by S. H. Ball: U. S. Geol. Survey Prof. Paper 63, 422 p.

Theodore, T. G., 1970, Petrogenesis of mylonites of high metamorphic grade in the Peninsular Ranges of southern California: Geol. Soc. America Bull., v. 81, p. 435-450.

Thompson, J. B., Jr., 1957, The graphical analysis of mineral assemblages in pelitic schists: Am. Mineralogist, v. 42, p. 842-858.

Thompson, J. B., Jr., 1959, Local equilibria in metasomatic processes, in Abelson, P. H., ed., Researches in Geochemistry: New York, Wiley, p. 427-457.

Thornton, C. and Tuttle, O., 1960, Chemistry of igneous rocks: I Differentiation Index: Am. Jour. Sci., v. 258, p. 664-684.

Turner, F. J., 1968, Metamorphic petrology - mineralogical and field aspects: New York, McGraw Hill Book Co., 403 p.

Turner, F. J. and Verhoogen, J., 1960, Igneous and metamorphic petrology: New York, McGraw-Hill, 694 p.

Turner, F. J. and Weiss, L. E., 1963, Structural analysis of metamorphic tectonites: New York, McGraw Hill Book Co., Inc., 545 p.

Tweto, O., 1960,scheelite in the Precambrian gneisses of Colorado: Econ. Geology, v. 55, p. 1406-1428.

Velde, B., 1964, Low grade metamorphism of micas in pelitic rocks: Carnegie Inst. Wash. Yearbook, v. 3, p. 142.

Watanabe, R. Y., 1965, Petrology of cataclastic rocks of northeastern Alberta: University of Alberta, unpub. Ph.D. thesis, 219 p.

Wells, J. D., 1967, Geology of the Eldorado Springs quadrangle Boulder and Jefferson Counties, Colorado: U. S. Geol. Survey Bull. 1221-D, 85 p.

White, A. J. R., 1966, Genesis of migmatites from the Palmer region of South Australia: Chem. Geol., v. 1, p. 165-200.

Winkler, H. E. F., 1967, Petrogenesis of metamorphic rocks, 2nd ed.: New York, Springer-Verlag, 237 p.

Wohlford, D. D., 1965, Petrology and structure of Precambrian rocks in the Cache La Poudre Canyon - Livermore area, Colorado: Colo. Univ., unpub. Ph.D. thesis, 123 p.

Wones, D. R., and Eugster, H. P., 1965, Stability of biotite - Experiment, theory and application: Am. Mineralogist, v. 50, p. 1228-1272.

Wright, T. L., 1968, Xray and optical study of alkali feldspar: II An xray method for determining the composition and structural state from measurement of 2θ values for three refractions: Am. Mineralogist, v. 53, p. 88-104.

Yoder, H. S., Jr., and others, 1957, Ternary feldspars: Carnegie Inst. Wash. Yearbook 56, p. 206-214.

Zen, E-An, 1961, Mineralogy and petrology of the system of Al_2O_3 - SiO_2 - H_2O in some pyrophyllite deposits of North Carolina: Am. Mineralogist, v. 46, p. 52-66.

Zen, E-An, 1963, Components, phases, and criteria of chemical equilibrium in rocks: Am. Jour. Sci., v. 261, p. 929-942.

APPENDIX 1

METAMORPHIC ASSEMBLAGES

The following summary of metamorphic mineral assemblages is based on the observation of phases over the area of a single thin section. Rarely were four phases actually found in physical contact, three phases being the common assemblage. Because of the large number of components in these systems and the common absence of obvious disequilibrium textures it was assumed that all phases present within a single thin section were part of an equilibrium assemblage. There are some notable exceptions which will be discussed below and the assumption needs to be tested analytically before undue faith is put in these assemblages.

As was discussed in some detail in an earlier section the origin of the muscovite in the knotted mica schists, the migmatitic biotite schists and the quartzofeldspathic mica schists remains ambiguous. It is difficult to distinguish secondary from primary muscovite in some cases. A large part of the muscovite is probably secondary. No distinction has been made between these in the following summary.

Those assemblages containing andalusite and cordierite are from near the Skin Gulch shear zone and may represent disequilibrium assemblages produced by superposition of a later thermal metamorphism on the main regional metamorphic assemblages.

The order of listing does not imply relative proportions. Brackets indicate only trace amounts were present.

Pelitic and Quartzo-feldspathic Assemblages

Migmatitic biotite schist

1) Biotite-muscovite-quartz
2) Biotite-muscovite-sillimanite

3) Biotite-quartz-plagioclase-microcline
4) Biotite-muscovite-quartz-plagioclase-microcline
5) Biotite-muscovite-quartz-plagioclase-sillimanite
6) Biotite-muscovite-quartz-andalusite-sillimanite
7) Biotite-muscovite-quartz-plagioclase-microcline-sillimanite

Knotted mica schist

8) Biotite-muscovite-quartz
9) Biotite-muscovite-quartz-sillimanite
10) Biotite-muscovite-quartz-andalusite
11) Biotite-muscovite-quartz-plagioclase-andalusite-sillimanite
12) Biotite-muscovite-quartz-andalusite-cordierite
13) Biotite-muscovite-quartz-plagioclase-andalusite-sillimanite
14) Biotite-muscovite-quartz-plagioclase-sillimanite
15) Biotite-muscovite-quartz-plagioclase-microcline-sillimanite

Quartzofeldspathic mica schist

16) Biotite-quartz-plagioclase
17) Biotite-quartz-plagioclase-microcline
18) Biotite-quartz-muscovite-plagioclase
19) Biotite-quartz-muscovite-sillimanite
20) Biotite-quartz-muscovite-plagioclase-sillimanite
21) Biotite-quartz-plagioclase-garnet
22) Biotite-quartz-muscovite-plagioclase-microcline
23) Biotite-quartz-muscovite-plagioclase-microcline-sillimanite
24) Biotite-quartz-muscovite-plagioclase-microcline-garnet
25) Biotite-quartz-muscovite-plagioclase-microcline-garnet (sillimanite)
26) Biotite-quartz (muscovite)-plagioclase-microcline-garnet-sillimanite

Clinozoisite biotite schist

27) Biotite-quartz-muscovite-plagioclase-microcline-clinozoisite

Microcline-quartz-plagioclase-biotite gneiss

28) Biotite-quartz-plagioclase-microcline
29) Biotite-quartz-plagioclase-(microcline)-(muscovite)
30) Biotite-quartz-muscovite-plagioclase-microcline

Basic and Calcareous Assemblages

Amphibolite

1) Hornblende-plagioclase-quartz
2) Hornblende-plagioclase-quartz-diopside
3) Hornblende-plagioclase-quartz-epidote
4) Hornblende-plagioclase-quartz-actinolite
5) Hornblende-plagioclase-quartz-biotite
6) Hornblende-plagioclase-quartz-biotite-microcline
7) Hornblende-plagioclase-biotite
8) Hornblende-plagioclase
9) Hornblende-plagioclase-clinozoisite
10) Hornblende-plagioclase-orthorhombic amphibole(?)
11) Hornblende-plagioclase-diopside-clinozoisite
12) Hornblende-quartz-garnet-clinozoisite

Hornblende-microcline gneiss

13) Quartz-microcline-hornblende
14) Quartz-microcline-actinolite-clinozoisite

Calc silicate gneiss

15) Quartz-plagioclase-tremolite
16) Quartz-plagioclase-epidote
17) Quartz-epidote-actinolite
18) (Quartz)-plagioclase-diopside-actinolite-clinozoisite
19) Quartz-plagioclase-microcline-actinolite-diopside-clinozoisite
20) Quartz-plagioclase-hornblende-biotite-diopside-tremolite
21) Quartz-plagioclase-hornblende-diopside-clinozoisite-tremolite

22) Quartz-plagioclase-clinozoisite

23) Quartz-plagioclase-clinozoisite-augite

24) Quartz-calcite-diopside-clinozoisite-(tremolite)

Figures 61 and 62 are AKF and ACF diagrams for the microcline + sillimanite and muscovite + sillimanite zones of the upper amphibolite facies assemblages. These are primarily compatibility diagrams, not phase diagrams and the crossing tie lines should not necessarily be interpreted as evidence of disequilibrium. They may represent disequilibrium, univariant equilibrium or divariant equilibrium. The exact chemistry of the participating phases must be known in order to distinguish between these alternatives.

Correlation of the listed mineral assemblages with these diagrams is hampered by the equivocal nature of muscovite however it is clear that representation of the majority of these assemblages requires the presence of crossing tie lines.

Figure 63 gives the ACF and AKF diagrams for the andalusite-cordierite bearing assemblages adjacent to the Skin Gulch shear zone. These assemblages are typical of hornblende-hornfels facies metamorphism. The significance of the muscovite and sillimanite in these assemblages is also unclear. Muscovite was probably stable during this metamorphic event. Sillimanite may be a metastable relict of the earlier high grade metamorphism.

An alternative method of graphical representation of metamorphic mineral assemblages is the AFM projection of Thompson (1957). It is designed to accurately portray reactions within the system MgO, FeO, K_2O and Al_2O_3 by projections from muscovite or potassium feldspar onto the MgO-FeO-Al_2O_3 side of the quaternary. The utility of this approach is particularly great for demonstrating chemical reactions taking place within the lower to upper middle grades of

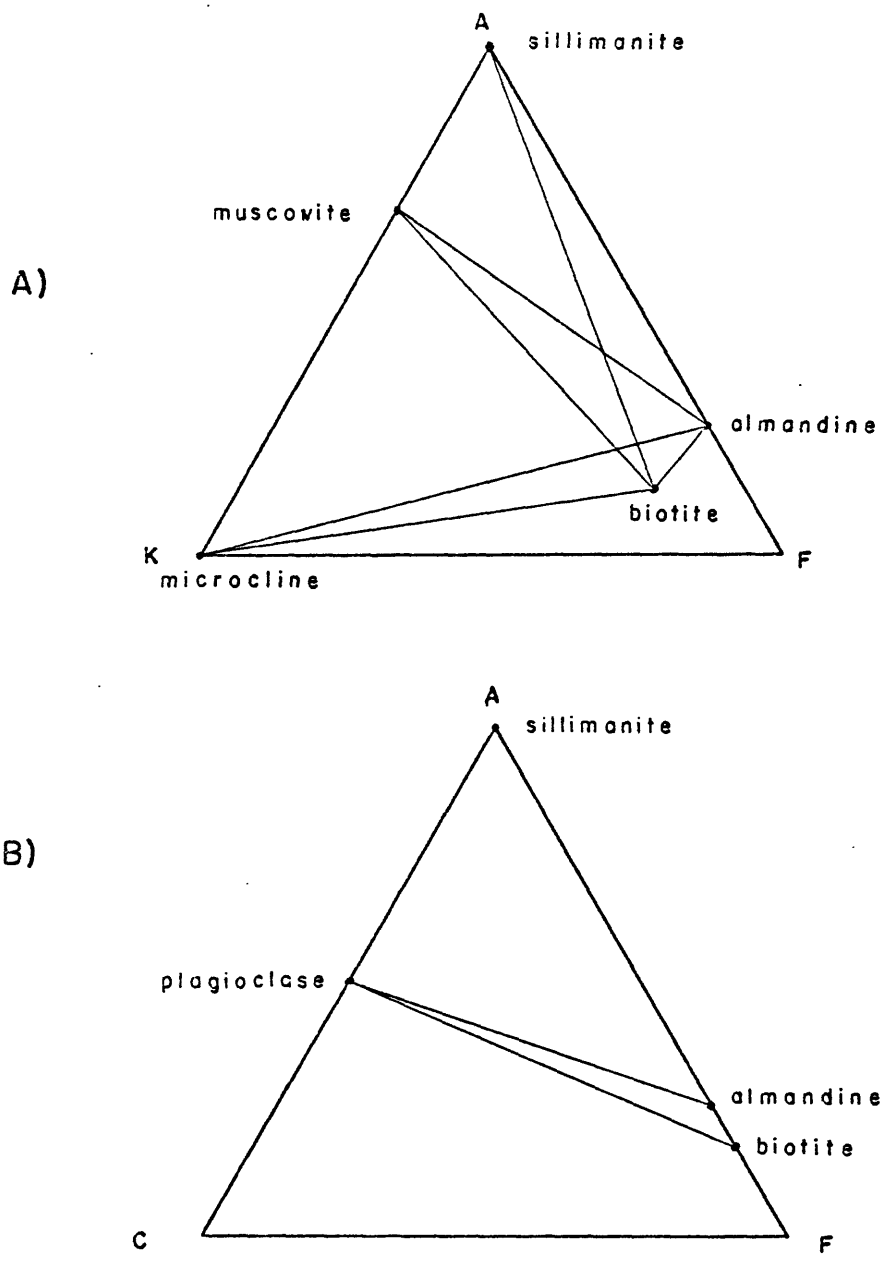

Figure 61: Upper amphibolite facies: muscovite + sillimanite zone. AKF and ACF diagrams for pelitic and quartzofeldspathic rocks with excess SiO_2 and K_2O. (a) AKF diagram. Plagioclase is a possible additional phase. (b) ACF diagram. Microcline and muscovite are possible additional phases.

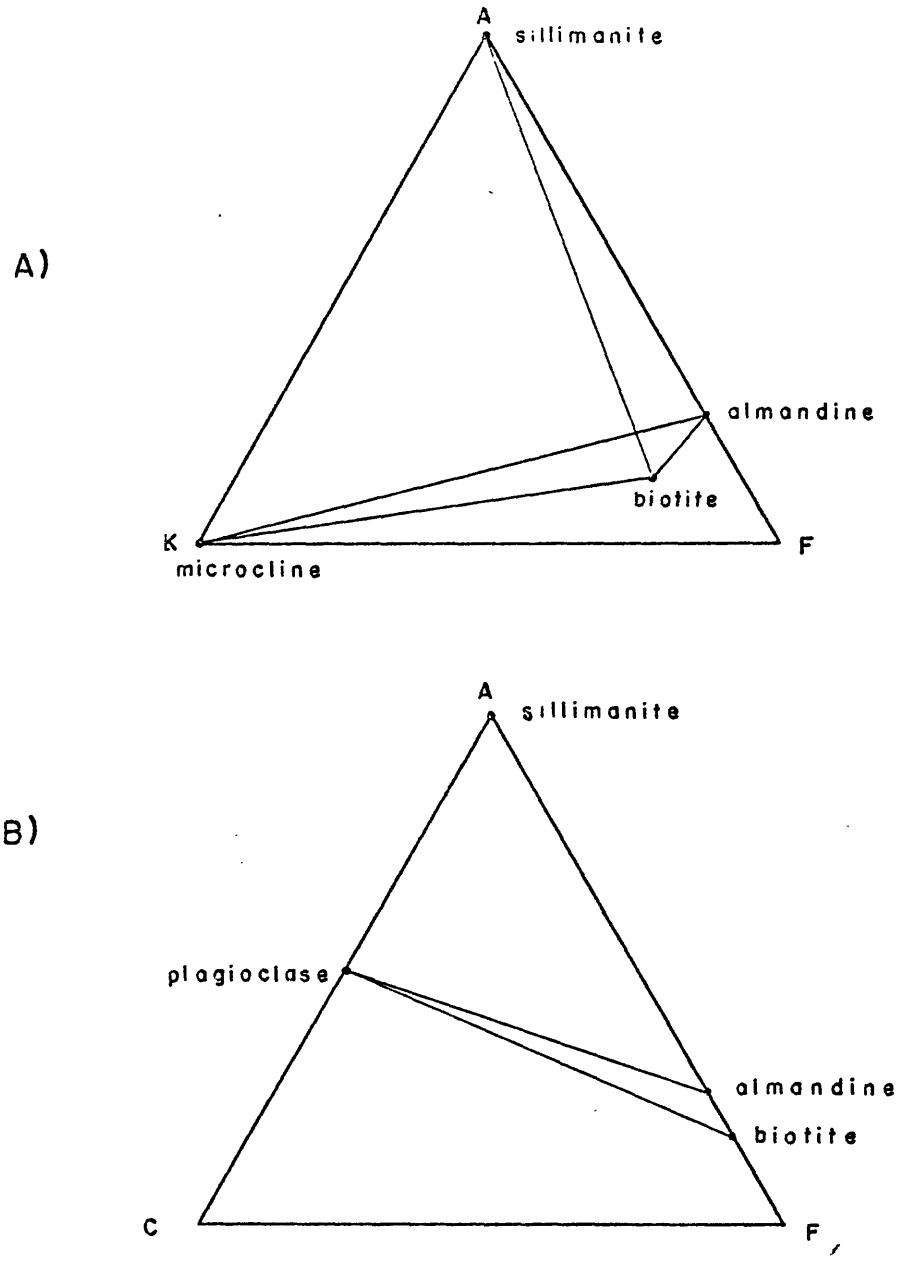

Figure 62: Upper amphibolite facies: microcline + sillimanite zone. AKF and ACF diagram for pelitic and quartzofeldspathic assemblages with excess SiO_2 and K_2O. (a) AKF diagram. Plagioclase is a possible additional phase. (b) ACF diagram. Microcline is a possible additional phase.

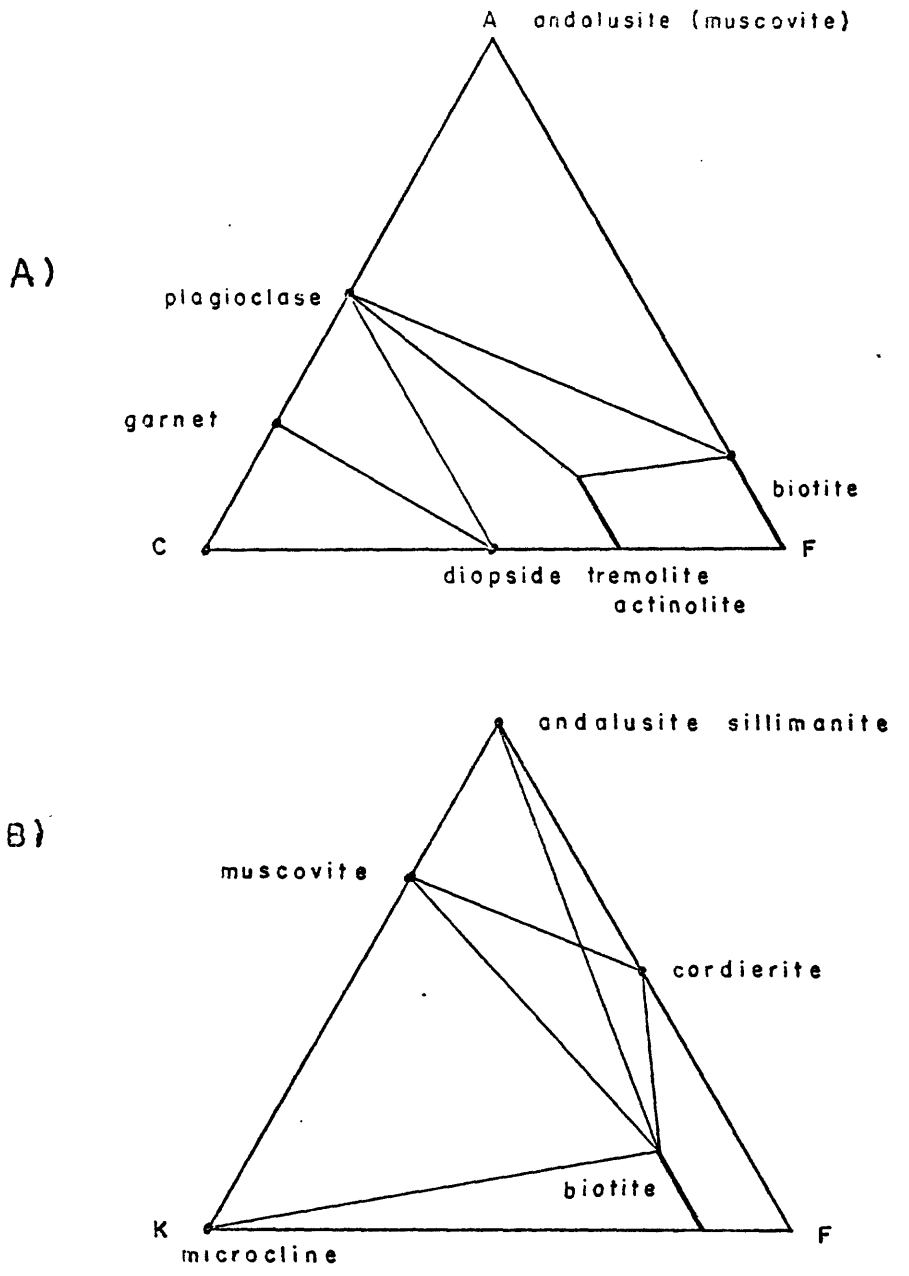

Figure 63: Hornblende hornfels facies. AKF and ACF diagrams for rocks with excess SiO_2 and K_2O. (a) ACF diagram. Quartz and microcline are possible additional phases. (b) AKF diagram. Quartz and plagioclase are possible additional phases.

metamorphism in pelitic rocks where accurate chemical analyses (particularly Fe-Mg ratios) of the participating phases are known.

APPENDIX 2

SUMMARY OF STATISTICAL PROCEDURES AND RESULTS OF

A TREND SURFACE ANALYSIS

OF THE

MODAL VARIATION IN

MICROCLINE-QUARTZ-PLAGIOCLASE-BIOTITE GNEISS

Introduction

Trend surface analysis is an effective means for testing for large scale variation in geologic populations and has an extensive and rapidly expanding geologic literature (Krumbein, 1959; Morton et. al., 1969; Peikert, 1965; Hall, 1969).

It has hoped that trend surface analysis might provide information useful for deciding whether the microcline-quartz-plagioclase-biotite gneiss is igneous or sedimentary in origin, independent of other criteria. A regular, pronounced trend showing a high correlation with the outer contacts of the unit might indicate regular, progressive crystallization and fractionation of an igneous magna (Morton and others, 1969). Poorly developed trends might be the result of random sedimentation processes in a tectonically active depositional basin or the result of the rapid accumulation of heterogeneous volcanics.

The following analysis represents a preliminary test of these ideas. The application of the results is discussed in the section on the origin of the metamorphic rocks.

Procedures

Sampling techniques have evolved rapidly and sophisticated statistical procedures have been developed to permit accurate representations of a geologic population. Krumbein (1959) and Baird, et. al., (1967) have discussed sampling procedures in some detail. The present study was designed as an initial test for variability and trend and therefore a completely thorough sampling procedure was not carried out. Theoretically a rectilinear grid

should be used to specify sampling sites and samples should be collected from as close as possible to the predetermined site in order to minimize sampling bias. Furthermore, in order to check variability on the outcrop and hand specimen scale suites of samples should be collected at each sample site. Logistics and economics prevented such a procedure. Eighty-six samples were collected over the entire area of the unit. Sample sites were selected to provide as uniform coverage as topography and exposure permitted. One sample was collected at each site with the exception of a few sites where multiple samples were obtained. Plate F shows the areal distibution of sample sites.

Thin sections were prepared from each sample and all slides were stained for potassium-feldspar. Complete modal analyses were carried out on each slide using standard point counting techniques. A counting grid was set up so that 1000 counts were uniformly distributed over approximately four-fifths of a standard 20 by 40 mm thin section. Chayes (1956), Van der Plas and Tobi (1965), Solomon (1963) and others have discussed the statistics of counting. Chayes presented data indicating what level of significance might be attached to the counting statistics for rocks of a given grain size. The majority of the gneiss samples have IC (Chayes, 1956, p. 72) numbers in excess of 100. Thus one normal thin section is sufficient to guarantee an analytical error of $\leq$ 2 percent for the major mineral components (Chayes, 1956). Use of the nomograph of Van der Plas and Tobi for a count length of 1000 also indicates an analytical error of approximately 2 percent at the 95 percent confidence level.

Four slides were recounted five times each using different orientations of the counting grid in order to test the effect of a possible mineralogical banding on counting statistics, and the variance on the level of a single thin section. These four sections were chosen to represent a cross-section of the variation in the megascopic textures present in these units. The counting paths were oriented both parallel with, and normal to, the foliation. It is assumed that with the fine to medium grain size any mineralogical banding present should be apparent on the thin section scale. By moving the counting grid between each replication any significant mineralogical variation would be indicated by the counting statistics. No detailed study of within outcrop variance was completed.

The trend surface analysis was carried out on a CDC 6400 computer using a program written by Esler et. al., (1968). The program uses standard matrix techniques to solve for the desired regression coefficients. The program permits computation of up to the seventh order trend surface. Standard statistical tests are also carried out.

Results

Means, ranges and standard deviations for the modal variation of quartz, plagioclase, microcline and biotite are given in Table 18. Clearly the standard deviation of each variate is a substantial percentage of the total range of variation.

The results of the replication study of four thin section are presented in Table 19. These data indicate that the variance on the thin section scale is substantially less than that of the unit wide

variance. Chayes (1956) has shown that operator counting error approaches quite close to binomial expectation. It is assumed that this was the case in this study for these data do not provide a direct test of operator precision. The data indicate that the grain size is sufficiently small and the mineralogical variation sufficiently uniform (i.e., no significant mineralogical banding) to justify the use of modal analyses on these foliated gneisses in a larger trend analysis study.

The results of the trend analysis study are presented in Tables 20-25 and figures 64-67. Each table summarizes the statistical data for a specific major mineral component for 1st through 3rd order surfaces. The calculated F values and the indicated confidence levels are listed. Table 23 lists the percent total sums of squares explained for each surface.

The problem of analyzing the significance of trend surfaces is a difficult, and still largely unsolved, one. Krumbein and Graybill (1965) have indicated techniques for determining confidence levels for 1st order surfaces but no generalized procedure for higher order surfaces is available. Howarth (1967) has determined the percent sum of squares levels which can be used as the lower limits for data with a significant trend and the upper levels for random data. These are 6, 12 and 16.2 percent sums of squares explained by the first, second and third order surfaces respectively. Applying these criteria to the data from the Mt. McConnel layer it is apparent that only the first order surface of quartz and the first and third order surfaces of biotite have any significance beyond the random data level.

An F test is utilized to determine the significance of a variance ratio, in this case the ratio of mean squares of the variance within a trend surface of a given order and the residual variance of that surface. Failure of significance at a given level indicates that the variance for that order surface is not significantly different from that attributable to random error. The confidence levels indicated by the F test results show that only the first order surface of quartz is significant at the 90 percent level. Clearly any attempt to carry out trend calculations to higher order surfaces would achieve no significant purpose. Recently Chayes (1970), also using the F test, has demonstrated the futility of carrying trend surface calculations to higher and higher order surfaces.

Mandelbaum (1963) has shown that the parameter $^{ss}X_{dev}(N-P)$ can be utilized as an indicator of the significance of the trend component in a surface of a given level. The trend surface for a given variate which shows the minimum value for $^{ss}X_{dev}(N-P)$ should most closely represent any regional trend present. Table 25 summarizes computed values of this parameter. The data are in agreement with the results from the other statistical tests. The first order surface of quartz and the third order surfaces of plagioclase, microcline and biotite have minimum values.

All of these tests indicate that any regional trend which may be present, whatever its geologic origin, has a marginal to nonexistent statistical significance. The trend surface data suggests that the distribution of the major mineral phases within this body of microcline-quartz-plagioclase-biotite gneiss is random.

Figures 64-67

First through third order trend surfaces for quartz, plagioclase, microcline and biotite.

Contour interval for each surface is one modal percent except for the third order plagioclase and microcline trend surfaces for which it is two modal percent.

The boundaries of the microcline-quartz-plagioclase-biotite gneiss are shown. Locations of individual data points are given on plate 7.

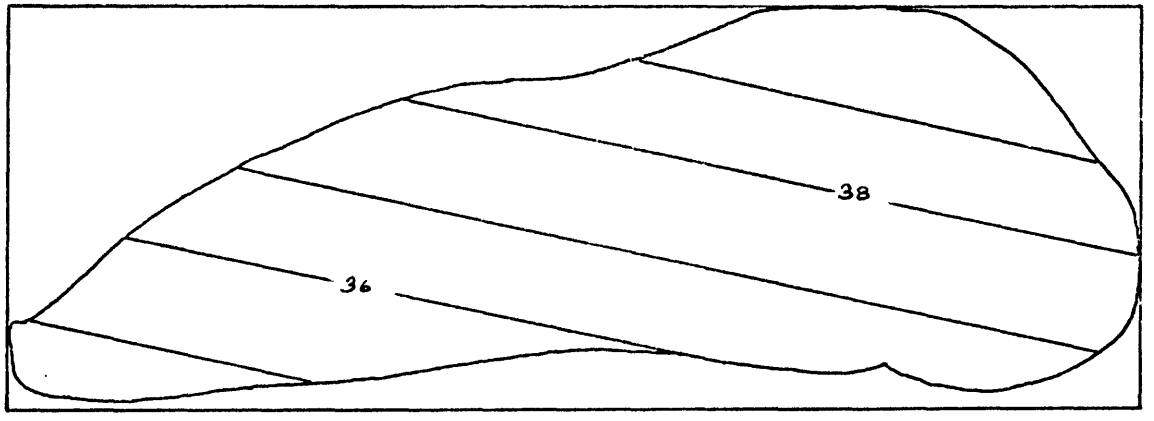

First order surface

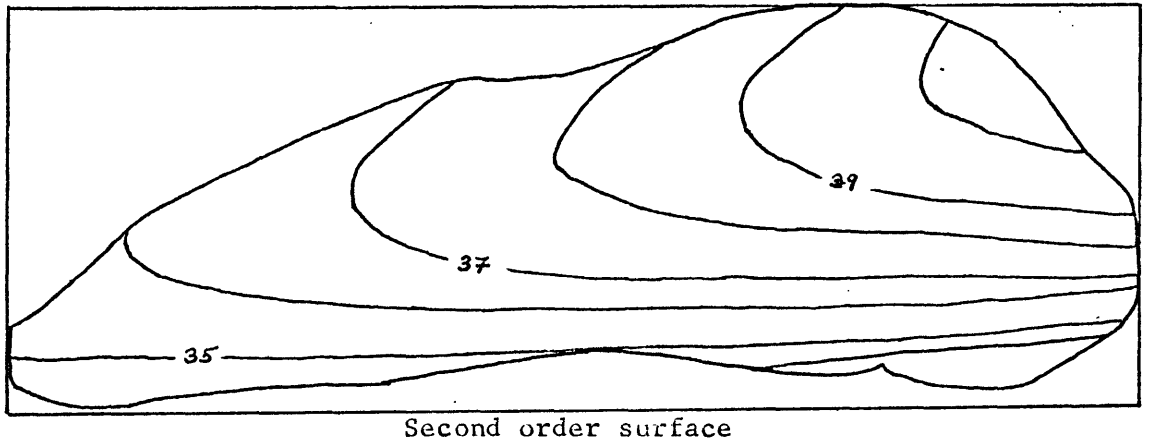

Second order surface

Figure 64: First through third order trend surfaces for modal quartz

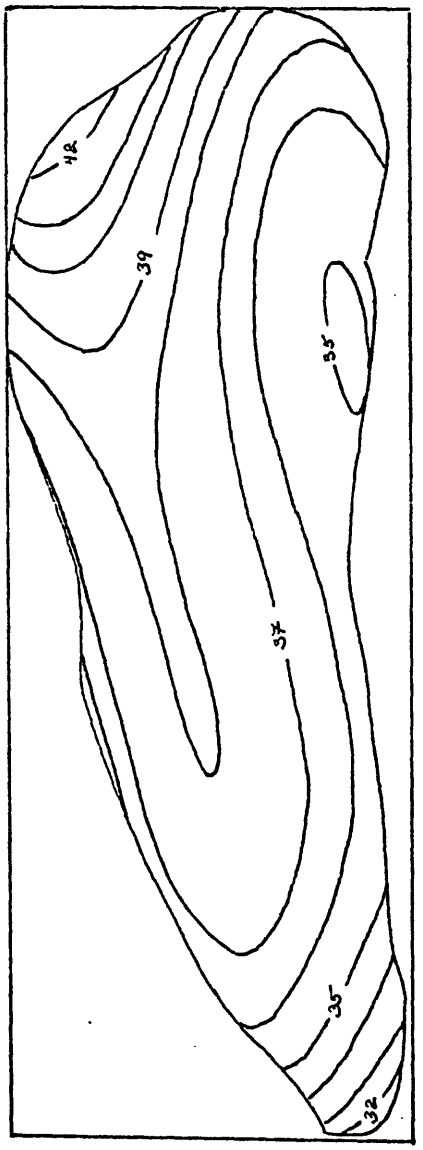

Third order surface

Figure 64: continued

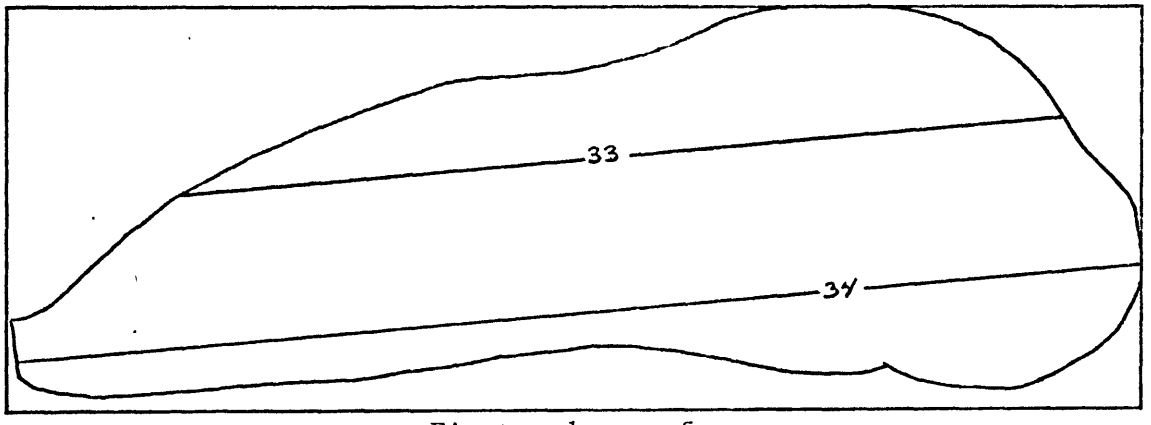

First order surface

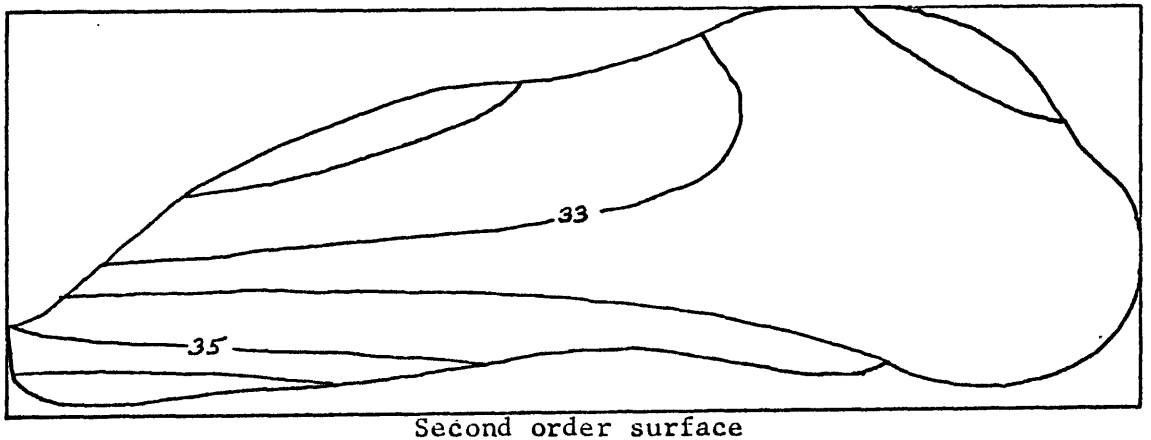

Second order surface

Figure 65: First through third order trend surfaces for modal plagioclase

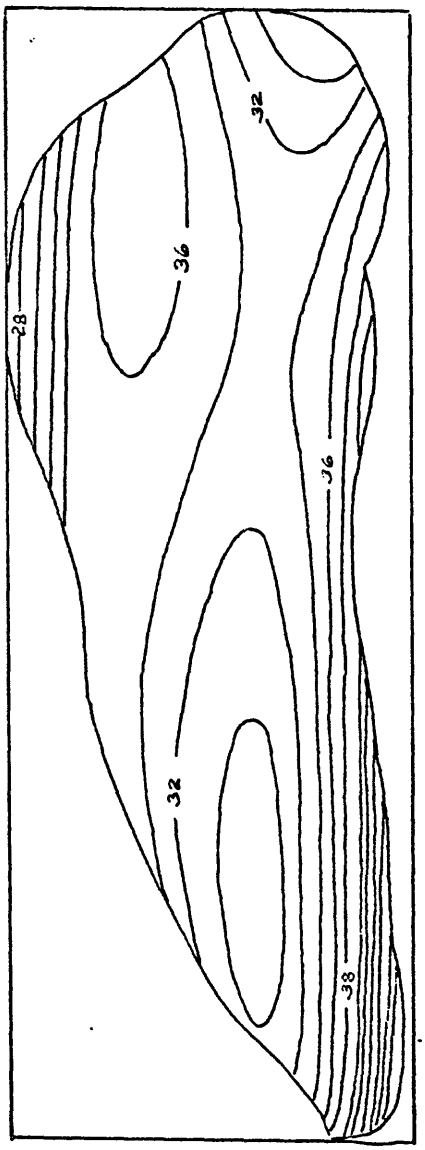

Third order surface

Figure 65: continued

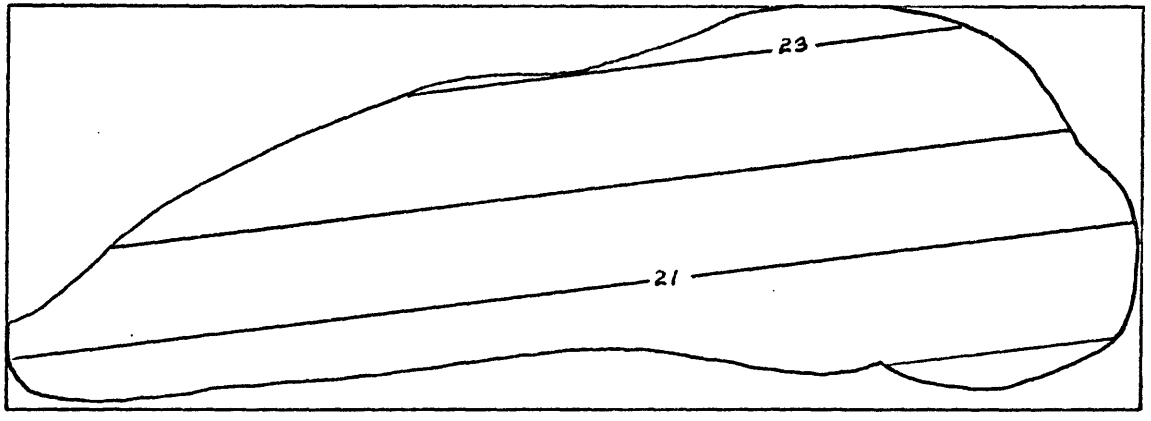

First order surface

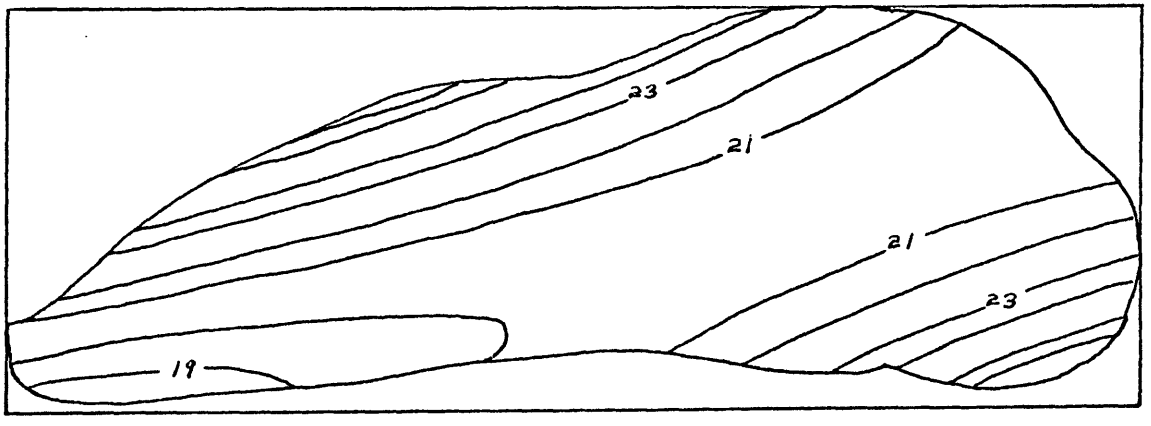

Second order surface

Figure 66: First through third order trend surfaces for modal microcline

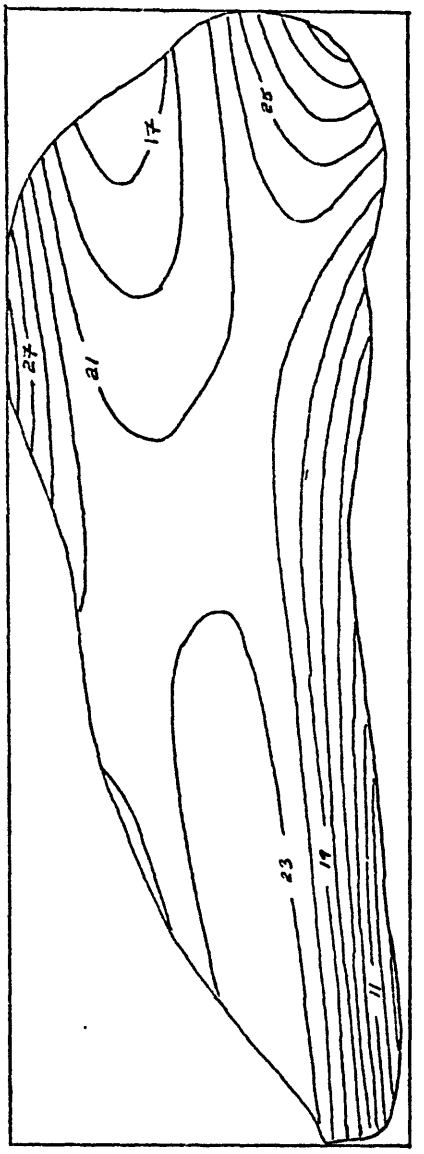

Third order surface.

Figure 66: continued

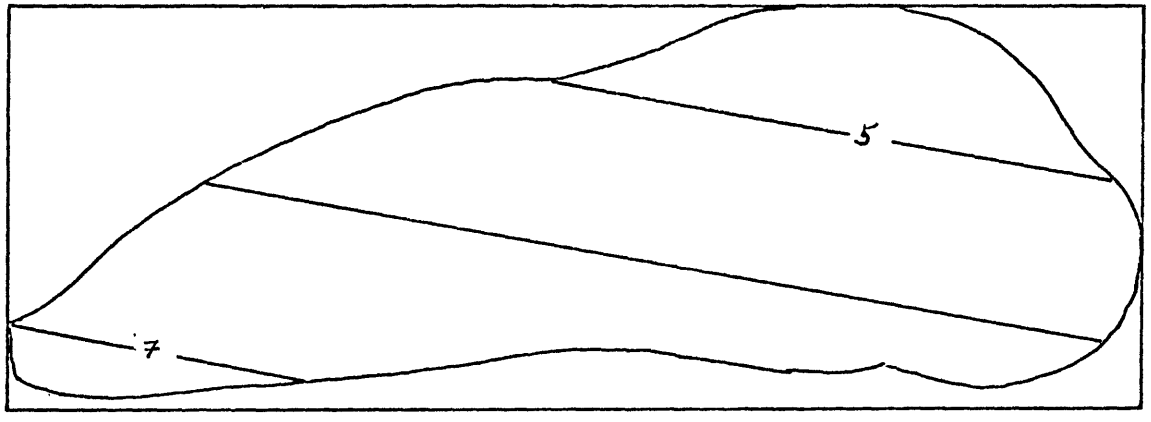

First order surface

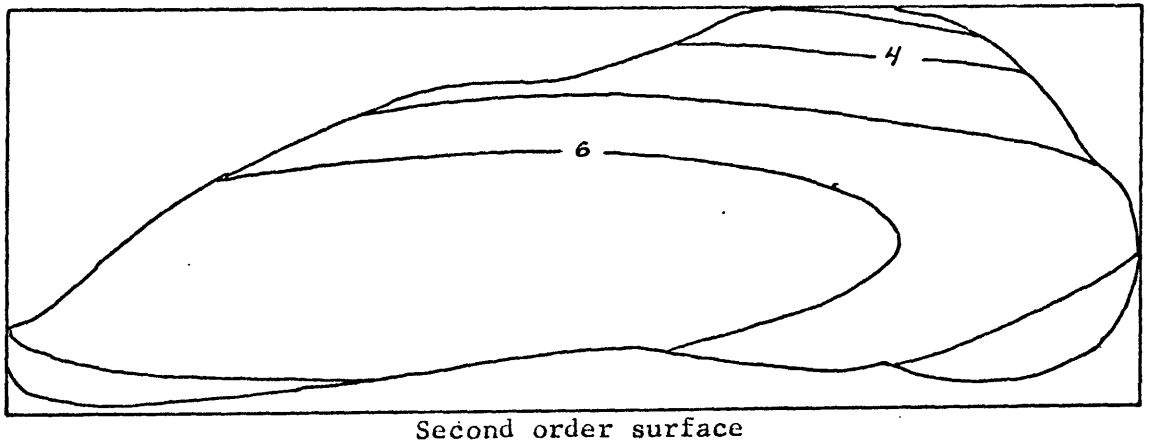

Second order surface

Figure 67: First through third order trend surfaces for modal biotite

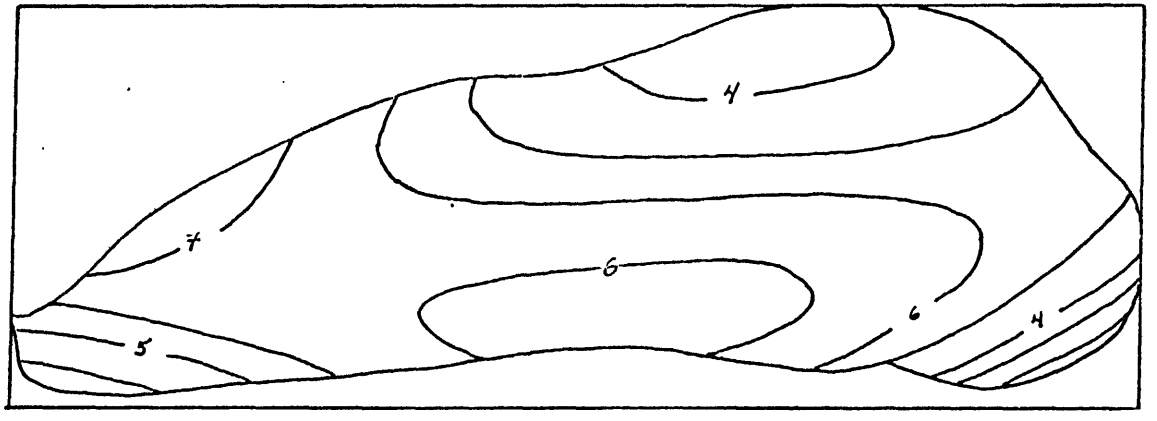

Third order surface

Figure 67: continued

TABLE 18

Summary of standard deviations of modal composition of microcline-quartz-plagioclase-biotite gneiss

	$\bar{X}$	Range	s
Quartz	37.3	27.1 - 51.8	4.36
Plagioclase	33.4	17.2 - 62.6	7.68
Microcline	21.8	0.0 - 43.3	8.42
Biotite	5.7	0.3 - 16.4	2.81

TABLE 19

Summary of thin section variance study

	Range of s	Mean s
Quartz	1.064 - 3.000	2.012
Plagioclase	1.160 - 2.776	1.744
Microcline	0.959 - 1.425	1.143
Biotite	0.277 - 0.913	0.728

TABLE 20

Summary of analysis of variance

and trend of modal quartz

Level	Sum of squares	Degrees of freedom	Mean Square	F	Confidence Level %
Due to 1st order surface	145.59	3	48.50	2.61	90+
Deviation from 1st order surface	1521.74	82	18.56		
Due to 2nd order surface	183.74	6	30.62	1.63	75+
Deviation from 2nd order surface	1483.50	79	18.78		
Due to 3rd order surface	242.58	10	24.26	1.28	50+
Deviation from 3rd order surface	1424.65	75	19.00		
Total	1667.24				

TABLE 21

Summary of analysis of variance

and trend of modal plagioclase

Level	Sum of squares	Degrees of freedom	Mean Square	F	Confidence Level %
Due to 1st order surface	24.05	3	11.35	0.13	5+
Deviation from 1st order surface	4985.68	82	60.80		
Due to 2nd order surface	70.52	6	11.75	0.19	1+
Deviation from 2nd order surface	4939.20	79	62.52		
Due to 3rd order surface	720.85	10	72.09	1.26	50+
Deviation from 3rd order surface	4288.87	75	57.18		
Total	5009.73				

TABLE 22

Summary of analysis of variance

and trend of modal microcline

Level	Sum of squares	Degrees of freedom	Mean Square	F	Confidence Level %
Due to 1st order surface	55.24	3	18.41	0.25	10+
Deviation from 1st order surface	5966.87	82	72.77		
Due to 2nd order surface	223.97	6	37.33	0.51	10+
Deviation from 2nd order surface	5798.15	79	73.39		
Due to 3rd order surface	704.65	10	70.46	0.99	50+
Deviation from 3rd order surface	5317.47	75	70.90		
Total	6022.11				

TABLE 23

Summary of analysis of variance

and trend of modal biotite

Level	Sum of squares	Degrees of freedom	Mean Square	F	Confidence Level %
Due to 1st order surface	42.46	3	14.15	1.92	75+
Deviation from 1st order surface	603.60	82	7.36		
Due to 2nd order surface	68.80	6	11.47	1.57	75+
Deviation from 2nd order surface	577.26	79	7.31		
Due to 3rd order surface	114.70	10	11.47	1.62	75+
Deviation from 3rd order surface	531.35	75	7.08		
Total	646.05				

TABLE 24

Percent reduction in total sums of squares due to least-squares trend (polynomial) surfaces based on U, V coordinates

	Degree 1	Degree 2	Degree 3	Degree 4
Quartz	8.73	11.02	14.55	16.66
Plagioclase	0.48	1.41	14.39	25.21
Microcline	0.90	3.68	11.67	20.41
Biotite	6.57	10.65	17.75	25.05

TABLE 25

Mandelbaum's test for the trend surface that best distinguishes the regional from the local trends. Computed values are for $^{ss}X_{dev}(N-P)$

	Degree 1	Degree 2	Degree 3
Quartz	18.33	18.54	18.74
Plagioclase	60.07	61.74	56.43
Microcline	71.88	72.48	69.97
Biotite	7.27	7.22	6.99

Where:

$^{ss}X_{dev}$ is the sum of the squares of the deviations from a surface of a given order;

N is the total number of sample points;

P is the number of terms in the polynomial expansion for a surface of a given order.